

1-2020

**PULMONARY AND SYSTEMIC PATHOPHYSIOLOGICAL IMPACT
OF SILVER NANOPARTICLES: EFFECTS OF COATING, TIME, AND
DOSE**

Zannatul Ferdous

Follow this and additional works at: https://scholarworks.uaeu.ac.ae/all_dissertations

 Part of the [Medicine and Health Sciences Commons](#)

United Arab Emirates University

College of Medicine and Health Sciences

PULMONARY AND SYSTEMIC PATHOPHYSIOLOGICAL
IMPACT OF SILVER NANOPARTICLES: EFFECTS OF COATING,
TIME AND DOSE

Zannatul Ferdous

This dissertation is submitted in partial fulfilment of the requirements for the degree
of Doctor of Philosophy

Under the Supervision of Professor Abderrahim Nemmar

January 2020

Declaration of Original Work

I, Zannatul Ferdous, the undersigned, a graduate student at the United Arab Emirates University (UAEU), and the author of this dissertation entitled "*Pulmonary and Systemic Pathophysiological Impact of Silver Nanoparticles: Effects of Coating, Time and Dose*", hereby, solemnly declare that this dissertation is my own original research work that has been done and prepared by me under the supervision of Professor Abderrahim Nemmar, in the College of Medicine and Health Sciences at UAEU. This work has not previously been presented or published or formed the basis for the award of any academic degree, diploma or a similar title at this or any other university. Any materials borrowed from other sources (whether published or unpublished) and relied upon or included in my dissertation have been properly cited and acknowledged in accordance with appropriate academic conventions. I further declare that there is no potential conflict of interest with respect to the research, data collection, authorship, presentation and/or publication of this dissertation.

Student's Signature: _____



Date: _____

30/1/2020

Copyright © 2020 by Zannatul Ferdous
All Rights Reserved

Advisory Committee

1) Advisor: Abderrahim Nemmar

Title: Professor

Department of Physiology

College of Medicine and Health Sciences

2) Member: Abdu Adem

Title: Professor

Department of Pharmacology

College of Medicine and Health Sciences

3) Member: Suhail Al-Salam

Title: Professor

Department of Pathology

College of Medicine and Health Sciences

Approval of the Doctorate Dissertation

This Doctorate Dissertation is approved by the following Examining Committee Members:

- 1) Advisor (Committee Chair): Abderrahim Nemmar

Title: Professor

Department of Physiology

College of Medicine and Health Sciences

Signature 


Date 20/01/2020

- 2) Member: Abdu Adem

Title: Professor

Department of Pharmacology

College of Medicine and Health Sciences

Signature 

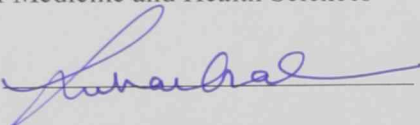
Date 20/01/2020

- 3) Member: Suhail Al-Salam

Title: Professor

Department of Pathology

College of Medicine and Health Sciences

Signature 

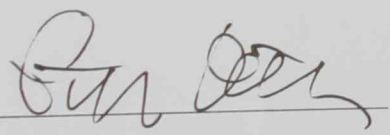
Date 20/01/2020

- 4) Member: Günter Oberdorster

Title: Professor

Department of Environmental Sciences


Institution: University of Rochester, School of Medicine and Dentistry, New York, USA

Signature 

Date 20/01/2020

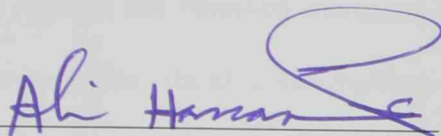
This Doctorate Dissertation is accepted by:

Dean of the College of Medicine and Health Sciences: Professor Juma al Kaabi

Signature 

Date 30-1-2020

Dean of the College of Graduate Studies: Professor Ali Al-Marzouqi

Signature 

Date 30/1/2020

Copy 10 of 10

Abstract

Nanotechnology is rapidly developing, and the engineered materials (ENMs) are utilized in a wide array of end user products owing to their unique physiochemical properties. Of the various forms of ENMs, silver nanoparticles (AgNPs) have gained much attention for potential uses in commercial applications. Due to their unique features, particularly antimicrobial properties, there had been a surge in the production of AgNPs-based products, hence increasing the potential of both occupational and consumer exposure. Among the various routes of human exposure, pulmonary exposure to AgNPs has received increased interest due to their potential to cause pulmonary injury, cross the alveolar-capillary barrier, and distribute to remote organs. However, the mechanism by which pulmonary exposure to AgNPs may induce pathophysiological effects on the cardiovascular system and other major remote organs (including liver, kidney, spleen and brain) is not well understood. Thus, the primary objective of this dissertation was to evaluate, in mice, the coating [(polyvinylpyrrolidone (PVP) and citrate (CT)], time (1 day and 7-days) and dose-dependent (0.05, 0.5 and 5 mg/kg) effects of pulmonary exposure to 10 nm AgNPs, on the cardiovascular system and other major organs including liver, kidney, spleen and brain. Moreover, since AgNPs are able to translocate from the airways into the bloodstream, they can, consequently, interact with circulatory cells such as erythrocytes. However, information regarding the pathophysiological effects and possible mechanism of action of AgNPs on the erythrocytes are still inadequately studied. Hence, to address this, we evaluated the effects of PVP- and CT- AgNPs (10 nm) at three different concentrations (2.5, 10, and 40 $\mu\text{g/ml}$) on mouse erythrocytes *in vitro*. For the *in vivo* experiments, AgNPs exposure in mice was achieved by single

intra-tracheal instillation and various cardiac and systemic endpoints were assessed including thrombosis, inflammation, oxidative stress, DNA damage and apoptosis following 1 and 7-days of exposure. Pulmonary deposited AgNPs induced dose-dependent cardiovascular effects including thrombosis, oxidative stress, inflammation, coagulation and apoptosis, with some of the effects persisting even after 7-days post-exposure. A biodistribution of AgNPs showed that, besides the presence of AgNPs in the lung, these nanoparticles were also found in the spleen, liver and to a lesser extent in the kidney, heart and brain. In addition, both PVP- and CT- AgNPs induced inflammation and oxidative stress in these latter organs as evidenced by significant elevations of tumor necrosis factor α , interleukin-6, glutathione, total antioxidants, nitric oxide and 8-isoprostane, as well as DNA damage and apoptosis in lung, heart, liver and brain, as shown by 8-hydroxy-2-deoxyguanosine and TUNEL assay. Our *in vitro* study revealed that both coating AgNPs induced significant and dose-dependent hemolysis, oxidative stress and increase cytosolic Ca^{2+} , annexin V binding and calpain activity. In conclusion, our data showed that firstly AgNPs deposition in the lungs induced pulmonary inflammation and oxidative stress. Secondly, the particles translocated and distributed to the remote organs including heart, liver, kidney, spleen and brain and caused alteration in oxidative stress markers, inflammatory cytokines, DNA damage and apoptosis. Thirdly, AgNPs induced prothrombotic actions, and altered coagulation markers. Fourthly, *in vitro* data indicated that both PVP- and CT- AgNPs induced erythrocyte hemolysis and eryptosis. Overall, these *in vivo* and *in vitro* results, not only reinforced the previously established mechanisms of DNA damage caused by reactive oxygen species, resulting in cellular dysfunction and apoptosis, but also provided a novel mechanistic insight into the pathophysiological effects and tissue distribution of AgNPs following pulmonary exposure.

Keywords: Silver nanoparticles, oxidative stress, inflammation, eryptosis, apoptosis, DNA damage.

Title and Abstract (in Arabic)

الأثر الفيزيولوجي – المرضي لمركبات الفضة النانوية على الرنتين والأجهزة الأخرى: تأثيرات وضع طبقة خارجية، والزمن، والجرعة

الملخص

تتطور التقنية النانوية بسرعة، وتستخدم المواد الهندسية في طيف واسع من منتجات المستهلك النهائي، ومرد ذلك هو خواصها الفيزيائية والكيميائية المتفردة. ومن بين الأشكال المتعددة لمنتجات المستهلك النهائي وجدت مركبات الفضة النانوية اهتماما كبيرا في العديد من الاستخدامات التجارية الممكنة. ونسبة للمزايا المتفردة التي تتمتع بها مركبات الفضة النانوية (خاصة عملها كمضادات للجراثيم) تضاعف انتاج المنتجات التي يعتمد انتاجها على هذه المركبات. وهذا مما شأنه أن يزيد من احتمال تعرض البشر في المجالات المهنية والاستهلاكية لتلك المركبات. ولقي تعرض البشر لهذه المركبات النانوية عن طريق التنفس اهتماما كبيرا نسبة لما قد تحدثه من أضرار بالرنتين، ولقدرتها على عبور الحاجز بين الشعيرات الدموية والأسناخ، وأن تتوزع إلى أعضاء في الجسم بعيدة عن الرنتين. غير أن الآلية التي يحدث بها التعرض التنفسي لمركبات الفضة النانوية آثارا فيزيولوجية – مرضية على الجهاز القلبي الوعائي، والأعضاء البعيدة الأخرى (مثل الكبد والكلى والطحال والدماغ) ليست مفهومة تماما. لذا فقد كان الهدف الرئيس من هذه الأطروحة هو تقييم تأثيرات وضع طبقة خارجية من مادة بولي فينيل بايرونولون والسترات على آثار التعرض لمركبات الفضة النانوية (10 nm) عن طريق التنفس في الجهاز القلبي الوعائي والأعضاء الأخرى (مثل الكبد والكلى والطحال والدماغ) في الفئران. وكان الهدف من الدراسة أيضا دراسة تأثير التعرض لتلك المركبات ليوم واحد أو سبعة أيام، ودراسة تأثير الجرعات المعطاة (0.05, 0.5 and 5 mg/kg). وبما أن بإمكان مركبات الفضة النانوية أن تترافق / تنقل من المسالك الهوائية إلى مجرى الدم، فإن بإمكانها نتيجة لذلك أن تتفاعل مع خلايا الدم (مثل كريات الدم الحمراء). إلا أن الآثار الفيزيولوجية – المرضية التي تحدثها تلك المركبات على كريات الدم الحمراء، وآلية عملها المحتملة لم تدرس بعد دراسة وافية. لذا فقد قمنا بعمل دراسة مختبرية خارج الجسم الدراسة لتقييم آثار وضع طبقة خارجية من مادة بولي فينيل بايرونولون والسترات (10 nm) في جرعات ثلاث (2.5, 10 and 40 µg/ml) على كريات الدم الحمراء المعزولة من فئران. أما في التجارب داخل الجسم فقد قمنا بإعطاء المادة عن طريق التسليل الرغامي، وقمنا بعد ذلك بدراسة مختلف النقاط النهائية القلبية والجهازية، والتي شملت

الختار والالتهاب والاجهاد التأكسدي، وضرر الحامض النووي عقب يوم أو سبعة أيام من التعرض. وأحدث ترسب مركبات الفضة النانوية في الرئة آثارا قلبية وعائية معتمدة على الجرعة شملت الخثار والالتهاب والاجهاد التأكسدي وضرر الحامض النووي والموتُ الخَلَوِيُّ المُبَرِّمَج. وبقيت تلك الآثار حتى بعد سبعة أيام من التعرض للمركبات. ودرسنا أيضا توزيع هذه المركبات في أعضاء غير الرئة، فوجدناها في الطحال والكبد، وإلى حد أقل في الكلى والقلب والدماغ. ووجدنا أيضا أن مركبات الفضة النانوية المغطاة بمادتي بولي فينيل بايرولدون والسترات قد أحدثت التهابا واجهدا تأكسديا في تلك الأعضاء المذكورة كما وضح من الارتفاع المعتد به إحصائيا في عامل نخر الورم الفا، وانترليوكين - 6، وغلوتاثيون، ومضادات الأوكسدة الكلية، واكسيد النترريك، ومادة 8 - ايسو بروتستين، إضافة للضرر في الحامض النووي واحداث الموتُ الخَلَوِيُّ المُبَرِّمَج في الرئة والقلب والكبد والدماغ، المقاس بطريقتي 8 - هيدروكسي - 2 - ديوكسي قوانيزين و TUNEL. ووجدنا في الدراسات المخبرية (خارج الجسم) أن تغطية مركبات الفضة النانوية بالمادتين المذكورتين سببت انحلالا في الدم وإجهادا تأكسديا، وزيادة في تركيز ايونات الكالسيوم في العصارة الخلوية، وفي الاتحاد مع مادة انكسين، وفي نشاط بروتين كالبيين. وكانت كل تلك الأفعال معتدة إحصائيا ومعتمدة على الجرعة.

خلصت الدراسة إلى أن ترسب مركبات الفضة النانوية في الرئة قد أفضى إلى التهاب وإجهاد تأكسدي. وخلصت أيضا إلى أن هذه المركبات تنتقل من الرئة وتنتزع إلى أعضاء بعيدة عنها شملت القلب والكبد والكلى والطحال والدماغ، وتسببت في ارتفاع مؤشرات الاجهاد التأكسدي، والسيتوكينات الالتهابية، وكذلك في ضرر الحامض النووي واحداث الموتُ الخَلَوِيُّ المُبَرِّمَج. وجد أيضا أن مركبات الفضة النانوية تسبب أفعالا تقود إلى زيادة التخرثر، وتغير من مؤشرات التجلط. وأثبتت النتائج التي تحصلنا عليها من تجارب مخبرية (خارج الجسم) أن مركبات الفضة النانوية مع مادة بولي فينيل بايرولدون والسترات تسبب انحلالا في الدم وتحدث الموتُ الخَلَوِيُّ المُبَرِّمَج في الكريات الحمراء. وعلى وجه الإجمال، النتائج المتحصل عليها من داخل وخارج الجسم لا تؤكد فقط الآليات المعروفة عن طريقة إحداث ضرر الحامض النووي الذي تسببه المواد المحدثة للتأكسد، والتي تقضي إلى اختلال وظائف الخلايا واحداث الموتُ الخَلَوِيُّ المُبَرِّمَج، بل تعرض آلية مبتكرة للآثار المرضية - الفيزيولوجية الناتجة عن التعرض لمركبات الفضة النانوية عن طريق الرئة، وعن توزيعها في الأنسجة الأخرى.

مفاهيم البحث الرئيسية: مركبات الفضة النانوية، الإجهاد التأكسدي، الالتهاب، موت الخلايا المبرمج ، ضرر الحمض النووي.

Acknowledgements

First and foremost, I bow down before “Almighty Allah” with solicity to express my deepest sense of gratitude to His blessing, mercy, wisdom, faithfulness and thus enabling me to accomplish this venture.

With an utmost degree of sincerity, I avail this opportunity to express my heartfelt thanks to my incomparable advisor, Prof. (Dr.) Abderrahim Nemmar, Department of Physiology, CMHS, UAEU, for the supervision and guidance throughout the research work. The critical evaluation of the research work at different stages and valuable suggestions went a long way in bringing this research work to this stage. He has not only been a fathomless ocean of knowledge and wisdom to me but most of all his words of care and hands of blessing has been my pillar of strength and courage to complete this task. My dream has been converted into reality because of his blessings and fatherly behavior. My fortune may not give anything more but has given me the opportunity to work under this great teacher and human being. “Thank you, Sir”.

I would like to thank my PhD advisory committee, Professor Suhail Al-Salam and Professor Abdu Adem for their guidance, support, and assistance throughout my project. I am grateful for their precious time, expertise, feedback and encouragement during the progress of my project and preparation of my thesis. I would like to also thank all members of the Department of Physiology, UAEU for assisting me all over my studies and research. My special thanks are extended to the Library Research Desk for providing me with the relevant reference material.

Special thanks go to my parents, husband and children for their supreme sacrifice & eternal benediction in evolving my personality. Their words of

encouragement, care & good wishes, always being spring of inspiration, have made this work a great success.

Dedication

To my beloved family

Table of Contents

Title	i
Declaration of Original Work	ii
Copyright	iii
Advisory Committee	iv
Approval of the Doctorate Dissertation	v
Abstract	vii
Title and Abstract (in Arabic)	x
Acknowledgements	xiii
Dedication	xv
Table of Contents	xvi
List of Tables.....	xviii
List of Figures	xix
List of Abbreviations.....	xxii
Chapter 1: Introduction	1
1.1 Nanotechnology	1
1.1.1 Engineered nanomaterials	2
1.2 Silver nanoparticles	8
1.2.1 AgNPs synthesis and characterization	9
1.2.2 AgNPs physicochemical properties	11
1.2.3 AgNPs application and mechanism of action	13
1.2.4 Routes of exposure and biodistribution.....	14
1.2.5 Pathophysiological effects of AgNPs.....	20
Chapter 2: Hypothesis, Aims and Objectives	42
2.1 Hypothesis.....	42
2.2 Aims and Objectives	43
Chapter 3: Methods	44
3.1 Research design.....	44
3.2 Material and Methods	44
3.3 Study one: Pulmonary exposure to silver nanoparticles impairs cardiovascular homeostasis: effects of coating, dose and time.....	46
3.3.1 Background	46
3.3.2 Methods	49
3.3.3 Results	57
3.3.4 Discussions	77

3.4 Study two: Coating and time-dependent effect and biodistribution of pulmonary instilled silver nanoparticles in remote organs	84
3.4.1 Background	84
3.4.2 Methods	86
3.4.3 Results	89
3.4.4 Discussions	105
3.5 Study three: The <i>in vitro</i> effect of polyvinylpyrrolidone and citrate coated silver nanoparticles on erythrocytic oxidative damage and eryptosis	111
3.5.1 Background	111
3.5.2 Materials and Methods	112
3.5.3 Results	118
3.5.4 Discussions	127
Chapter 4: Conclusions, Limitations of study and Future directions.....	134
4.1 Conclusions	134
4.1.1 <i>In vivo</i> studies: Pulmonary exposure to AgNPs and pathophysiological effects.....	135
4.1.2 <i>In vitro</i> studies: Effect of AgNPs on incubated mouse erythrocytes	138
4.2 Limitations of study	140
4.3 Future directions.....	140
References	142
List of Publications	168

List of Tables

Table 1: Common nanoparticles and their major applications.....	6
Table 2: Toxicity and distribution of AgNPs following pulmonary exposure in rodents via inhalation	28
Table 3: Toxicity and distribution of AgNPs following pulmonary exposure in rodents via intratracheal instillation	30
Table 4: Toxicity and biodistribution of AgNPs in rodents via oral exposure	34
Table 5: Toxicity and biodistribution of AgNPs in rodents via intravenous injection	39
Table 6: Main physicochemical properties of tested AgNPs provided by the manufacturer and reported in the datasheet	45
Table 7: Size distribution and zeta potential measurements of polyvinylpyrrolidone and citrate coated silver nanoparticles	58
Table 8: Concentrations of Ag ($\mu\text{g/g}$) in lung, heart, brain, kidney, spleen and liver following 1-day and 7-days of intra-tracheal instillation of polyvinylpyrrolidone or citrate silver nanoparticles or silver acetate in mice.	104

List of Figures

Figure 1: Schematic representation of biodistribution and toxicity of silver nanoparticles (AgNPs) following various routes of exposure.....	16
Figure 2: Transmission electron microscope analysis of polyvinylpyrrolidone or citrate coated silver nanoparticles.....	59
Figure 3: Representative light microscopy sections of lung tissues of control mice and those treated with polyvinylpyrrolidone (PVP) silver nanoparticles (AgNPs) at dose of 0.05, 0.5, 5 mg/kg, stained with H&E and of control mice and those treated with citrate silver nanoparticles (AgNPs) at dose of 0.05, 0.5, 5 mg/kg, stained with H&E.	62
Figure 4: TNF- α and IL-6 levels in heart tissues following 1-day and 7-days of intra-tracheal instillation of saline (control) or citrate 2 mM (control) or polyvinylpyrrolidone (PVP) or citrate (CT) silver nanoparticles (AgNPs) or silver acetate (AgAc) in mice.....	64
Figure 5: Total antioxidants, reduced glutathione (GSH) and 8-isoprostane levels in heart tissues following 1-day and 7-days of intra-tracheal instillation of saline (control) or citrate 2 mM (control) or polyvinylpyrrolidone (PVP) or citrate (CT) silver nanoparticles (AgNPs) or silver acetate (AgAc) in mice.....	66
Figure 6: 8-hydroxy-2-deoxyguanosine (8-OH-dG) levels in heart tissues following 1-day and 7-days of intra-tracheal instillation of saline (control) or citrate 2 mM (control) or polyvinylpyrrolidone (PVP) or citrate (CT) silver nanoparticles (AgNPs) or silver acetate (AgAc) in mice.....	67
Figure 7: Estimation of apoptotic cells by an in situ TUNEL assay in heart sections and their representative images, following intra-tracheal instillation of saline (control) or citrate 2 mM (control) or polyvinylpyrrolidone (PVP) or citrate (CT) silver nanoparticles (AgNPs) or silver acetate (AgAc) in mice.....	69
Figure 8: Fibrinogen, plasminogen activator inhibitor-1 (PAI-1, C, D) concentrations in plasma, following 1-day and 7-days of intra-tracheal instillation of saline (control) or citrate 2 mM (control) or polyvinylpyrrolidone (PVP) or citrate (CT) silver nanoparticles (AgNPs) or silver acetate (AgAc) in mice.....	72
Figure 9: Plasma brain natriuretic peptide (BNP) following 1-day and 7-days of intra-tracheal instillation of saline (control) or citrate 2 mM (control) or polyvinylpyrrolidone (PVP) or citrate (CT) silver nanoparticles (AgNPs) or silver acetate (AgAc) in mice.....	73

Figure 10: Prothrombin time (PT) and activated partial thromboplastin time (aPTT) measured following 1-day and 7-days of intra-tracheal instillation of saline (control) or citrate 2 mM (control) or polyvinylpyrrolidone (PVP) or citrate (CT) silver nanoparticles (AgNPs) or silver acetate (AgAc) in mice.....	74
Figure 11: Thrombotic occlusion time in pial arterioles or venules following 1-day and 7-days of intra-tracheal instillation of saline (control) or citrate 2 mM (control) or polyvinylpyrrolidone (PVP) or citrate (CT) silver nanoparticles (AgNPs) or silver acetate (AgAc) in mice.....	76
Figure 12: In vitro effect after the administration of saline (control) or citrate 2 mM (control) or polyvinylpyrrolidone (PVP) or citrate (CT) silver nanoparticles (AgNPs) or silver acetate (AgAc) on platelet aggregation in whole blood of untreated mice.....	77
Figure 13: Representative light microscopy sections of lung, brain, kidney, spleen, liver and heart tissues of control mice and those treated with polyvinylpyrrolidone (PVP) silver nanoparticles (AgNPs) at dose of 5 mg/kg , stained with H&E and of control mice and those treated with citrate (CT) silver nanoparticles (AgNPs) at dose 5 mg/kg, stained with H&E.....	90
Figure 14: TNF- α concentrations in lung, brain, kidney, spleen and liver tissues following 1-day and 7-days of intra-tracheal instillation of saline (control) or citrate 2 mM (control) or polyvinylpyrrolidone (PVP) or citrate (CT) silver nanoparticles (AgNPs) or silver acetate (AgAc) in mice.....	92
Figure 15: IL-6 concentrations in lung, brain, kidney, spleen and liver tissues following 1-day and 7-days of intra-tracheal instillation of saline (control) or citrate 2 mM (control) or polyvinylpyrrolidone (PVP) or citrate (CT) silver nanoparticles (AgNPs) or silver acetate (AgAc) in mice.....	93
Figure 16: Reduced glutathione (GSH) levels in lung, brain, kidney, spleen and liver tissues following 1-day and 7-days of intra-tracheal instillation of saline (control) or citrate 2 mM (control) or polyvinylpyrrolidone (PVP) or citrate (CT) silver nanoparticles (AgNPs) or silver acetate (AgAc) in mice.....	95
Figure 17: Total NO levels in lung, brain, kidney, spleen and liver tissues following 1-day and 7-days of intra-tracheal instillation of saline (control) or citrate 2 mM (control) or polyvinylpyrrolidone (PVP) or citrate (CT) silver nanoparticles (AgNPs) or silver acetate (AgAc) in mice.....	96
Figure 18: 8-isoprostane levels in lung, brain, kidney, spleen and liver tissues following 1-day and 7-days of intra-tracheal instillation of saline (control) or citrate 2 mM (control) or	

polyvinylpyrrolidone (PVP) or citrate (CT) silver nanoparticles (AgNPs) or silver acetate (AgAc) in mice.....	97
Figure 19: 8-hydroxy-2-deoxyguanosine (8-OH-dG) levels in lung, brain, kidney, spleen and liver tissues following 1-day and 7-days of intra-tracheal instillation of saline (control) or citrate 2 mM (control) or polyvinylpyrrolidone (PVP) or citrate (CT) silver nanoparticles (AgNPs) or silver acetate (AgAc) in mice.....	99
Figure 20: Estimation of apoptotic cells by an in situ TUNEL assay in tissue sections and their representative images, following 1-day and 7-days of intra-tracheal instillation of saline (control) or citrate 2 mM (control) or polyvinylpyrrolidone (PVP) or citrate (CT) silver nanoparticles (AgNPs) or silver acetate (AgAc) in mice.	101
Figure 21: Transmission electron microscope analysis of polyvinylpyrrolidone or citrate coated silver nanoparticles.....	119
Figure 22: Hemolytic effect of polyvinylpyrrolidone (PVP) and citrate (CT) silver nanoparticles (AgNPs) on mouse erythrocytes.	120
Figure 23: Transmission electron microscope (TEM) analysis of erythrocytes after in vitro incubation with saline (control), polyvinylpyrrolidone (PVP) silver nanoparticles (AgNPs) 2.5, 10, 40 µg/ml, 2 mM citrate (control) or citrate (CT) coated AgNPs 2.5, 10, 40 µg/ml.	121
Figure 24: Effect of polyvinylpyrrolidone (PVP) and citrate (CT) silver nanoparticles (AgNPs) on concentration of malonaldehyde (MDA), reduced glutathione (GSH) and catalase activity measured in the incubation medium of erythrocytes.	123
Figure 25: Effect of polyvinylpyrrolidone (PVP) and citrate (CT) silver nanoparticles (AgNPs) on intracellular calcium concentration measured in incubated erythrocytes.....	124
Figure 26: Effect of polyvinylpyrrolidone (PVP) and citrate (CT) silver nanoparticles (AgNPs) on the concentration of bound Annexin V in the incubation medium of erythrocytes.....	125
Figure 27: Effect of polyvinylpyrrolidone (PVP) and citrate (CT) silver nanoparticles (AgNPs) on erythrocyte caspase 3 activity and caspase 3 expression assessed by western blotting.....	126
Figure 28: Effect of polyvinylpyrrolidone (PVP) and citrate (CT) silver nanoparticles (AgNPs) on calpain activity measured in incubated erythrocytes.	127

List of Abbreviations

AgNPs	Silver Nanoparticles
ALT	Alanine Aminotransferase
AST	Aspartate Aminotransferase
APTT	Activated Partial Thromboplastin Time
BBB	Blood Brain Barrier
Bl	Bladder
BNP	Brain Natriuretic Peptide
Br	Brain
CAT	Catalase
Ce	Cecum
CNTs	Carbon Nanotubes
CT	Citrate
DAB	Diaminobenzene
ENM	Engineered Nanomaterials
Fe	Feces
FeO	Iron Oxide
GSH	Reduced Glutathione
Ht	Heart
IL-6	Interleukin 6
I.p	Intraperitoneal
ISO	International Organization of Standardization
It	Intestine
I.t	Intratracheal

I.v	Intravenous
Ki	Kidney
LDH	Lactate Dehydrogenase
Lu	Lung
Li	Liver
MDA	Malondialdehyde
NMs	Nanomaterials
Ob	Olfactory Bulb
PAI-1	Plasminogen Activator Inhibitor 1
Pl	Placenta
PT	Prothrombin Time
PVP	Polyvinylpyrrolidone
QD	Quantum Dots
ROS	Reactive Oxygen Species
Sp	Spleen
St	Stomach
TEM	Transmission Electron Microscope
Th	Thymus
TiO	Titanium Oxide
TNF- α	Tumor Necrosis Factor α
TUNEL	Terminal Deoxynucleotide Transferase Mediated dUTP Nick End Labelling
Ur	Urine
Ut	Uterus
8-OH-dG	8-Hydroxy-2-Deoxy Guanosine

Chapter 1: Introduction

1.1 Nanotechnology

The concept of the novel nanoscale technology was introduced in 1959 in the lecture of physicist Richard Feynman entitled “*There is plenty of room at the bottom*”; which discussed the importance of manipulating and controlling things at the atomic scale [1]. The term nanotechnology was first introduced by Professor Norio Taniguchi in 1974, and the American engineer Kim Eric Drexler, popularized the concept of molecular nanotechnology by using it in his 1986 book *Engines of Creation; The Coming Era of Nanotechnology* [1]. However, it was only after 1981 following invention of the scanning tunneling microscope and atomic force microscope that the growth of nanotechnology spurred [1]. The emerging and exponential nanotechnology involves manipulation, design and precision placement of atoms and molecules at the nanoscale level [1]. Over the past two decades, nanotechnology has witnessed breakthroughs in the fields of medicine, environment, therapeutics, drug development and biotechnology. This is due to unique properties of nanomaterials (NMs), such as small size, large surface area to volume ratio, high reactivity, high carrier capacity and easy variation of surface properties, which makes them desirable for commercial and medical applications [2]. Considering the broad spectrum use of NMs, nanotechnology has a great potential in improving treatment of various disorders and *in vitro* diagnostics. These wide applications raise questions as to potential environmental and health effects that might result from occupational exposures during manufacture and use of NMs at the consumer end [3]. NMs can enter the bloodstream via inhalation or ingestion and are able to cross biological membranes and access cells, tissues and organs that larger-sized particles normally cannot [3]. This may lead to both

genotoxicity and biochemical toxicity [4]. Toxic effect of NMs on humans has recently gained much attention in the health industry [5, 6]. As NMs are involved for medicine, diagnostic and other technological advances, an understanding of the toxicology of these new materials is therefore much needed.

Some of the most commonly applied NMs include fullerenes, carbon nanotubes (CNTs), silver nanoparticles (AgNPs), gold nanoparticles (AuNPs), titanium oxide nanoparticles (TiO₂), zinc oxide nanoparticles, iron oxide (FeO) and silica nanoparticles (SiNP) [7]. Among these NMs, AgNPs have gained strong popularity in research over the past few decades [7]. Initial investigations on AgNPs were more focused on synthesizing and characterizing them using chemical approaches. However, current works are concentrated more on their biological effects and applications for several purposes [8]. AgNPs are also known to have unique properties in terms of toxicity, surface plasmon resonance, and electrical resistance [8]. Based on these, intensive works have been conducted to investigate their properties and potential applications for several purposes such as antimicrobial agents in wound dressings, water disinfectants, electronic devices and anticancer agents [8, 9].

1.1.1 Engineered nanomaterials

A major element of nanotechnology comprises of the engineered nanomaterials (ENMs). According to European commission NMs means “*A natural, incidental or manufactured material containing particles, in an unbound state or as an aggregate or as an agglomerate and where, for 50% or more of the particles in the number size distribution, one or more external dimensions is in the size range 1 nm - 100 nm*” [10]. The International Organization for Standardization (ISO) defines NMs “*as a material*

having any external dimension in the nanoscale or having internal structure or surface structure in the nanoscale". ISO classifies NMs in two main categories: Nano-objects and nanostructured materials. Nanoparticles (NPs) are nano-objects with all external dimensions at the nanoscale where lengths of the longest and shortest axes of the nano-object do not differ significantly.

NMs are comprised of 3 layers; a) the outer surface layer which may be modified by variety of small molecule, metal ions, surfactant and polymers, b) the intermediate shell layer and c) the core, which is the central portion and usually refers to the NPs itself [11]. Based on their origin, NMs can be grouped in 3 main categories, i.e naturally produced, incidental and engineered nanoparticles (ENPs). Naturally produced NMs can be found in the bodies of organisms, insects, plants, animals and human bodies [4]. In fact, nanostructures contribute to the basic foundation for all life forms on Earth as evident by nanometer sized genetic materials (DNA or RNA), proteins, antibodies, enzymes and other secretions that are highly beneficial for the proper functioning of human body. Incidental NMs are produced incidentally as a byproduct of industrial processes such as NPs produced from vehicle engine exhaust, welding fumes, combustion processes and even some natural process such as forest fires, volcanic eruptions, dust storms and photochemical reactions [4]. Incidental and naturally occurring NMs are continuously being formed within and distributed throughout soil, water and air. ENPs are type of synthetic NPs, deliberately developed by humans to be used in applications, for e.g., carbon black, fumed silica, titanium dioxide (TiO_2), iron oxide (FeO), quantum dots (QDs), fullerenes, carbon nanotubes (CNTs) and dendrimers [12]. One of the main differences between incidental and ENPs is that the morphology (i.e. size, shape and composition) of engineered ENPs can usually be better controlled as compared to incidental NMs.

NMs can also be classified in the basis of their overall shape; 0 dimensional (D), 1 dimensional (1D), 2 dimensional (2D) and 3 dimensional (3D) NMs [13]. Electrons in D are confined in all directions and NPs are isolated from each other [13]. 1D NPs include nanowire, nanorods and are often used as circuitry of computer chips and for anti-reflective properties and hard coatings on eyeglasses [13]. 2D NPs include graphene and are often used as nanocoating or nanopore filters used for small particle separation and filtration [13]. 3D nanomaterials have all their dimensions at macroscale, hence usually not covered under nanoparticles [13]. NPs can also be categorized depending on their physical and chemical properties. Some of the well-known classes include carbon based, metallic, ceramic, semiconductors, polymeric and lipid-based NPs [2].

ENPs can be prepared from a variety of materials such as proteins, polysaccharides and synthetic polymers and their preparation method usually includes dispersion of preformed polymers, ionic gelation or coacervation of hydrophilic polymers and polymerization of monomers [14]. Two broad approaches are applied for synthesis of NPs, top down syntheses and bottom up syntheses. In top down syntheses, larger molecules are decomposed into smaller units which are converted into NPs [2]. This destructive method uses microfabrication technique where extremely controlled tools cut, mill and shape materials in desired shape and size [15]. The bottom up syntheses are employed in reverse. uses smaller molecular components to form complex assemblies, and therefore, called as building approach [2]. Examples of this case are sedimentation and reduction techniques [2].

Nanomaterials have unique properties relative to bulk counterpart which impart them beneficial characteristics; ironically, they may also bestow them with unique mechanisms of toxicity. In general, toxicity has been thought to originate from

nanomaterials' size and surface area, composition, shapes, and so on. For instance, the main reasons why materials built of ENPs have different electrical, magnetic, chemical and mechanical properties from their bulk counterparts are that in this size-range quantum effects start to predominate, and the surface-area-to-volume ratio becomes very large [1]. The surface to volume of most materials increases gradually as their particles become smaller, which results in increased adsorption of the surrounding atoms and changes their properties and behavior. Once particles become small enough, they start to obey the quantum mechanical laws. The nanoscale size also influences their optical properties, reactivity and toughness and it is the optical property, which imparts different colors to various NPs, due to absorption in the visible region. Moreover, materials reduced to the nanoscale can suddenly show very different properties, compared to what they exhibit on the macro-scale, which again enables unique applications. For example, opaque substances become transparent (copper); stable materials become combustible (aluminum); inert materials become catalysts (platinum); insulators become conductors (silicon); solids turn into liquids at room temperature (gold) [3].

The unique characteristics of NPs make them suitable candidates for various domestic, commercial and environmental applications. A list of common NPs and their major applications is presented in Table 1. NPs enabled products range from cosmetics to sporting goods and serve a variety of functions: everything from acting as UV-blocking agents to making plastics that are extremely light, but stronger than steel.

Table 1: Common nanoparticles and their major applications.

Nanoparticles	Application	References
Ag	Medicine (wound dressings, drug delivery, biosensors and medical diagnostics, orthopedics), food and textile industries, and water disinfection systems	[16]
Fe/Fe ₂ O ₃	Environmental remediation: degradation of organic dyes, chlorinated organic pollutants and heavy metals removal, MRI, magnetic data storage, Contrast agent for targeted tumor imaging, magnetic sensing probes for <i>in vitro</i> diagnostics, drug and gene carriers, therapeutic agents in chemotherapy	[17]
CNT	Consumer electronics Air and water filtration, thermal materials, catalysts support	[18]
TiO ₂	Paints and coating for antimicrobial properties Degrading organic contaminants and germs Cosmetics as UV absorber	[19]
Fullereness	Drug delivery, anti-ageing and anti-damaging agent in cosmetics Anti-viral agents	[20]
Au	Medical diagnostics, sensing, targeted drug delivery, imaging, photothermal and photodynamic therapy	[21]

The rapid expansion and application of nanotechnology naturally leads to increased potential of exposure of ENMs both at occupational and consumer end. Production, use, disposal, and waste treatment of products containing nanoproducts are the prime reasons for the environmental release of nanoparticulate in the original

or modified forms. These particles released in human environment can be inhaled and most exposure to airborne NMs occurs in the work place [22]. Workers may be exposed to nano-scale materials while manufacturing these materials, formulating them into products, transporting them or handling them in the storage facilities. Additionally, as nanotechnology is available on the market for great variety of applications, widespread consumer exposure via direct contact with ENP-containing product is likely. The small size of NPs facilitates translocation of active chemical species from natural barriers such as the skin, lung, body tissues and organs [23]. For example, NPs that are inhaled can effortlessly reach the bloodstream and interact with blood cells and other sites in the human body including the liver, heart or brain [23]. Reactive oxygen species generation, protein denaturation, mitochondrial disconcertion and perturbation of phagocytic functions are acute toxic effects of NPs [4]. On the other hand, uptake by the reticuloendothelial system, nucleus, neuronal tissue and the generation of neoantigens that causes possible organ enlargement and dysfunction are common chronic toxic effects of NPs [4]. Other than penetration, electrostatic charges, van der Waals forces, interfacial tension effects and steric interaction of NPs bind with cellular components and cause cell death [4]. A wide variety of NPs can create reactive oxygen species and cause cellular damage via lipid peroxidation, protein alteration, DNA disruption, signaling function interference and gene transcription modulation [4]. The fate of oxidative products relies on the chemistry, shape, size and location of the NPs. NPs can relocate or distribute to various cellular sites such as the cytoplasm, components of cytoplasm and nucleus. NPs can harm cell organelles or DNA and cause cell mortality with their cellular localization effect [15].

Though NPs are useful for many applications, but still there are some health hazard concerns due to their uncontrollable use and discharge to natural environment,

Hence, nanotoxicology warrants intensive research studies in order to consider the use of NPs more convenient and environment friendly.

1.2 Silver nanoparticles

Of all the ENMs developed and characterized thus far, AgNPs assume a significant position owing to their potential uses in commercial applications [24, 25]. Silver, symbolized as Ag, is lustrous, soft, ductile and malleable metal, having the highest electrical conductivity of all metals and is widely used in fabricating printed electrical circuits and as a vapour-deposited coating for electronic conductors in electrical appliances [26]. This precious metal is chemically inactive, stable in water and does not oxidize in air, hence, used in manufacturing of coins, ornaments and jewelry [26]. Silver can be obtained from pure deposits as well as from silver ores such as horn silver and argentite. Most silver is derived as a by-product along with deposits of ores containing gold, copper, or lead [26]. It is estimated that nearly 320 tons of Ag NPs are manufactured every year and used in nanomedical imaging, biosensing and food products [27, 28]. AgNPs exhibit special properties relative to their bulk components due to their unique physicochemical properties including small size, greater surface area, surface chemistry, shape, particle morphology, particle composition, coating/capping, agglomeration, rate of particle dissolution, particle reactivity in solution, efficiency of ion release, and the type of reducing agents used for the synthesis of AgNPs [9, 16]. In addition, AgNPs are also well known for their antimicrobial, optical, electrical, and catalytic properties [8]. Owing to their unique properties, AgNPs have been extensively used in house-hold utensils, food storage, health care industry, environmental, and biomedical applications such as wound dressings, surgical instruments and disinfectants [16]. Further, due to their optical

activities these NPs have been used in catalysis, electronics and biosensors [16].

1.2.1 AgNPs synthesis and characterization

Numerous methods have been adopted for synthesis of AgNPs in order to meet the increasing requirements. The conventional physical method of synthesis includes spark discharge and pyrolysis [29, 30]. Chemical method which can be top down or bottom up approach involves three main components; metal precursors, reducing agents, stabilizing/capping agents [9]. The common approach usually is chemical reduction by organic or inorganic reducing agents, such as, sodium citrate, ascorbate, sodium borohydride, elemental hydrogen, polyol process, Tollens reagent, N, N-dimethylformamide, and polyethylene glycol-block copolymer [9]. Other procedures includes cryochemical synthesis, laser ablation, lithography, electrochemical reduction, laser irradiation, sono-decomposition and thermal decomposition [9]. The major advantage of chemical method is high yield unlike the physical method which has low yield [31]. However, contrary to physical method, chemical method is extremely expensive, toxic and hazardous [31]. In order to overcome the later limitations, biologically mediated synthesis of NPs have emerged as better options. This simple, cost effective and environment friendly approach uses biological systems including bacteria, fungi, plant extracts, and small biomolecules like vitamins, amino acids and enzymes for the synthesis of AgNPs [32]. The green approach is widely accepted due to availability of a vast array of biological resources, decreased time requirement, high density, stability, and the ready solubility of prepared NPs in water [32].

Characterization of AgNPs is a very crucial step to evaluate the functional effect of synthesized particle [9]. It has been documented in various studies that

biological activity of AgNPs depends on morphology, structure, size, shape, charge and coating/capping, chemical composition, redox potential, particle dissolution, ion release and degree of aggregation [28, 33-36]. Like all other NPs, these parameters can be determined using various analytical techniques, such as dynamic light scattering (DLS), zeta potential, advanced microscopic techniques as atomic force microscopy, scanning electron microscopy (SEM) and transmission electron microscopy (TEM), UV-vis spectroscopy, X-ray diffractometry (XRD), fourier transform infrared spectroscopy (FTIR), and X-ray photoelectron spectroscopy (XPS) [9, 37]. To capture the concept of importance of AgNPs characterization, it must be noted that from toxicological perspective studies using similar AgNPs provided by the same manufacturer demonstrated different results. For example, a repeated exposure study by Vandebriel RJ *et al.* [38] in rats showed that AgNPs are cytotoxic to various cells. Contradicting to that, Boudreau M.D *et al.* [39] using similar particles, showed dose dependent accumulation of AgNPs in various tissues of rats, without causing significant cytotoxicity. Moreover, some published nanotoxicity studies reported characteristics of the particles, using only manufacturer's data without investigators confirming the characteristics or using single analytical tool which provides limited information about the particle-type being studied [38, 40-42]. This brings in the importance of adequate physicochemical characterization of AgNPs prior to undertaking toxicity assessments studies. In addition, a standardized measurement approach like the application of validated methods and use of reference materials specific to AgNPs, needs to be more developed in order to assure the comparability of results among toxicity studies using similar AgNPs.

1.2.2 AgNPs physicochemical properties

Size is an important property that influence the NPs uptake and effect. In this regard, a review study reported that the common sizes of AgNPs used in general applications range from 1 to 10 nm [43]. The reason behind this is smaller particles displayed better antimicrobial and cytotoxic activity as demonstrated in various studies [41, 44, 45]. Furthermore, as the particle size gets smaller, the specific surface area increases and hence greater proportion of its atoms are displayed on the surface [3]. This implies that for the same mass of a NP, biological interactions and toxicity are more dependent on particle number and surface area than by particle mass. The properties of AgNPs can be further enhanced by functionalization of the NPs by using various coatings which in turn influences NPs' surface charge, solubility, and/or hydrophobicity. There are considerable literatures that suggests fate and toxicity of AgNPs are determined by the types of coating [46, 47]. Various types of surface coatings applied to AgNPs, particularly to improve their biocompatibility and stability against agglomeration are trisodium citrate (CT-AgNP), sodium bis(2-ethylhexyl) sulfosuccinate, cetyltrimethylammonium bromide, polyvinylpyrrolidone (PVP-AgNP), poly(L-lysine), bovine serum albumin, Brij 35 and Tween 20 [48]. Among the latter, CT- and PVP- coating are the most commonly used as stabilizing agent [43]. Furthermore, the coating also modifies their charge which again influence the toxic effect in cells. For example, positively charged NPs are considered more suitable drug delivery tool for anticancer drug as they can stay for a long time in the blood stream compared to negatively charged particles [9]. Shape-dependent effects were also reported in studies using varying size AgNPs. For instance, silver nanocubes showed greater antibacterial effect against *E.coli* compared to spheres and wires in a study

using 55 nm AgNPs [49]. Pal. S *et al.* [50] also successfully demonstrated a shape dependent interaction with *Escherichia coli* where truncated triangular had stronger biocidal action than spherical and rod shaped AgNPs. Contrarily, Actis *et al.* [51] reported no biocidal effect on *Staphylococcus aureus* using spherical, triangular and cuboid AgNPs. Cellular uptake and biological responses are also defined by the agglomeration state of NPs and there are sufficient evidences that interaction of the AgNPs with biological media and biomolecules can lead to particle agglomeration as well as aggregation [52, 53]. Though easy penetration of agglomerated AgNPs in mesenchymal stems cells and nuclei were reported in several studies, reduced cytotoxicity were also evident with agglomerated particles compared to free AgNPs [52, 54]. A good amount of research has also been conducted on various types of surface corona resulting from interfacial interactions between AgNPs and biological fluid [55]. This included studies involving both single and complex molecule protein coronas like bovine and human serum albumin, tubulin, ubiquitin, fetal bovine serum etc [56]. The formation of corona depending on composition have shown to interfere with the AgNPs dissolution to Ag ions and thus toxicity [56]. Researchers also successfully established the importance of various AgNPs formulation during synthesis with respect to biomedical applications [57]. For example, loading of AgNPs inside multiwalled carbon nanotubes demonstrated improved targeting of AgNPs to sperm cells and hence potential for development as diagnostic tool for the infertility management [58]. Similarly, Bilal *et al.* [59] synthesized AgNPs loaded chitosan-alginate construct which interestingly showed excellent biocompatibility to normal cell line (L929) and cytotoxicity to cancer cells (HeLa cells). Azizi *et al.* [60] formulated albumin coated AgNPs with the aim of developing new anticancer agents and showed that the latter was taken specifically by tumor cells and induced apoptosis.

1.2.3 AgNPs application and mechanism of action

Among various metal salts and NMs that are known to be effective in inhibiting the growth of many bacteria, AgNPs are accounted for their strong inhibitory and bactericidal effects [61, 62]. The use of AgNPs as well as Ag salts in catheters, cuts, burns and wounds to protect them against infection have been well established [63-66]. However, the exact mechanism underlying the antimicrobial effects of AgNPs is still unresolved, though literature suggests that these particles can interact with the membranes of bacteria [67, 68]. A potential pathway proposed is AgNPs, on interaction with bacteria, induce reactive oxygen species and free radicals damaging the intracellular organelles and modulating the intracellular signaling pathways towards apoptosis [69]. Another widely accepted mechanism of bacterial cytotoxicity is adhesion of AgNPs to bacterial wall, followed by infiltration of the particles, bacterial cell membrane damage leading to leakage of cellular contents and death [67, 70]. In this context, the antimicrobial activity assessment of small sized AgNPs (12 nm) by Das *et al.* [71] demonstrated these NPs to be excellent inhibitors against both Gram positive and Gram negative bacteria including, *Staphylococcus Basillus*, *Staphylococcus Aureus*, and *Pseudomonas Aeruginosa*. This indicate that both membrane thickness and surface charge facilitates particle attachment onto the cell membrane [72]. Finally, large surface area of AgNPs releasing silver ions (Ag^+) is another crucial factor contributing to the cytotoxic activity. As it is well established, smaller AgNPs have a faster rate of Ag^+ dissolution in the surrounding microenvironment due to their larger surface area to volume ratio, and hence results in increased bioavailability, enhanced distribution, and toxicity of Ag compared with larger ones [73, 74]. Furthermore, Ag^+ ions release rate is dependent on number of

factors including size, shape, concentration, capping agent and colloidal state of NPs [75, 76]. In particular, the rate of Ag⁺ ion release was shown to be associated with the presence of chlorine, thiols, sulfur, and oxygen [77]. Released Ag⁺ ions are suggested to interact with respiratory chain proteins on the membrane, interrupt intracellular O₂ reduction, and induce ROS production causing cellular oxidative stress in microbes and death [78]. AgNPs are also familiar for their antifungal, antiviral and anti-inflammatory activity [76]. Several studies reported potent anti-fungal activity of AgNPs against several phytopathogenic fungi (e.g. *Alternaria alternate*, *Sclerotinia sclerotiorum*, *Macrophomina phaseolina*, *Rhizoctonia solani*, *Botrytis cinerea* and *Curvularia lunata*) as well as human pathogenic fungi (e.g. *Candida* and *Trichoderma sp*) [79, 80]. Likewise, AgNPs have demonstrated efficient inhibitory activities against several viruses including human immunodeficiency virus, hepatitis B virus, herpes simplex virus, human parainfluenza virus, peste des petits ruminants virus and bean yellow mosaic virus, a plant pathogenic virus [81-85]. Inflammation is an early immunological response against foreign particles by tissue and interestingly, AgNPs have been recently recognized to play important role as anti-inflammatory agents. Studies evaluating the anti-inflammatory effect of AgNPs showed significant reduction in wound inflammation, modulation of fibrogenic cytokines, down regulation of pro-inflammatory cytokines and apoptosis in inflammatory cells [65, 86, 87].

1.2.4 Routes of exposure and biodistribution

The major routes of entry of NPs are ingestion, inhalation, dermal contact and, directly in systemic circulation via intraperitoneal (i.p.) or intravenous (i.v.) injection [22]. The various mode of exposure to AgNPs, their biodistribution and mechanisms

underlying the effects is illustrated in Figure 1. As AgNPs are extensively used in various household and biomedical products, the following section would discuss the various potential routes of entry of these NPs.

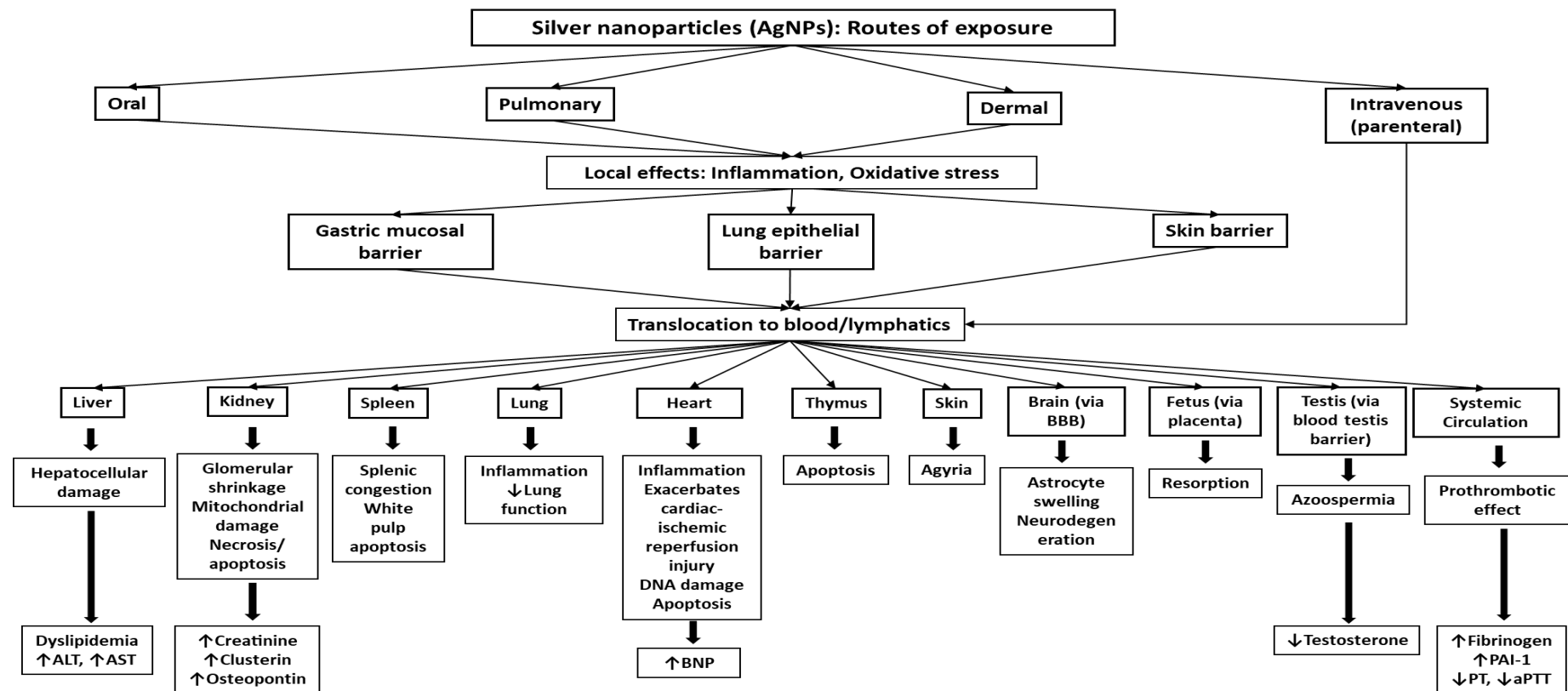


Figure 1: Schematic representation of biodistribution and toxicity of silver nanoparticles (AgNPs) following various routes of exposure. After their exposure, AgNPs are able to induce inflammation and oxidative stress at the site of exposure. Moreover, they can cross various biological barriers and enter the systemic circulation. Intravenously administered AgNPs are directly available in the circulation. Then onwards, AgNPs are distributed to various organs and cause organ specific pathophysiological effects. It remains to establish whether the effects observed in the distant organs are due to direct impact of the translocated AgNPs or ions and/or particle-induced inflammatory and oxidative stress response at the site of exposure.

1.2.4.1 Respiratory exposure

The release of AgNPs in the environment during manufacture, washing or disposal of products enables the NPs to enter the human respiratory system through inhalation [88]. Exposure assessment in a NMs manufacturing facility, showed significant release of AgNPs during processing as soon as the reactor, dryer and grinder were opened, leading to a potential occupational exposure even for wet production processes [89]. Similar studies evaluating workplace exposure and health hazard have reported that concentrations of AgNPs in the processes of manufacturing and integration of AgNPs into various consumer products can reach up to $1.35 \mu\text{g}/\text{m}^3$ [90, 91]. Several healthcare, hygiene and antibacterial spray products containing AgNPs have now entered in our daily use. Nazarenko *et al.* [92] and Lorenz *et al.* [93] reported that, use of nanotechnology based consumer sprays containing AgNPs, can lead to the generation of nanosized aerosols and the release of NPs near the human breathing zone. Furthermore, Ag-treated textiles can be a source of AgNPs in the washing solution when laundering fabrics, regardless of either conventional Ag or nano Ag treatment [94]. A recent study, evaluating the effluent from a commercially available silver nanowashing machine showed that AgNPs at an average concentration of $11 \mu\text{g}/\text{L}$ was released in the environment [95]. AgNPs with maximum concentration of $145 \mu\text{g}/\text{L}$ was also reported to be released from the outdoor paints during the initial runoff events [96]. An occupational study in silver manufacturing plant revealed that AgNPs in the air increases during production and peak area concentration of more than $290 \mu\text{g}/\text{m}^3$ can be been detected [90]. The authors suggested the possibility for workers to be exposed to airborne AgNPs at concentrations ranging from 0.005 to $0.289 \text{ mg}/\text{m}^3$. In spite of considerable studies evaluating pulmonary exposure and toxicity, there is still a lack of long-term toxicity

data, consumer exposure data, and human health effect of AgNPs information. Nevertheless, an occupational exposure limit of $0.19 \mu\text{g}/\text{m}^3$ for AgNPs, have been proposed recently based on a subchronic rat inhalation toxicity study and taking in consideration the human equivalent concentration with kinetics [97]. Following inhalation, the transport and deposition of NPs is not uniform and is influenced by several factors including flow rate, structure of airway, pulmonary function, age and most importantly, the particle size [88]. Particles smaller than $0.1 \mu\text{m}$ have been shown to deposit in lungs and trachea-bronchial region [22, 98]. Consequently, due to deeper particle deposition, the clearance mechanism takes longer leading to prolonged particle-tissue interaction and resulting in more pathophysiological effect [22]. In addition, translocation in blood capillaries is relatively easy for particles with a diameter lower than $0.1 \mu\text{m}$ [22]. The alveolar-capillary barrier consists of a very thin monolayer of epithelial cells, endothelial cells of the capillaries and basement membrane between the two cells, and maintains the homeostasis of the lung [22]. NPs penetration have been demonstrated following damage to the epithelial layer of the alveolar capillary membrane [22, 99].

1.2.4.2 Oral exposure

In the food industry, AgNPs are used in packaging and storage in order to increase the shelf life and quality of the food [100]. Moreover, urban and industrial effluents enter the aquatic ecosystem and accumulate along the trophic chains [101]. Thus, AgNPs in dietary supplements, coated food containers, water contamination or accumulation in food fish and other aquatic organisms provides the potential sources of oral exposure [100]. Recent studies also demonstrated that AgNPs incorporated in food packaging can migrate from packaging into food under several usage conditions

[102, 103]. Inhalation exposure during manufacture also leads ultimately to oral exposure since particles cleared via the mucociliary escalator are swallowed and cleared through the GIT. It is estimated that the amount of daily consumption of silver in humans by ingestion is around 20-80 μg [22]. After ingestion the GIT serves as a mucosal barrier that selectively promotes the degradation and uptake of nutrients such as carbohydrates, peptides, and fats. NPs can act on the mucus layer and translocate to blood stream and consequently access each organ upon crossing the epithelium. It has been reported that the uptake of NPs with a diameter lower than 100 nm occurs mainly by endocytosis in epithelial cells [104]. Within the enterocytes, AgNPs can trigger oxidative stress, DNA damage and inflammations [22].

1.2.4.3 Skin and parenteral exposure

Human exposure to AgNPs may also take place through the skin, the largest organ of the body and first-line of defense between the external environment and internal environment. The potential of solid NPs to penetrate the healthy as well as breached human skin and to diffuse into underlying structures have been well demonstrated [105, 106]. In this context, the use of AgNPs in cosmetics production have been estimated to reach up to 20%. In addition to cosmetics, dermal contact to wound dressings and antibacterial textiles have also shown large diffusion of AgNPs [107]. In the laboratory set up, i.v., i.p., subcutaneous injection enables the AgNPs to directly gain access into systemic circulation. Further, the development of AgNPs based drugs or drug carrier would enable the entry of these particles directly in human circulatory system.

Following exposure, the distribution and toxicity of AgNPs is further discussed broadly under the *in vivo* toxicity section of this introduction. In general, an exposure

and gender related difference, in target tissue AgNPs accumulation were evident in previous researches [108-111]. Next to biodistribution, assessment of clearance behavior of NPs is an important indicator of cumulative toxicity. In this context, there are several studies that have investigated the post exposure clearance kinetics following subacute inhalation, i.v, and oral exposure to various sizes of AgNPs and Ag⁺ ions [111-114]. These studies revealed silver clearance from most organs post recovery period which was 17-days to 4 months. However, tissues with biological barriers like brain and testis exhibited persistence of silver in long term oral exposure studies, suggesting difficulty of the silver to be cleared from these organs [113, 114]. Persistence of silver in these organs also enhances the chances of increased toxicity.

1.2.5 Pathophysiological effects of AgNPs

The immense growth in manufacture of AgNPs based products, owing to their unique physicochemical and functional properties, and their wide application has raised concern about their possible impact on the environment and subsequently human health. Hence, despite the favorable properties of AgNPs the increasing concern about the possible impact has directed researchers to focus on the *in vitro* and *in vivo* toxicity induced by these particles.

1.2.5.1 In vitro effects

In vitro cytotoxicity studies often are used to characterize the biological response to AgNPs and the results of these studies may be used to identify hazards associated with exposure to AgNPs. Some important studies that have shown toxic effect of AgNPs on different cell lines including, macrophages (RAW 264.7), including bronchial epithelial cells (BEAS-2B), alveolar epithelial cells (A549), hepatocytes (C3A, HepG2), colon cells (Caco2), skin keratinocytes (HaCaT), human

epidermal keratinocytes (HEKs), erythrocytes, neuroblastoma cells, embryonic kidney cells (HEK293T), porcine kidney cells (Pk 15), monocytic cells (THP-1) and stem cells [55, 115-124], are discussed below.

Exposure of A549 cells to increasing concentrations of AgNPs for 24 hrs, caused morphological changes including cell shrinkage, few cellular extensions and restricted spreading pattern, and cell death in a dose-dependent manner [125]. In another study using the same type of cell, treatment with 20 nm AgNPs induced DNA damage and overexpression of metallothioneins at a concentration of 0.6 nM up to 48 hrs [126]. Size-dependent changes in cellular morphology was observed in rat alveolar macrophage cell line incubated with hydrocarbon-coated AgNPs of different sizes (15, 30 and 55 nm) [127]. Gliga *et al.* [34] explored the mechanism of toxicity in BEAS-2B cells exposed to CT- AgNPs of different particle sizes (10, 40 and 75 nm) as well as to 10 nm PVP coated and 50 nm uncoated AgNPs. In the latter study, cytotoxicity was evaluated using Almar Blue and lactate dehydrogenase (LDH) assay. The Almar Blue assessed the cell viability and proliferation based on the reduction potential of metabolically active cells. Their results showed cytotoxicity only of the 10 nm particles independently of surface coating, and toxicity observed was associated with the rate of intracellular Ag release, a 'Trojan horse' effect. Nguyen *et al.* [47] exposed macrophage cell line to uncoated (20, 40, 60 and 80 nm) and PVP- AgNPs (10, 50, and 75 nm) and found a cell shrinkage effect due to uncoated particles, whereas cell elongation was evident after treatment with PVP-coated particles. Exposure of BEAS-2B and RAW 264.7 cell lines to 20 and 110 nm PVP- and CT- Ag-AuNPs (AgNPs with a gold core) showed that the 20 nm Ag-AuNPs induced significant reduction in cell viability, in the dose range from 6.25-50 $\mu\text{g/mL}$ for 24 hrs [128]. In addition, significant reactive oxygen species (ROS) generation, intracellular calcium influx and

decline in mitochondrial membrane potential were also demonstrated in 20 nm CT- and PVP- AgNPs and 110 nm CT- AgNPs treated cells. Bastos V. *et al.* [129] also evaluated the cytotoxicity of 30 nm CT- AgNPs on RAW 264.7 cells, using parameters including viability, oxidative stress, and cytostaticity, at 24 and 48 hrs of exposure. Their findings revealed decreased cell proliferation and viability at a concentration of only 75 µg/mL, thereby suggesting low sensitivity of RAW 264.7 cells to lower doses of AgNPs. Recently, Gliga *et al.* [123], using a combination of RNA sequence and functional assays, showed that repeated, low dose (1 µg/ml), long term exposure (6 weeks) of BEAS-2B cells to 10 and 75 nm CT- AgNPs is profibrotic, indicated by upregulation of *TGFβ1* and induce epithelial-mesenchymal transition and cell transformation. These evidences suggest that the observed cellular effects are dose, size, coating and duration of exposure dependent.

Exposure of 20 nm AgNPs to C3A cells, at sublethal concentrations (1.95 µg/10⁶ cells), revealed size dependent cytotoxicity indicated by elevated LDH, increased release of inflammatory proteins (interleukin (IL) 8, tumor necrosis factor (TNF) α, oxidative stress and decrease in albumin synthesis [130]. Cell viability were also evaluated by 3-(4,5-dimethylthiazol-2-yl)-2,5-diphenyl tetrazolium bromide (MTT) assay, a colorimetric assay measuring cell metabolic activity based on NADPH-dependent cellular oxidoreductase enzymes, in human hepatoblastoma HepG2 and mice primary liver cells. Interestingly, AgNPs caused a concentration dependent decrease of cell viability in both cell types [131]. A study by Xue *et al.* [132] in HepG2 cells demonstrated that AgNPs are able to cause time (24 and 48 hrs) and dose dependent (40, 80, 160 µg/ml) decrease in cell viability and induce cell-cycle arrest in the G2/M phase, significantly increasing the apoptosis rate and ROS generation. Similar study using PVP and CT- AgNPs at concentration of 1-100 mg/L

also showed coating (CT causing more effect than PVP) and dose dependent reduction in cell viability along with inhibition of albumin synthesis, decrease in alanine transaminase activity and apoptosis in HepG2 cells indicating therapeutic potential of the AgNPs against hepatic cancer [133]. Intestinal cells treated with Ag showed induction of cytokine release and higher genotoxicity compared to other inorganic metallic NPs (TiO₂ and silicon dioxide) [134]. Böhmert *et al.* [135] analyzed the toxicity of AgNPs with a primary size of 7.02 ± 0.68 nm in Caco-2 cells using NP concentrations between 1 and 100 µg/ml. Partial aggregation between digested and not-digested particles was observed by field fractionation (A4F) combined with DLS and X-ray dispersion at small angles. The authors concluded that AgNPs entered the GIT barrier without forming large aggregates in digestive fluids. These results confirmed the importance of body fluids on NP behavior and toxicity.

Samberg *et al.* [136] assayed the potential cytotoxicity of AgNPs in HEKs cells, following 24 hrs exposure and reported that unwashed and uncoated AgNPs caused significant dose-dependent decrease of HEK cell viability and increase in inflammatory cytokines, whereas washed and carbon-coated AgNPs did not induce any effect. Moreover, *in vitro* percutaneous penetration of Ag study revealed the accumulation of Ag and silver chloride aggregates of size less than 1 µm both in the epidermis and dermis [137].

NPs readily enters systemic circulation and may interact with circulatory components like blood cells, heart and blood vessel [138-140]. The potential impact of AgNPs on hemolysis, platelet activity and coagulation associated with human exposure have recently gained an interest. Studies using human erythrocytes have investigated the effects of AgNPs on hemolysis, morphology and their uptake [139,

141]. In our recent *in vitro* study, we assessed the effect of coating and dose of AgNPs on oxidative damage and eryptosis on mouse erythrocytes [118]. Both PVP and CT-AgNPs induced oxidative stress and increased cytosolic calcium, annexin V binding and calpain activity. The latter data may explain the mechanism of hemolysis and eryptosis induced by AgNPs. These NPs could also prevent platelet responses as evidenced by the inhibitory effects of AgNPs of different sizes (13-15 nm, 30-35 nm and 40-45 nm) on platelet aggregation [142]. Conversely, *Bian et al.* [143] recently compared the AgNPs (<100 nm) with Ag macro particle (5-8 μm) and showed that the former can promote phosphatidylserine (PS) exposure and microvesicles generation in freshly isolated human erythrocytes, mainly through ROS generation and intracellular calcium increase and hence suggesting that AgNPs may have prothrombotic risks by promoting procoagulant activity of RBCs, more importantly at non-hemolytic concentrations ($\leq 100 \mu\text{g/mL}$). These discrepancies in results, though not fully understood, could be related to different cell type used in the studies. The various blood biological effects of AgNPs, such as, hemolysis, interference on plasma coagulation, enhancement of platelet aggregation and inhibition of lymphocyte proliferation, are size, coating and concentration dependent [118, 144, 145]. *Lin et al.* [146] studied the potential toxicity of AgNPs on cardiac electrophysiology. The particles caused concentration dependent (10^{-9} - 10^{-6} g/ml) depolarization of resting membrane potential, diminished action potential and subsequently led to loss of excitability in mice cardiac papillary muscle cells *in vitro*. *Milic M et al.* [120] investigated the interaction of CT-AgNPs (13-61 nm) with porcine kidney (Pk15) cells, and compared the effect of the particles to ionic form. Both forms of silver, concentration (1-75 mg/l) dependently decreased the viability of Pk15 cells after 24 hrs.

Furthermore, AgNPs exhibited increased toxicity in stem cells which were attributed to their properties such as size, concentration and coating. For eg., the biocompatibility of 100 nm AgNPs was tested in human mesenchymal stem cells (hMSCs) by Greulich C *et al.* [147] and there was a dose (0.5-50 µg/ml) dependent effect on cytotoxicity exhibited by decreased cell proliferation and chemotaxis. In addition, He W *et al.* [148], showed increased LDH release and ROS production and reduction in both cell viability and mitochondrial membrane potential in hMSCs exposed to 30 nm AgNPs. Murine spermatogonial stem cells showed less cell viability, LDH leakage, and prolonged apoptosis after exposure to 15 nm AgNPs at concentrations of 5, 10, 25, 50, and 100 µg/ml [149]. Similarly, neural stem cells showed an increase in cell death, LDH leakage, induction of ROS, upregulation of pro-apoptotic Bax protein, and increased in apoptosis when exposed to various concentrations (0.01-80 µg/mL) of PVP- Ag-NPs [150]. In the latter study, AgNPs induced neurotoxicity was compared to Ag⁺ ions, and the authors demonstrated that AgNPs caused cell apoptosis by inducing intracellular ROS generation coupled with JNK phosphorylation while Ag ions caused cell necrosis via altering the cell membrane integrity and binding with cellular thiol groups directly.

Results of the *in vitro* studies indicated that AgNPs are toxic to the mammalian cells derived from skin, liver, lung, brain, vascular system and reproductive organs [151]. Cytotoxicity of AgNPs depends on their size, shape, surface charge, coating/capping agent, dosage, oxidation state, agglomeration and the type of pathogens against which their toxicity is investigated [45, 115, 152, 153]. Despite the number of studies, the toxicological mechanism is still unclear. Several studies reported DNA damage and apoptosis induced by NPs. In this context, AgNPs were shown to cause apoptosis in mouse embryonic stem cell [154]. A follow up by the

same group also demonstrated involvement of AgNPs in activation of apoptotic markers, caspase 3 and caspase 9, at concentration of 50 and 100 $\mu\text{g}/\text{mL}$ [155]. DNA damage at concentration of 0.1 $\mu\text{g}/\text{mL}$ of AgNPs, was also reported in a study investigating the chromosomal aberration in human mesenchymal cells [156]. Furthermore, the potential of AgNPs to induce genes associated with cell cycle progression, cause chromosomal damage, cell cycle arrest and cell death in human cells BEAS-2B, umbilical vein endothelial cells and hepatocellular liver carcinoma cells, at various concentrations were also reported [151]. In spite of these numerous studies, a major limitation of the *in vitro* study in hazard identification with respect to human health, is related to the doses used in the *in vitro* study which may not be comparable to realistic exposure doses in human. Hence, this necessitates *in vivo* toxicity research which are presented in the following section based on the potential routes of exposure.

1.2.5.2 In vivo toxicity

In vivo biodistribution and toxicity studies in rats and mice have demonstrated that AgNPs administered by inhalation, ingestion, i.v., or i.p. injection were subsequently detected in blood and caused toxicity in several organs including lung, liver, kidney, intestine and brain [157-159].

Inhalation is a proposed major route of exposure not only during manufacturing of Ag containing materials but also during use of aerosolized products. Table 2 and 3 summarizes the important toxicity and biodistribution studies of AgNPs in rodents following pulmonary exposure via inhalation and intratracheal (i.t.) instillation, respectively. The data from these studies showed diverse outcomes related to biodistribution and remote organ toxicity. Some studies showed no induction of

adverse effects [160, 161], while other studies reported adverse effects varying from a minimal inflammatory response to the presence of inflammatory lesions in the lungs [110, 111, 162, 163]. For instance, a 28-days inhalation toxicity study on rats showed no significant changes in the haematology and blood biochemistry in either the male or female rats following 11-14 nm AgNPs at concentration of $1.73 \times 10^4/\text{cm}^3$, $1.27 \times 10^5/\text{cm}^3$ and 1.32×10^6 particles/ cm^3 [161]. Hyun *et al.* [164] also exposed rats to 12-15 nm AgNPs for similar duration and doses and showed no remarkable histopathological changes in the nasal cavity and lung, in the NPs exposed group compared to the control group. Nevertheless, Lee *et al.* [165] found that a short term (14 days) nose only exposure of mice to 20 nm AgNPs at concentration of 1.91×10^7 particles/ cm^3 led to alterations in brain gene expression. Sub-chronic (90 days) inhalation studies exhibited mild, dose-dependent pulmonary inflammation and alterations in pulmonary function in rats exposed to 18 nm AgNPs [163]. In addition, inhaled AgNPs may also enter the systemic circulation to become distributed to extra-pulmonary organs such as the liver and brain as demonstrated in studies using ~15 nm NPs at concentrations of $1-3 \times 10^6$ particles/ cm^3 [161, 166]. A 90 days inhalation study by Sung *et al.* showed alterations in lung function and inflammatory responses in 18 nm AgNPs exposed rats [163]. Additionally, accumulation of Ag in lungs and liver were more evident in rats after 90 days of inhalation [110]. Silver accumulation have been also observed in brain, olfactory bulb, kidney and spleen [110, 167, 168]. Moreover, AgNPs (18-20 nm) have also been shown to reach and cross mouse placenta in an inhalation study, where pregnant females were exposed to freshly produced aerosols for either 1 or 4 hrs/day, during the first 15-days of gestation, at a particle number concentration of 3.80×10^7 part/ cm^3 [169].

Table 2: Toxicity and distribution of AgNPs following pulmonary exposure in rodents via inhalation.

Size	Dose	Model	End-point measurement	Effect	Tissue accumulation	References
11-14 nm	1.73 x 10 ⁴ /cm ³ (low dose), 1.27 x 10 ⁵ /cm ³ (middle dose), (1.32 x 10 ⁶ particles/cm ³ (high dose)	Sprague–Dawley rats	Inhalation 6 h/day, 5 days/wk, for 4 wk, sacrificed 1-day post last exposure	AgNPs concentration below the American Conference of Governmental Industrial Hygienists silver dust limit (100 µg/m ³) did not produce significant toxic effects	Lu, Li, Br, Ob	[161]
18 nm	0.7 × 10 ⁶ particles/cm ³ (low dose), 1.4 × 10 ⁶ particles/cm ³ (middle dose), and 2.9 × 10 ⁶ particles/cm ³ (high dose)	Sprague–Dawley rats	Inhalation 6h/day, 5 days/wk, for 90 days, sacrificed 1-day post last exposure	Subchronic exposure to AgNPs compromised the lung function	N/A	[163]
18 nm	0.6 × 10 ⁶ particle/cm ³ , 49 µg/m ³ (low dose), 1.4 × 10 ⁶ particle/cm ³ , 133 µg/m ³ (middle dose) and 3.0 × 10 ⁶ particle/cm ³ , 515 µg/m ³ (high dose)	Sprague–Dawley rats	Inhalation 6 h/day, 5 days/week, for 90 days, sacrificed 1-day post last exposure	Silver accumulation in kidney was gender dependent. Dose-dependent increase of bile duct hyperplasia in AgNP exposed liver	Lu, Li, Br, Ob, Ki	[110]
10 nm	3.3 ± 0.5 mg/m ³ or 31 µg/g lung	Male C57Bl/6 mice	Inhalation 4h/day, 5 days a week, for 10 days, sacrifice at 1 hr and 21-days post last exposure	Subacute inhalation of AgNPs induced minimal pulmonary toxicity	Lu	[162]

Table 2: Toxicity and distribution of AgNPs following pulmonary exposure in rodents via inhalation (cont'd).

Size	Dose	Model	End-point measurement	Effect	Tissue accumulation	References
15 nm; 410 nm	179 $\mu\text{g}/\text{m}^3$ and 167 $\mu\text{g}/\text{m}^3$ or 7.9×10^6 particles/ mm^3 and 118 particles/ mm^3 for 15 and 410 nm, respectively	Male Fischer rats	Inhalation 6h/day, 4 consecutive days, sacrifice at 1- and 7-days post exposure	Size dependent effect on pulmonary toxicity after inhalation of similar mass concentration of 15 and 410 nm AgNPs	Lu, Li	[168]
15 nm	8, 28 μg	Brown-Norway and Sprague-Dawley rats	Inhalation 3h for 1 day or 3h for 4 days. Sacrifice at 1 and 7-days post last exposure	AgNPs induced an acute pulmonary neutrophilic inflammation with the production of proinflammatory and pro-neutrophilic cytokines	Lu	[170]
20 nm; 110 nm (CT)	7.2 ± 0.8 mg/m^3 and 5.3 ± 1.0 mg/m^3 or 86 and 53 $\mu\text{g}/\text{rat}$ for C20 and C110 nm, respectively	Male Sprague-Dawley rats	Inhalation 6h/1day, sacrifice at 1, 7, 21, 56 days postexposure	Delayed peak and short-lived inflammatory and cytotoxic effects in lungs with greater response due to smaller sized nanoparticles	N/A	[171]
18-20 nm	3.80×10^7 part./ cm^{-3}	Female C57BL/6 mice	Inhalation for 1 hr/day or 4 hrs/day, for first 15 days of gestation, sacrificed 4 hrs post last exposure	Increased number of resorbed fetuses associated with reduced oestrogen levels, in the 4 hrs/day exposed mothers	Lu, Sp, Li, Pl	[169]

Table 3: Toxicity and distribution of AgNPs following pulmonary exposure in rodents via intratracheal instillation.

Size	Dose	Model	End-point measurement	Effect	Tissue accumulation	References
20 nm; 110 nm (PVP & CT coated)	0.5, 1 mg/kg	Male Sprague– Dawley rats	Single i.t. instillation, sacrifice at 1, 7- and 21- days post exposure	Coating and size dependent AgNPs retention in lungs. PVP coated AgNPs had less retention over time and larger particles were more rapidly cleared from large airways than smaller particles	Lu	[172]
20 nm; 110 nm (PVP & CT coated)	0.1, 0.5, 1 mg/kg	Male Sprague– Dawley rats	Single i.t. instillation, sacrifice at 1, 7- and 21- days post exposure	Smaller sized AgNPs produced more inflammatory and cytotoxic response. Larger particles produce lasting effects post 21 days instillation	N/A	[173]
20 nm (CT capped)	1 mg/kg	Male Sprague– Dawley rats	Single i.t. instillation, sacrifice at 1- and 7-days post exposure	AgNP resulted in exacerbation of cardiac ischcemic- reperfusion injury	N/A	[174]
50 nm; 200 nm (PVP coated)	0.1875, 0.375, 0.75, 1.5, 3 mg/kg	Female Wistar rats	Single i.t. instillation, sacrifice at 3- and 21-days post exposure	Focal accumulation of Ag in peripheral organs along with transient inflammation in lung	Li, Sp, Ki	[167]

Table 3: Toxicity and distribution of AgNPs following pulmonary exposure in rodents via intratracheal instillation (cont'd).

Size	Dose	Model	End-point measurement	Effect	Tissue accumulation	References
20 nm; 110 nm	1 mg/kg	Male Sprague–Dawley rats	Single i.t. instillation, sacrifice at 1- and 7-days post exposure	Both sizes of AgNP resulted in exacerbation cardiac I/R injury 1 day following instillation independent of capping agent. Persistence of injury was greater for 110 nm PVP capped AgNP following 7 days instillation	N/A	[175]
50 nm; 200 nm (PVP, CT coated)	0.05, 0.5, 2.5 mg/kg	Female Balb/C mice	Single i.t. instillation, sacrifice 1-day post instillation	Size, dose and coating dependent pro-inflammatory effects in healthy and sensitized lungs following pulmonary exposure to AgNPs	N/A	[107]
10 nm	0.05, 0.5, 5 mg/kg	Balb/C mice	Single i.t. instillation, sacrifice at 1- and 7-days post exposure	Oxidative stress, DNA damage, apoptosis in heart. Prothrombotic events and altered coagulation markers	N/A	[176]

In several cases, a gender-dependent difference for AgNPs accumulation in kidneys has been reported, with females exhibiting a higher concentration than males [108, 163, 177]. One possible explanation for the sex differences in the distribution of Ag may be hormonal regulation in the rat kidney [39]. Gender-dependent difference was also reported in terms of persistence of pulmonary inflammation and decrease in lung function in male rats following termination of exposure, while females showed gradual improvement in lung inflammation following cessation of exposure [111]. However, the exact mechanism of sex related differences is still not clear.

The potential mechanisms of the cardiovascular effects of lung deposited particles have been previously discussed by Nemmar *et al.* [178]. In this context, Holland *et al.* [174] investigated the effect of 20 nm AgNPs on cardiovascular injury and showed exacerbation of cardiac ischemic-reperfusion injury following single i.t. instillation in rats. The authors further evaluated the impact of size (20 and 110 nm) and coating (PVP and CT) of AgNPs and demonstrated that the acute effect was size and coating independent, whereas the persistence of injury was greater for 110 nm PVP- AgNPs [175]. A significant dose dependent effect of pulmonary exposed PVP- and CT- AgNPs on cardiovascular homeostasis was also demonstrated in our recent study [176]. The mechanism through which lung injury occurs and how the physicochemical properties of inhaled AgNPs affect their interactions with the lung have recently began to be investigated *in vivo*. [107, 168, 172, 173]. For instance, a greater pulmonary inflammatory response was observed with instillation of 20 nm size than a 110 nm size but with little influence imposed by CT or polyvinyl phosphate-capping in rats [179]. In addition, i.t. instillation of 5-150 μg AgNPs (50 nm) caused a reversible inflammation while 300 μg led to DNA damage, accelerated cell proliferation and progressively increased numbers of neutrophilic granulocytes in rat

lungs [167]. Along with the *in vitro* studies, *in vivo* results suggest that size, coating and dose affect pulmonary inflammation and cellular toxicity.

As mentioned above, besides respiratory exposure, consumer exposure to AgNPs via ingestion can also occur due to incorporation of AgNP into products such as food containers and dietary supplements. Table 4 summarizes the important toxicity and biodistribution studies of AgNPs in rodents via oral exposure. The deposition of orally exposed AgNPs in the GIT has been widely demonstrated in previous studies [39, 180]. Jeong *et al.* [181] showed an increase of goblet cells in the intestine, together with high mucus granule release in mice treated with AgNPs (60 nm), orally, at a concentration of 30 mg/kg bw/day for 28-days. In addition, AgNPs (5-20 nm) orally administered for 21-days in mice (20 mg/kg of BW) disrupted epithelial cell microvilli and intestinal glands [113]. Distribution of PVP- AgNPs (14 nm) to multiple organs including intestine, liver, kidney, lung and brain following oral administration have been reported [180]. Several other investigators also showed that oral exposure to AgNPs may lead to liver, intestinal and neuronal damage [159, 182, 183]. Cases of argyria, a condition characterized by irreversible gray or bluish gray pigmentation of the skin, and irreversible neurologic toxicity and death have been reported upon long-term ingestion of colloidal silver [184]. Liver appears to be a major accumulation site of circulatory AgNPs [157]. In fact, PVP- AgNPs (20-30 nm) have been shown to increase oxidative stress, enhance autophagy and deplete insulin signaling pathway following oral exposure for 90-days in the liver of male rats [159]. Changes in blood parameters indicated by significant elevation of alanine transaminase (ALT) and aspartate transaminase (AST) and hepatotoxicity, shown by histological damages (necrosis, hepatocytic inflammation, and resultant aggregation of lymphocytes in liver tissue, were also observed in study evaluating toxic effect of 14-days orally exposed

AgNPs (40 nm) at doses 20 and 50 ppm in Balb/C mice [185]. Moreover, Tiwari *et al.* [186] determined the effect of 60-days AgNPs (10-40 nm) treatment on kidneys of female Wistar rats at doses of 50 ppm and 200 ppm and demonstrated significant mitochondrial damage, increased levels of serum creatinine and early toxicity marker such as KIM-1, clusterin and osteopontin.

Table 4: Toxicity and biodistribution of AgNPs in rodents via oral exposure.

Size	Dose mg/kg	Model	End-point measurement	Effect	Tissue accumulation	References
56 nm	30, 125, 500	F344 rats	Daily exposure for 90 days, sacrifice 24 hrs post last exposure	Accumulation of silver in kidneys was gender dependent, with 2-fold increase in female kidneys. Liver is the target of silver toxicity for both male and female rats.	Li, Ki, Br, Lu, Bl	[109]
15 nm; 20 nm	90	Male Sprague Dawley rats	Daily exposure 28 days, sacrifice 24 hrs, 1 week, 8 weeks post last exposure	Main target organ for AgNPs and AgNO ₃ upon oral exposure are the liver and spleen. Silver was cleared from all organs after 8 weeks post dosing except brain and testis	Li, Sp, Te, Ki, Br, Lu, Bl, Blr, Ht	[113]
20 nm	820	Male Sprague Dawley rats	Daily exposure for 81 days, sacrifice 24 hrs post last exposure	AgNPs induces liver and cardiac oxidative stress and mild inflammatory response in liver	N/A	[187]
20 nm; 110 nm	10	Pregnant Sprague Dawley rats	Single exposure, sacrificed at 24 hrs and 48 hrs post exposure	Silver enters and crosses placenta regardless of route and form of silver	Ce, LI, Pl, Ki, Bl	[188]

Table 4: Toxicity and biodistribution of AgNPs in rodents via oral exposure (cont'd).

Size	Dose mg/kg	Model	End-point measurement	Effect	Tissue accumulation	References
20, nm; 110 nm (PVP and CT coated)	0.1, 1, 10	Male C57BL/6NCrl mice	3-days exposure, sacrifice at 1- and 7-days post exposure	Acutely ingested AgNP, irrespective of size or coating, are well-tolerated in rodents even in markedly high doses and associated with predominant fecal accumulation	Absence of tissue accumulation	[189]
10 nm; 75 nm; 110 nm	9, 18, 36	Sprague Dawley rats	Daily exposure for 13-weeks. Sacrifice 24-hrs post last exposure	Silver accumulation in tissues showed size dependent relationship 10>75>110. Statistically significant difference in distribution and accumulation of silver in male and female rats. No toxic effect on blood, reproductive and genetic system tested was observed	Ki, Sp, Li, Ht, Ut	[39]
91.71 ± 1.6 nm	0.5	Male Wistar rats	Daily exposure for 45-days, sacrificed 24-hrs post exposure	AgNPs caused significant oxidative stress compared to TiO ₂ NP _s with similar dose concentration	Bl, Li, Ki	[190]

Table 4: Toxicity and biodistribution of AgNPs in rodents via oral exposure (cont'd).

Size	Dose mg/kg	Model	End-point measurement	Effect	Tissue accumulation	References
20-30 nm (PVP coated)	50, 100, 200	Male Sprague Dawley rats	Daily exposure for 90-days, sacrifice 24hrs post last exposure	Though AgNPs accumulated in hepatic and ileum cells, no harmful effects in liver and kidney, as well as no histopathological, hematological and biochemical markers changes was observed	Il, Li, Ki, Br, Th, Spl	[191]
20-30 nm (PVP coated)	50, 100, 200	Male Sprague Dawley rats	Daily exposure for 90-days, sacrifice 24-hrs post last exposure	High dose showed an increase of sperm morphology abnormalities	N/A	[192]
10 ± 4 nm (CT capped)	0.2	Male Wistar rats	Daily exposure for 14-days, sacrifice 24 hrs post exposure	Prolonged low dose AgNPs exposure induced oxidative stress in brain but not in liver	N/A	[193]
20-30 nm (PVP coated)	50, 100, 200	Male Sprague Dawley rats	Daily exposure for 90-days, sacrifice 24-hrs post last exposure	High dose of AgNPs induced hepatocellular damage by increased ROS production, enhanced autophagy and depleted insulin signaling pathway	N/A	[159]

The use of AgNPs in wound dressings and other applications designed to regulate skin microbiome composition is an established strategy that has been shown to inhibit a broad range of bacteria, including *Pseudomonas aeruginosa*, *Escherichia*

coli and *Staphylococcus aureus* [61, 87]. Numerous reports indicate that AgNPs promote wound healing by decreasing the inflammatory response [194, 195]. Nevertheless, an aspect that remains sparsely researched is the possibility of sensitization of the skin by these NPs. It is well known that patients with wounds are at particular risk of developing either an allergic or irritant contact dermatitis, and silver compounds are widely used in wound care. Yet so far there has only been very few confirmed case of contact dermatitis secondary to silver-containing wound products like silver sulfadiazine and skin marker containing silver nitrate [196, 197]. Contrary, there are considerable evidence for significant transdermal penetration of AgNPs into capillaries during use of surgical dressings, textiles or cosmetics [198, 199]. In order to elucidate the mechanism of cytotoxicity, Samberg *et al.* [136] evaluated the potential ability of AgNPs to penetrate porcine skin and showed focal inflammation and localization of AgNPs on the surface and in the upper stratum corneum layers of porcine skin. Acute and sub-acute dermal studies conducted by Korani *et al.* [6], suggested a correlation between dermal exposure, tissue accumulations of AgNPs (100 nm) and dose-dependent histopathological abnormalities in skin which was exhibited by reduced thickness of papillary layer and epidermis. Compared to animals treated with single dose, animals that were subjected to sub-chronic exposure, showed considerable accumulation of AgNPs in other like liver and lung and dose dependent toxic response in several organs including spleen, liver and skin [200].

Other potential route of AgNPs entry in case of biomedical applications includes parenteral administration. A summary of important toxicity and biodistribution studies of AgNP in rodents via exposure of i.v. injection is given in Table 5. In a recent study, comparing the biodistribution and toxicological

examinations after repeated i.v. administration of AgNPs and AuNPs in mice showed more deposition of AgNPs in heart, lung and kidney than AuNPs [157]. Moreover, the AgNPs induced adverse effects in a dose-dependent manner (the concentrations tested were 4, 10, 20, 40 mg/kg) [157]. Another study, following subcutaneous administration of AgNPs of different size, in rats, also revealed that the particles translocated to the blood circulation and distributed throughout the main organs, especially in the kidney, liver, spleen, brain and lung [138]. The results also suggested the potential of AgNPs to cross blood-brain barrier and induce astrocyte swelling and neuronal degeneration [138]. A few studies reported the transfer of AgNPs across placenta in rats and mice [201, 202]. Following i.v. administration of 10 nm AgNPs, at a dose of 66 µg Ag/mouse to pregnant animals on gestational days 7, 8 and 9, Ag accumulation was revealed in all examined organs with highest being in maternal liver, spleen and visceral yolk sac and the lowest concentrations in embryos [201]. Another study comparing the administration methods (i.v. versus i.p.) showed similar localization of Ag in liver and spleen for both methods [202]. However, Ag was quickly excreted from the body with i.v. administration, compared with i.p. administration. The latter study also showed that the AgNPs could cross the placental barrier and the blood-testis resulting in accumulation in fetus and testis, respectively [202].

Table 5: Toxicity and biodistribution of AgNPs in rodents via intravenous injection.

Size	Dose	Model	End-point measurement	Effect	Tissue accumulation	References
15-40 nm	4,10,20,40 mg/kg	Male Wistar rats	32 days i.v, sacrifice 24-hrs post last i.v administration	AgNPs in doses < 10 mg/kg is safe, while > 20 mg/kg is toxic	Li, Ki	[203]
21.8 nm	7.5, 30, 120 mg/kg	ICR mice	Single i.v, parameters measured at 1,7,14-days post injection	Inflammatory reactions in lung and liver cells were induced in mice treated at the high dose of AgNPs. Gender related differences in distribution and elimination of AgNPs, elimination in female is longer than the males.	Sp, Li, Lu, Ki	[204]
20 nm; 200 nm	5 mg/kg	Male Wistar rats	Single i.v, sacrifice at 1, 7, 28-days post i.v administration	High tissue concentration of silver in tissues of 20 nm group as compared to 200 nm groups	Li, Sp, Ki, Lu, Br, Ur, Fe	[158]
7.2 ± 3.3 nm	5,10,45 mg/kg	Male Sprague-Dawley rats	Daily tail vein injection for 3 consecutive days, parameters measured at 1 and 3 rd day	Decrease in body weight and locomotor activity	N/A	[205]
3 ± 1.57 nm	11.4-13.3 mg/kg	Male KunMing mice	i.v. injection 2 times/week for 4 weeks, sacrifice at 1, 28, 56-days post injection	AgNPs preferentially accumulated in all major organs compared to other metallic NPs.	Li, Sp, Ki, He, Lu, Te, Fe, Bl, In, St, Br, SV	[157]

Table 5: Toxicity and biodistribution of AgNPs in rodents via intravenous injection (cont'd).

Size	Dose	Model	End-point measurement	Effect	Tissue accumulation	References
20, nm; 100 nm	0.0082, 0.0025, 0.074, 0.22, 0.67, 2, 6 mg/kg	Wistar rats	28-days, repeated i.v, sacrifice at 24 hrs post last injection	Immune system is the most sensitive parameter affected by AgNPs; reduced thymus weight, increased spleen weight and spleen cell number, strongly reduced NK cell activity, and reduced IFN- γ production were observed	N/A	[40]
20 nm	0.0082, 0.0025, 0.074, 0.22, 0.67, 2, 6 mg/kg	Male Wistar rats	28-days, repeated i.v, sacrifice at 24-hrs post last injection	AgNPs suppress the functional immune system	N/A	[38]
10 nm (CT coated)	1 mg/kg	CD1 mice	IV administration, once every 3 days, sacrifice at 15, 60 120-days post initial exposure	AgNPs induced toxicity to male reproduction, altered Leydig cell function, increased testosterone level	Te	[206]
10 nm; 75 nm; 110 nm (CT coated)	0.1 mg/kg	Female Balb/C mice	Single dose injection sacrifice at 4 hrs, 1, 3 or 7-days post injection. Multi dose: i.v injection on day 1, 4 and 10, sacrifice at 7-days post last injection	Injection of a single dose of AgNPs induced a less toxicity in liver and lung tissues than that induced by multi-dose injections. The toxic effect of AgNPs was time dependent	N/A	[207]

Table 5: Toxicity and biodistribution of AgNPs in rodents via intravenous injection (cont'd).

Size	Dose	Model	End-point measurement	Effect	Tissue accumulation	References
10 nm; 40 nm, 100 nm (PVP or CT coated)	10 mg/kg	Male CD-1 (ICR) mice	Single i.v, sacrifice at 24-hrs post injection	10 nm AgNP group showed increased silver distribution and overt hepatobiliary toxicity compared to larger ones.	Sp, Li, Lu, Ki, Bl, Br	[73]
20 nm; 110 nm	1 mg/kg	Pregnant Sprague Dawley rats	Single exposure, sacrificed at 24-hrs and 48-hrs post exposure	silver crosses the placenta and is transferred to the fetus regardless of the form of silver	Sp, Pl, Li, Lu, Ce, Bl, Ki	[188]
6.3- 629 nm	5 mg/kg	Female Sprague Dawley rats	Single exposure, sacrificed at 24-hrs	Histopathologically AgNPs caused mild irritation in thymus and spleen and significantly increased chromosome breakage and polyploidy cell rates	Lu, Sp, Li, Ki, Th, Ht	[208]
20 nm; 110 nm (PVP or CT)	701.75 μ g/kg	Pregnant female Sprague Dawley rats	Single i.v administration	Exposure to CT- AgNPs, is associated with changes in fetal growth and increased contractile force in both uterine and aortic vessels	N/A	[209]

Chapter 2: Hypothesis, Aims and Objectives

2.1 Hypothesis

Among the various routes of exposure discussed in the introduction section, inhalation through the lung provides a major pathway for the human exposure of AgNPs. The latter is most likely to happen during particle synthesis, handling of dry powders, aerosolization of liquid suspensions, along with the manufacture and machining of composites containing AgNPs. Exposure is also probable beyond the scope of occupational exposure, via the utilization of AgNPs in consumer products such as disinfecting sprays or deodorants which have the potential to directly aerosolize AgNP, which may lead to a direct pulmonary exposure to AgNPs. Furthermore, AgNPs are a dynamic area of research of inhalable therapies for respiratory infections and allergic airway inflammation.

Consequently, pulmonary exposure to AgNPs has received increased attention due to their potential to cause pulmonary injury, cross the alveolar-capillary barrier as NPs or solubilized form, and distribute to remote organs. In this context, though there are considerable studies reporting into how pulmonary exposure to AgNPs may impact pulmonary toxicity, the mechanism by which pulmonary deposited AgNPs may induce pathophysiological effects on the cardiovascular system and other major remote organs (including liver, kidney, spleen and brain) is not well understood. In addition, understanding the interactions of AgNP coating as well as the influence of particle doses at different post-exposure endpoints is an important, yet under investigated, step in understanding the cardiovascular and systemic mechanisms of pulmonary exposure to AgNPs. Furthermore, as AgNPs can translocate from the alveoli into the bloodstream, they can, consequently, interact with erythrocytes and information

regarding the pathophysiological effects and possible mechanism of action of AgNPs on the erythrocytes are still inadequately studied. Hence, we hypothesize that pulmonary deposited AgNPs could alter cardiovascular hemostasis, induce pathophysiological effect on major distant organs, interact with erythrocytes and induce hemolysis and eryptosis.

2.2 Aims and Objectives

The aim of the study was to investigate the following:

i) Coating (PVP and CT), post exposure time (1 day and 7-days) and dose-dependent (0.05, 0.5 and 5 mg/kg) effects of pulmonary exposure to 10 nm AgNPs, on the cardiovascular system.

ii) Coating (PVP and CT) and post exposure time (1 and 7-days) dependent effect of pulmonary exposed 10 nm AgNPs on major distant organs including liver, kidney, spleen and brain.

iii) *In vitro* effects of PVP- and CT- AgNPs (10 nm) at three different doses (2.5, 10, and 40 µg/ml) on mouse erythrocytes *in vitro*.

Chapter 3: Methods

3.1 Research design

In the present study, we, firstly, assessed the effects of pulmonary exposed 10 nm AgNPs on cardiovascular homeostasis. Secondly, we evaluated the biodistribution and pathophysiological effects of 10 nm AgNPs in local and major remote organs including lung, liver, kidney, brain and spleen, following pulmonary exposure. Thirdly, we investigated the *in vitro* effects of AgNPs on mouse erythrocytes.

3.2 Material and Methods

Particles

Suspensions of silver nanoparticles of 10 nm (BioPure™), coated with either PVP or CT were purchased from NanoComposix (San Diego, CA, USA). Details provided by the manufacturer on the physico-chemical properties of the studied AgNPs are reported in Table 6.

Table 6: Main physicochemical properties of tested AgNPs provided by the manufacturer and reported in the datasheet.

	Biopure Silver Nanoparticles	10 nm PVP AgNPs	10 nm CT-AgNPs
	Lot no.	HKE0023	JEA0236
DLS	Mean hydrodynamic diameter (nm)	19	14
UV-Vis	λ_{max} (nm)	390	389
TEM	Diameter (mean \pm SD) (nm)	10.1 \pm 1.8	9.0 \pm 1.7
	Surface area (m ² /g)	53.5	59.0
	Variation coefficient (%)	17.5	19.2
	Mas concentration (mg/ml)	1.08	1.07
	Particle concentration (particles/ml)	1.9E+14	2.6E+14
	Endotoxin level (EU/ml)	<5	<5
	Zeta potential (mV)	-26	-33
	pH of solution	7.4	7.5
	Solvent	MilliQ water	Aqueous 2 mM citrate

For the *in vivo* experiments, AgNPs exposure in Balb/C mice was achieved by single i.t. instillation. As mice are obligate nose breathers, which results in most of the inhaled particles being removed by filtration, we chose i.t. instillation to simulate pulmonary exposure to NPs that enabled controlled and consistent dose deposition, and consequently, accurate determination of dose response [210, 211]. Various cardiac and systemic endpoints were assessed including thrombosis, inflammation, oxidative stress, DNA damage and apoptosis following 1 and 7-days post exposure. For *in vitro* experiments, we evaluated hemolytic, oxidative stress and eryptosis of mouse erythrocytes following 4 hours incubation with 10 nm AgNPs.

The studies are structurally presented along with results and discussions in the following section.

3.3 Study one: Pulmonary exposure to silver nanoparticles impairs cardiovascular homeostasis: effects of coating, dose and time

3.3.1 Background

Of the various routes of introduction, pulmonary exposure to aerosolized particles is a prime concern regarding safety of ENMs. Inhalation exposure of AgNPs can occur at nanosilver-manufacturing industries during particle synthesis, handling of dry powders, as well as during manufacture of AgNPs containing products. In this regard, a study from air samples collected in the injection room of a nano-Ag manufacturing facility showed that it is possible for workers to be exposed to airborne AgNPs concentrations, ranging from 0.005 to 0.289 mg/m³ [212]. Beside occupational exposure, the extensive use of AgNPs also increases the risk of consumer exposure via inhalation of AgNPs that are used in spray application such as disinfectants, deodorants and nebulizers [99]. Despite several studies into how pulmonary exposure

to ENMs may impact pulmonary toxicity, there are much fewer investigations on the impact of pulmonary exposure on extra-pulmonary targets particularly cardiovascular toxicity [170, 175, 213]. Following pulmonary exposure, there is evidence showing that nanoparticles (NPs) such as titanium dioxides (TiO₂), nano-ceria and AgNPs may translocate from the lung to systemic circulation and eventually be deposited in remote organs causing toxicity [23, 167, 214]. A strong relationship between pulmonary exposure to particulate matter and cardiovascular toxicity has been previously reported [178, 215]. It has also been demonstrated that pulmonary exposure to other forms of ENMs are capable of inducing or exacerbating cardiovascular dysfunction via mechanisms including systemic inflammation, coronary artery dysfunction, metabolic derangement, autonomic dysregulation and oxidative stress [174, 175, 216, 217]. However, the mechanism by which pulmonary exposure to AgNPs causes cardiovascular toxicity is poorly understood.

Recent studies have demonstrated that the pathophysiological effect of AgNPs is size, coating and dose-dependent [73, 128, 168, 173]. It is well known that smaller sized NPs result in increased bioavailability, enhanced distribution, and toxicity of silver compared with larger ones [73, 74]. The inverse relationship between the particle size and surface area implies that smaller AgNPs may have a faster rate of silver ions (Ag⁺) dissolution in the surrounding microenvironment [218]. Stability of NPs is also differentially affected by the type of coating [47, 128, 173]. In this context, an appraisal of scientific literature revealed that citrate (CT) coating of AgNPs was the most commonly used stabilizing agent, followed by polyvinylpyrrolidone (PVP) and amines [43]. However, work by Huynh *et al.* [219] and Tejamaya *et al.* [220] suggested that PVP-coated NPs are more stable than those coated with CT. Furthermore, the toxicological effects are also demonstrated to be influenced by dose and time of

exposure to AgNPs [173, 221]. Until now, there has been much debate in the literature regarding the formulation of AgNPs that leads to toxicity [222]. The adverse effects might be the result of either the direct interaction of AgNPs themselves, or released Ag⁺ ions or a combination of both [73]. Though Ag⁺ ions are known to have toxic effects in various biological species, including bacteria, fungi and viruses, they are reported to exhibit low toxicity in mammalian cells, which may be due to the formation of insoluble salts with chloride and sulfide ions [223]. Furthermore, smaller AgNPs (≤ 10 nm) have proven to be more toxic than predicted on the basis of Ag⁺ ion release in the biological medium [34].

Most of the previous *in vivo* experiments on pulmonary exposure to AgNPs have been limited to studying only one particle type (one coating and/ one size), at limited dose range and/or post exposure time frame and mostly reporting effects in lung. An aspect that has not been evaluated extensively so far is the potential cardiovascular effect of pulmonary exposure to AgNPs. Hence, we hypothesize that pulmonary deposited AgNPs could alter cardiovascular hemostasis and tested the hypothesis by evaluating the impact of two different coatings (namely PVP and CT), 3 doses (0.05, 0.5 and 5 mg/kg) and 2 time points (1 and 7 days). As mice are obligate nose breathers, which results in most of the inhaled particles being removed by filtration, we chose i.t. instillation to simulate pulmonary exposure to NPs that enabled controlled and consistent dose deposition, and consequently, accurate determination of dose response [210, 211]. Following i.t. instillation, we evaluated the acute (1-day) and sub-acute (7-days) vascular, systemic and cardiac effects of well characterized 10 nm AgNPs, using physiological parameters including a well-established mouse model of thrombosis in pial microvessels *in vivo* and evaluation of several markers of

coagulation, oxidative stress, inflammation, DNA damage and apoptosis in plasma and heart of mice.

3.3.2 Methods

Nanoparticles, silver acetate and vehicles

Suspensions of AgNPs of 10 nm (BioPure™), coated with either PVP or CT, were purchased from NanoComposix (San Diego, CA, USA). The provided stock concentrations were 1.0 mg/ml with endotoxin level <5 EU/ml and silver purity of 99.99%. The surface areas of PVP- and CT- AgNPs were 53.5 m²/g and 59.0 m²/g, respectively. The pH of both the suspensions was 7.4. The suspending solvents of PVP- and CT- AgNPs were sterile saline (0.9% NaCl) and 2.0 mM sodium citrate, respectively. Silver acetate (AgAc), as the source of Ag⁺ ions, purchased from Sigma-Aldrich (#216674, St. Louis, MO, USA), was dissolved in sterile water to yield a stock concentration of 1 mg/ml. To minimize aggregation, the working stock particle suspensions were always sonicated (Clifton Ultrasonic Bath, Clifton, NJ, USA) for 15 min and vortexed for 30 sec before their dilution and/or instillation. The vehicle for PVP- AgNPs and AgAc control groups was prepared as 0.9% NaCl. The vehicle for CT- AgNPs was 2 mM sodium citrate (Sigma-Aldrich, St. Louis, MO) dissolved in deionized water.

Characterization of AgNPs: zeta potential measurement and transmission electron microscopy (TEM)

The size distribution and the zeta potential of the nanoparticles were analyzed in aqueous dispersion using Malvern zetasizer instrument (Malvern Panalytical, UK), and Zetasizer 7.11 software for the measurement and data processing. All

measurements were carried out at room temperature and were done in triplicate. TEM of AgNPs were performed by method described in our previous paper [118]. Briefly, the suspensions were subjected to sonication at room temperature for 15 min prior to processing for TEM. A drop of PVP- and CT- AgNPs suspensions were deposited on a 200 mesh Formvar/Carbon coated copper grid and allowed to dry for 1 hr at room temperature. Then the grids were examined and photographed at different magnifications using FEI Tecnai Biotwin Spirit G2 TEM (FEI, Eindhoven, Netherlands).

Animals, dosing and i.t instillation

Both male and female BALB/C mice of age 8-10 weeks (BW: 22-25g) (Taconic Farms Inc., Germantown, NY, USA) were housed in light- (12 hrs light: 12 hrs dark cycle) and temperature-controlled ($22 \pm 1^\circ\text{C}$) rooms. They had free access to commercial laboratory chow and were provided tap water *ad libitum*.

The animals were randomly and broadly divided into the following groups: i) 10 nm PVP- AgNPs, ii) 10 nm CT-AgNPs, iii) ionic silver control: Ag^+ ions, iv) 0.9% NaCl (vehicle control for PVP-AgNPs and Ag^+ ions and v) 2 mM citrate (vehicle control for CT-AgNPs). For *in vivo* studies, the AgNPs (group i and ii) were dosed at 0.05, 0.5 and 5 mg/kg BW and Ag^+ ions (group iii) at 8 mg/kg BW, which is equivalent to the highest dose of AgNPs (5 mg/kg) used and freshly made on the day of dosing using endotoxin free water. Each group contained 8 animals with equally distributed male and female mice for each dose and for each endpoint i.e. 1 and 7 days. In the case of *in vitro* analysis, while the concentrations prepared for AgNPs were 0.04, 0.2 and 1 $\mu\text{g}/\text{ml}$, the Ag^+ ion concentration used was 1.55 $\mu\text{g}/\text{ml}$, equivalent to the highest dose of AgNPs i.e. 1 $\mu\text{g}/\text{ml}$.

The *in vivo* concentrations used in our study may not reflect a practical standard of human exposure; however, they are comparable with those employed in previous animal models of i.t. administration of AgNPs [73, 173]. Considering various factors such as American Conference of Governmental Industrial Hygienists limits for soluble and insoluble silver (0.01 mg/m³ and 0.1 mg/m³ respectively), occupational exposure measured at 1.02 µg/m³ and estimated dose of 75 ng AgNPs from consumer product (2.43 µg/m³ and 1.02 µg/m³ for soluble and insoluble silver, respectively), the doses tested in the present study correlate to potential human exposure in countries where occupational safety is not much considered [212, 224]. A study in silver manufacturing plant has shown that AgNPs in the air increases during production and peak area concentration of more than 290 µg/m³ has been detected and the later concentration has been used to correlate our *in vivo* doses [212]. The alveolar epithelium surface area in human is more than 102 m² [225] and ventilation rate is 20 l/min. Hence, exposure to 290 µg/m³ AgNPs would produce more than 11, 55 and 218 µg AgNPs/m² alveolar epithelium after 1 day, 1 week and 1 month, respectively. The alveolar epithelium surface area of mouse is more than 0.05 m² [225], hence, the *in vivo* concentration used in this study; i.e. 0.05, 0.5 and 5 mg/kg would result in 25, 250 and 2500 µg AgNPs/m², respectively, in a mouse weighing an average of 25 g. These doses approximate human occupational exposure to AgNPs after 2 days, 5 weeks and 11 months. As our preliminary analysis showed that animals given the highest dose of AgNPs exhibited much more of a significant effect, we chose a concentration of Ag⁺ ions to be tested equivalent to the highest dose of AgNPs. Similar derivation of the equivalent dose for Ag⁺ ions has been used recently by Recordati et al. [73]. We related our *in vitro* doses to *in vivo* doses used in current study. If at least 10% of the instilled AgNPs is expected to translocate to the systemic circulation [226, 227] for a mouse

weighing an average of 25 g, the concentration that would be available after the highest *in vivo* dose instillation, which is 5 mg/kg, would be approximately 12 µg/ml. However, we used a much lower *in vitro* concentration in our study, the highest dose (1 µg/ml) representing 1.6% of the pulmonary instilled dose.

Pulmonary exposure was achieved by single i.t. instillation. Mice were anesthetized with isoflurane and placed supine with extended neck on an angled board. A Becton Dickinson 24 Gauge cannula was inserted via the mouth into the trachea. The NPs suspension, AgAc or vehicles was instilled (100 µL) via a sterile syringe, followed by an equal volume of air bolus. Following 1 and 7-days of pulmonary exposure to AgNPs, Ag⁺ ions or vehicles, mice were sacrificed with an overdose of sodium pentobarbital, lung inflammation and several cardiovascular events were assessed.

For each AgNPs type a sample size of 64 mice and for Ag ions group a sample size of 36 mice were used for pial vessel thrombosis study. Subsequent studies were completed using additional 64 and 36 animals for each NP type and Ag⁺ ions respectively, for lung pathology, determination of systemic markers of inflammation and cardiac apoptosis. Another set of 32 animals for each AgNPs type were used to study markers of coagulation and *in vitro* platelet aggregation. Animals were sacrificed with an overdose of sodium pentobarbital, after 1 day and 7-days single i.t. administration of either vehicle or AgNPs or Ag⁺ ions.

This study was reviewed and approved by the Institutional Review Board of the United Arab Emirates University, College of Medicine and Health Sciences, and experiments were performed in accordance with protocols approved by the Institutional Animal Care and Research Advisory Committee.

Histology of lungs

Lungs were excised, washed with ice-cold saline, blotted with filter paper and weighed. Each organ was dissected, casseted and immediately fixed in 10% neutral formalin for 24 hours, which was followed by dehydration in increasing concentrations of ethanol, cleared with xylene and embedded with paraffin. Five- μ m sections were prepared from paraffin blocks and stained with hematoxylin and eosin (H & E) [228]. The stained sections were evaluated using light microscopy by the histopathologist who participated in this project.

Measurement of tumor necrosis factor alpha (TNF- α) and interleukin 6 (IL-6) in heart

Immediately after sacrifice, the harvested heart was quickly rinsed with ice-cold PBS (pH 7.4) before homogenization in 0.1 M phosphate buffer, pH 7.4, containing 0.15 M KCl, 0.1 mM EDTA, 1 mM DTT, and 0.1 mM phenylmethylsulfonyl fluoride at 4°C. The homogenates were centrifuged at 14,000 rpm for 20 min at 4°C to remove cellular debris, and the supernatants were stored for biomolecular analysis [229]. The total concentration of protein was determined using bicinchoninic acid assay (BCA assay). TNF- α and IL-6 were measured using ELISA Kits (Duo Set, R & D systems, Minneapolis, MN, USA).

Oxidative stress and lipid peroxidation evaluation: Detection of total antioxidants, reduced glutathione (GSH) and 8-isoprostane in heart

Total antioxidant was assayed by a commercially available kit (Cayman, Ann Arbor, MI, USA) according to the manufacturer's instruction. The concentration of GSH was also measured using a commercially available kit (Sigma-Aldrich Fine

Chemicals, St Louis, MO, USA), as were 8-isoprostane concentrations (ELISA Kit, Cayman Chemicals, Michigan, USA) [230].

Oxidative DNA damage evaluation by measurement of 8-hydroxy-2-deoxyguanosine (8-OH-dG) in heart

8-OH-dG was quantified using an ELISA kit (Cayman, Ann Arbor, MI, USA) according to the manufacturer's instruction [231].

Detection of apoptosis in heart

Apoptotic myocytes were detected by terminal deoxynucleotide transferase mediated dUTP nick end-labelling (TUNEL) assay, using a TACS® 2 TdT diaminobenzidine (DAB) kit (Trevigen, Gaithersburg, MD, USA) according to the manufacturer's instruction [232]. Briefly, paraffin embedded heart tissues were cut into 5 µm sections and deparaffinized with xylene followed by rehydration with decreasing concentrations of ethanol. Rehydrated tissue sections were washed with PBS and incubated with proteinase K for 15 min at room temperature, washed and quenched with hydrogen peroxide before labeling with biotin labeled dUTP for 1 hr at 37°C. The labeling reaction was stopped by adding stop buffer as provided by the kit. The tissue sections were then incubated with horseradish peroxidase-conjugated streptavidin for 10 min at 37°C, washed, and immersed in DAB solution for color development. These sections were also counterstained with methyl green before mounting. Negative control of the TUNEL assay was confirmed by staining of the heart tissue in the same manner without labelling enzyme. The positive control of the TUNEL assay was confirmed by staining heart sections with a labelling mix that contained TACS-nuclease™. Preparations were observed and photographed using a

light microscope. Cells with green nuclei after TUNEL staining using methyl green were considered normal, whereas cells with brown nuclei were considered apoptotic. Apoptotic (TUNEL positive) cells were counted in at least ten areas per heart section, in eight individual sections from each animal, at 400X magnification.

Measurement of systemic markers of coagulation and fibrinolysis

The concentrations of fibrinogen (Molecular Innovation, Southfield, MI, USA) and plasminogen activation inhibitor (PAI-1, Molecular Innovation, Southfield, USA) were determined using an ELISA Kit. Brain natriuretic peptide (BNP), Phoenix Pharmaceuticals, Burlingame, California, USA) was measured spectrophotometrically using ELISA kits.

Prothrombin time (PT) and activated partial thromboplastin time (aPTT) measurements in plasma

The PT and aPTT were measured in plasma collected from treated mice by using TEClot PT-S and TEClot APTT-S kits (TECO GmbH, Dieselstr. 1, 84088, Neufahrn, NB, Germany), according to the manufacturer's instruction. Briefly, the PT and aPTT were measured in platelet poor plasma (PPP), pre- incubated at 37°C for 3 min, followed by addition of PT and aPTT reagent, using a Merlin coagulometer (MC 1 VET, Merlin, Lemgo, Germany).

Experimental pial arterioles and venules thrombosis model

In separate animals, *in vivo* thrombogenesis in the pial arterioles and venules was assessed after AgNPs and Ag⁺ ions exposure at the end of 1 and 7 days, according to a previously described technique [228]. Briefly, the animal was anesthetized with urethane (1 mg/g BW, i.p.), the trachea was intubated, and the right jugular vein was

cannulated with a 2F venous catheter (Portex, Hythe, UK) for the administration of fluorescein (Sigma, St. Louis, MO, USA). Thereafter, craniotomy was first performed on the right temporoparietal cortex with a hand-held microdrill, and the dura was stripped open. Only untraumatized preparations were used, and those showing trauma to either microvessels or underlying brain tissue were discarded. Cerebral microcirculation was directly visualized using a fluorescence microscope (Olympus, Melville, NY, USA) connected to a camera and DVD recorder. A heating pad was used, and body temperature was raised to 37°C, as monitored by a rectal thermoprobe connected to a temperature reader (Physitemp Instruments, NJ, USA). A field containing arterioles and venules 15-20 µm in diameter was chosen. Such a field was taped prior to, and during the photochemical insult, which was carried out by injecting fluorescein (0.1 ml/mouse of 5% solution) via the jugular vein, which was allowed to circulate for 30-40 sec. The cranial preparation was then exposed to stabilized mercury light. The photochemically induced injury to arterioles and venules, in turn, causes platelets to adhere at the site of endothelial damage and aggregate. Platelet aggregates and thrombus formation grow in size until complete vascular occlusion. The time from the injury until complete vascular occlusion (time to flow stop) in arterioles and venules was measured in seconds. At the end of the experiments, the animals were euthanized by an overdose of urethane.

In vitro platelet aggregation in mouse whole blood

The platelet aggregation assay in whole blood was performed as described in previous studies [228]. After anesthesia, blood from untreated mice was withdrawn from the inferior vena cava, placed in citrate (3.2%), and 0.1 mL aliquots were added to the well of a Merlin coagulometer (MC 1 VET; Merlin, Lemgo, Germany). The

blood samples were incubated at 37°C for 3 minutes and then stirred for another 3 minutes with either PVP- or CT- AgNPs at concentrations of 0.04, 0.2, or 1 µg/mL or Ag⁺ ions at 1.55 µg/mL. The control for PVP- AgNPs and Ag⁺ ions was saline, while for CT-AgNPs it was 2 mM citrate solution. At the end of this period, single platelets were counted in a VET ABX Micros with a mouse card (ABX, Montpellier, France). The degree of platelet aggregation following NPs and Ag⁺ ions exposure was calculated as a fall in the number of single platelets counted and expressed as a % of respective controls.

Statistics

Data are presented as mean ± standard error of the mean and the statistical significance was determined by one-way analysis of variance (ANOVA) followed by the Holm-Sidak comparison test. P ≤ 0.05 were regarded as significant using GraphPad Prism Ver. 5.01 (GraphPad Software Inc., La Jolla, CA, USA).

3.3.3 Results

Characterization of PVP- and CT- AgNPs

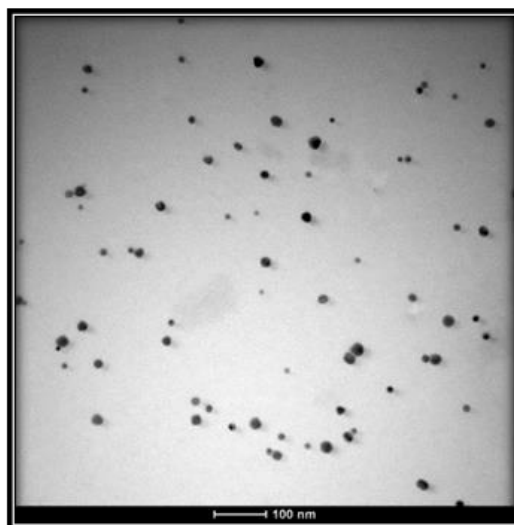
The TEM analysis showed primary particle of size ≈ 10 nm for both coating types (Figure 2). Agglomerated clusters were also seen (Figure 2 A & D). The results of size distribution and zeta potential measurements are represented in Table 7 and Figure 2 (B, C, E & F). Both PVP- and CT-coated AgNPs showed agglomeration with an average size of 93.2 ± 3.4 nm for PVP-AgNPs and 62.1 ± 0.27 nm for CT-AgNPs, and a highest particle size of 194.6 ± 3.2 nm for PVP-AgNPs and 157.9 ± 32.1 nm for CT-AgNPs. The Zeta potential for PVP-AgNPs was found to be - 0.305 ± 0.09 mV, whereas that of CT-AgNPs was - 36.25 ± 1.2.

Table 7: Size distribution and zeta potential measurements of polyvinylpyrrolidone (PVP) and citrate coated silver nanoparticles (AgNPs).

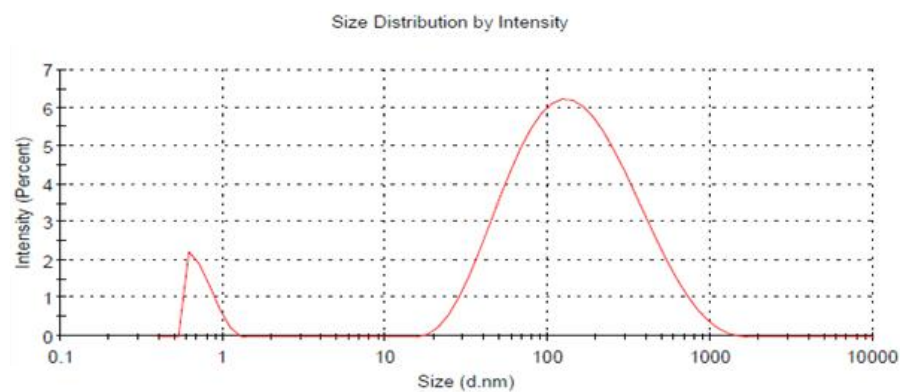
	Average size (nm)	Highest particle size (nm)	Zeta potential (mV)
PVP-AgNPs	93.2 ± 3.4	194.6 ± 3.2	- 0.305 ± 0.09
CT-AgNPs	62.1 ± 0.27	157.9 ± 32.1	- 36.25 ± 1.2

Data are mean ± SEM (n=3).

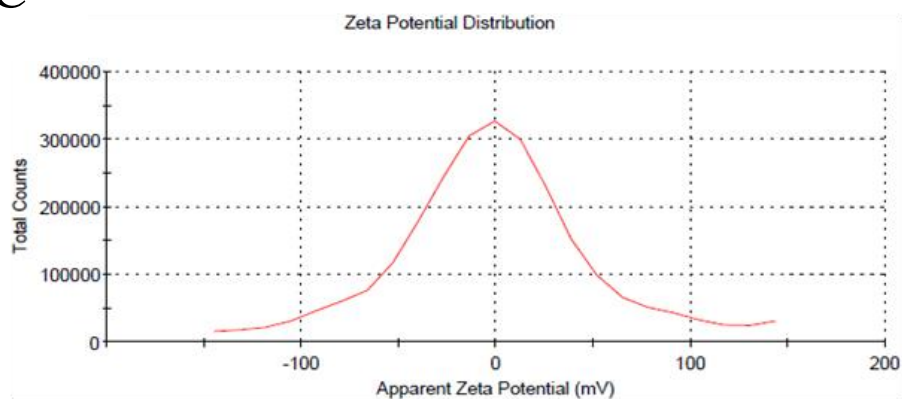
A



B



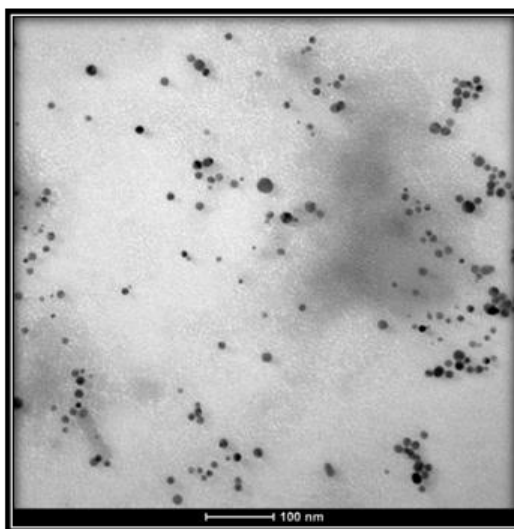
C



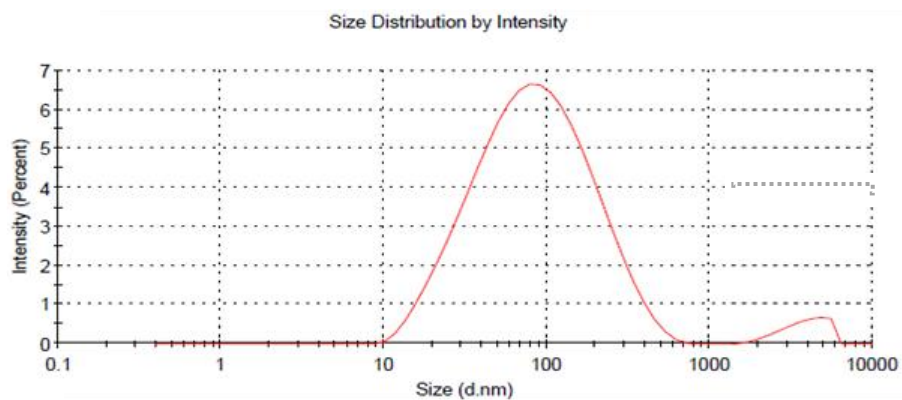
PVP- AgNPs

Figure 2: Transmission electron microscope analysis of polyvinylpyrrolidone or citrate coated silver nanoparticles. Representative images showing size distribution and zeta potential measurements of polyvinylpyrrolidone (PVP) or citrate (CT) coated silver nanoparticles (AgNPs).

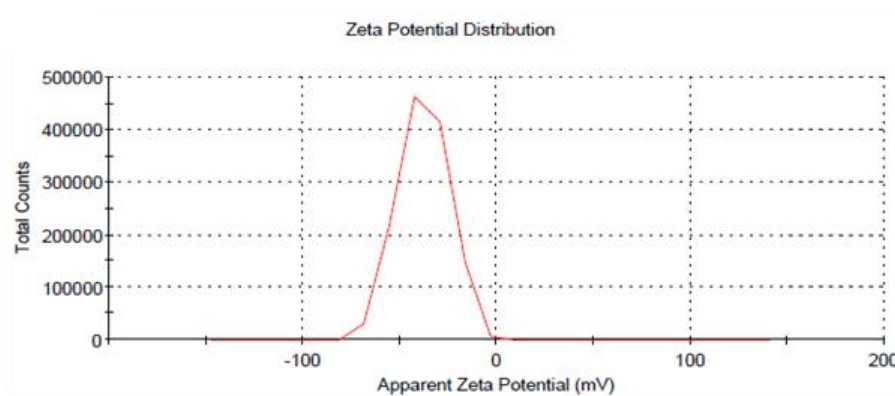
D



E



F



CT-AgNPs

Figure 2: Transmission electron microscope analysis of polyvinylpyrrolidone (A) or citrate (D) coated silver nanoparticles. Representative images showing size distribution and zeta potential measurements of polyvinylpyrrolidone (PVP) or citrate (CT) coated silver nanoparticles (AgNPs) (cont'd).

Histopathological examinations

Light microscopy analysis of the lung sections stained with H&E obtained from control mice (0.9% NaCl and 2 mM citrate) exhibited normal structure (Figure 3 A & B). Compared with their respective controls, there was marked increase of inflammatory infiltrate in the lung sections of mice i.t. instilled with either PVP- or CT- AgNPs at all doses (0.05, 0.5, and 5 mg/kg) and at both endpoints (1 and 7-days). The inflammatory infiltrate consisted of neutrophil polymorphs, macrophages, and lymphocytes. The intensity of infiltrate was almost similar after 1 and 7-days of exposure of any of the 3 doses for both the PVP- and CT- AgNPs group. Likewise, compared with the control there was mild peribronchial inflammatory cells infiltration consisting of neutrophil polymorphs and lymphocytes, following 1 and 7-days of i.t. instillation of Ag⁺ ions (figure not shown).

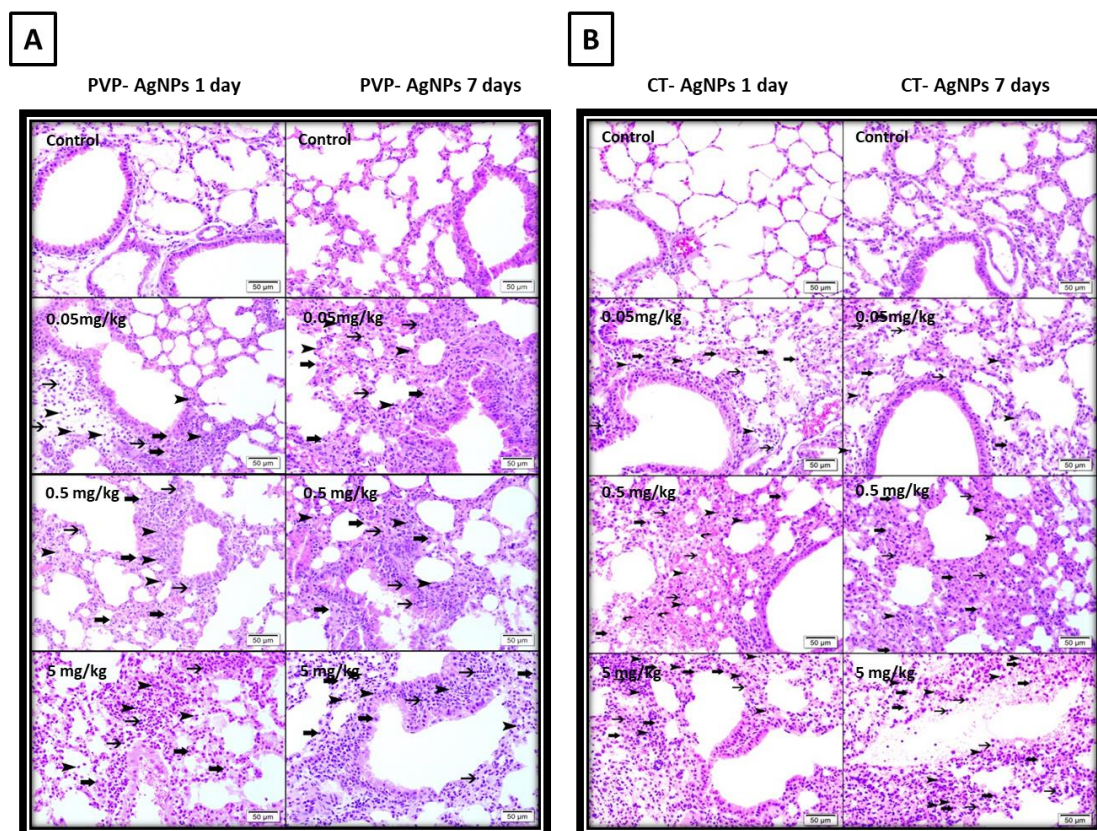


Figure 3: Representative light microscopy sections of lung tissues of control mice and those treated with polyvinylpyrrolidone (PVP) silver nanoparticles (AgNPs) at dose of 0.05, 0.5, 5 mg/kg, stained with H&E (A) and of control mice and those treated with citrate (CT) silver nanoparticles (AgNPs) at dose of 0.05, 0.5, 5 mg/kg, stained with H&E (B). All magnifications: 400X. The control group shows normal lung architecture and histology. PVP- and CT- AgNPs treated group shows increased interstitial inflammatory cells following 1-day and 7-days of intratracheal instillation of any of the three doses in alveolar and bronchial walls. The inflammatory infiltrate consists of neutrophil polymorphs (arrowhead), macrophages (thick arrow) and lymphocytes (thin arrow).

Effect of AgNPs and Ag⁺ on cytokines concentrations in heart homogenates

Concentrations of TNF- α and IL-6 are shown in Figure 4. After 1-day exposure, the administered AgNPs caused a dose-dependent increase in the levels of TNF- α in heart for both coating types (Figure 4 A). The increase was statistically significant at 5 mg/kg ($P < 0.001$) for the PVP group, and at all concentrations for CT-AgNPs ($P < 0.05$). Similarly, Ag⁺ significantly augmented the level of TNF- α ($P <$

0.001). In comparison with the control group, AgNPs caused significant increase of IL-6, at 5 mg/kg ($P < 0.001$) for PVP- and at 5 mg/kg ($P < 0.05$) for CT- AgNPs (Figure 4 C). The increase was significant for animals treated with Ag^+ ions ($P < 0.001$) also. Interestingly, no significant effect was observed at any of the concentrations for any of the particles following 7-days of i.t. instillation (Figure 4 B &D).

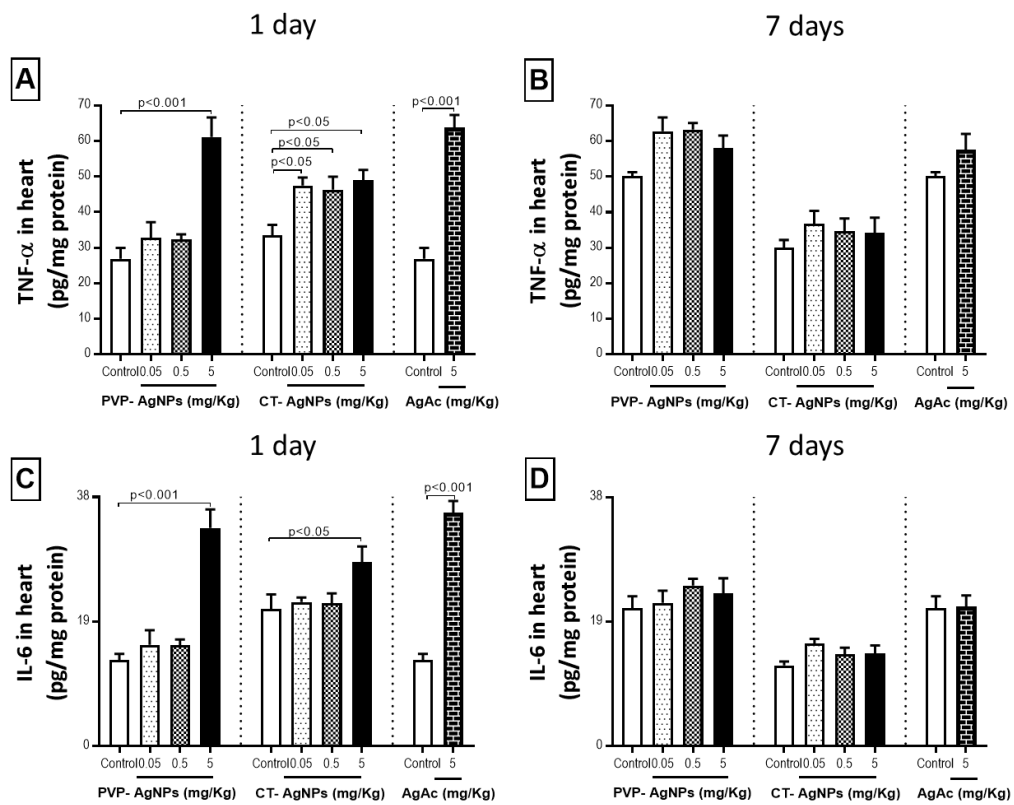


Figure 4: TNF- α and IL-6 levels in heart tissues following 1 day and 7 days of intra-tracheal instillation of saline (control) or citrate 2 mM (control) or polyvinylpyrrolidone (PVP) or citrate (CT) silver nanoparticles (AgNPs) or silver acetate (AgAc) in mice. Data are mean \pm SEM ($n=6-8$ in each group). Statistical analysis by one-way ANOVA followed by Holm-Sidak's multiple comparison test.

Effect of AgNPs and Ag⁺ ions on oxidative stress markers in heart homogenates

The assessments of total antioxidants, GSH and 8-isoprostane following the exposure to PVP- and CT- AgNPs and Ag⁺ are represented in Figure 5. Following 1-day exposure, a dose-dependent increase of total antioxidants was observed for both PVP- and CT- AgNPs (Figure 5 A). While the level of significance was achieved at 0.5 mg/kg ($P < 0.01$) and 5 mg/kg ($P < 0.001$) for PVP- AgNPs, the CT group showed significant increase at 5 mg/kg ($P < 0.01$). A significant increase was also observed for Ag⁺ ions ($P < 0.001$). After 7-days, a dose-dependent increase was found for both coating particles with significance achieved at the highest dose ($P < 0.05$) (Figure 5 B). The effect remained significant for Ag⁺ ions ($P < 0.05$). Compared with the control group, PVP- AgNPs caused an acute dose-dependent increase in GSH at 0.05 mg/kg ($P < 0.01$), 0.5 mg/kg ($P < 0.001$) and 5 mg/kg ($P < 0.001$) (Figure 5 C). Likewise, CT- AgNPs caused a significant increase at 0.05 mg/kg ($P < 0.05$) and 5 mg/kg ($P < 0.01$). Ag⁺ ions also produced significant increase ($P < 0.001$) compared with control. In the case of 8-isoprostane measurement, a dose-dependent increase was observed following 1-day treatment (Figure 5 E); significance was achieved at 5 mg/kg ($P < 0.001$) for PVP coated and at 5 mg/kg ($P < 0.01$) for CT coated AgNPs. After 7 days, significant increase of 8-isoprostane was only seen with PVP coating at 5 mg/kg ($P < 0.05$) (Figure 5 F). Interestingly, Ag⁺ ions did not produce any acute effect, but showed a significant increase ($P < 0.001$) after 7-days treatment.

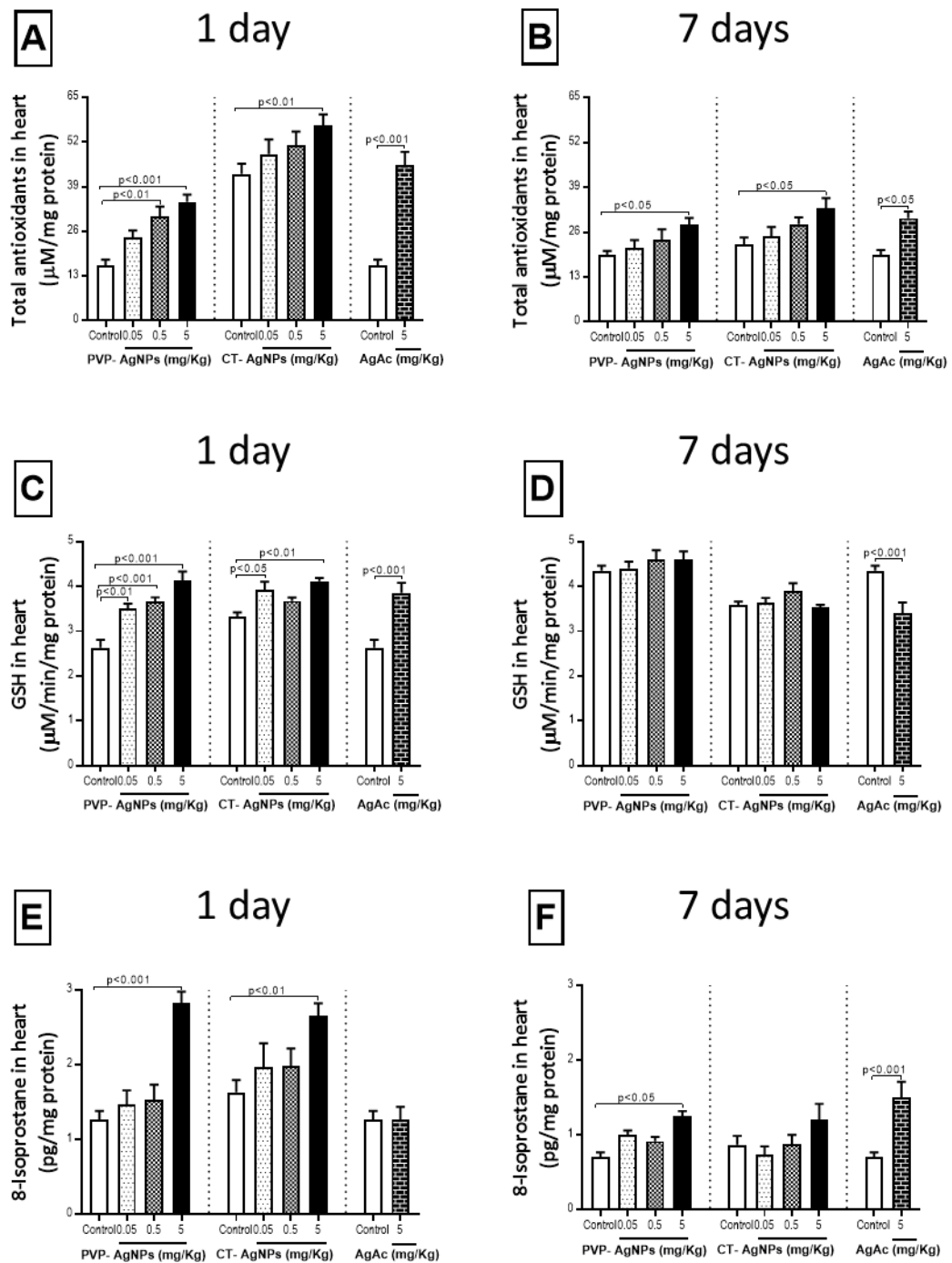


Figure 5: Total antioxidants (A, B), reduced glutathione (GSH, C, D) and 8-isoprostane (E, F) levels in heart tissues following 1 day and 7 days of intra-tracheal instillation of saline (control) or citrate 2 mM (control) or polyvinylpyrrolidone (PVP) or citrate (CT) silver nanoparticles (AgNPs) or silver acetate (AgAc) in mice. Data are mean \pm SEM ($n = 6-8$ in each group). Statistical analysis by one-way ANOVA followed by Holm-Sidak's multiple comparison test.

Effect of AgNPs and Ag⁺ ions on 8-OH-dG concentrations in heart homogenates

Figure 6 shows the concentration of 8-OH-dG in heart following 1 and 7 days of i.t. instillation of either AgNPs or Ag⁺. Following 1-day exposure, the concentration of 8-OH-dG increased dose-dependently for PVP- and CT- AgNPs (Figure 6 A). The level of significance was achieved at 0.5 mg/kg ($P < 0.05$) and 5 mg/kg ($P < 0.01$) in the case of PVP- AgNPs and at the highest dose for CT- AgNPs ($P < 0.001$). The significant effect persisted at 7 days with PVP- AgNPs at 0.5 mg/kg ($P < 0.01$) and 5 mg/kg ($P < 0.001$) (Figure 6 B). No effect on 8-OH-dG was observed with Ag⁺ ions at both time points.

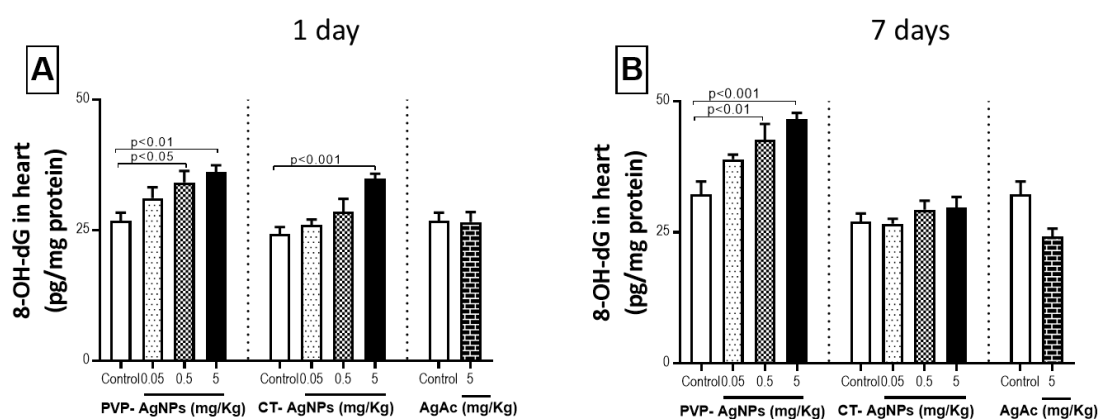
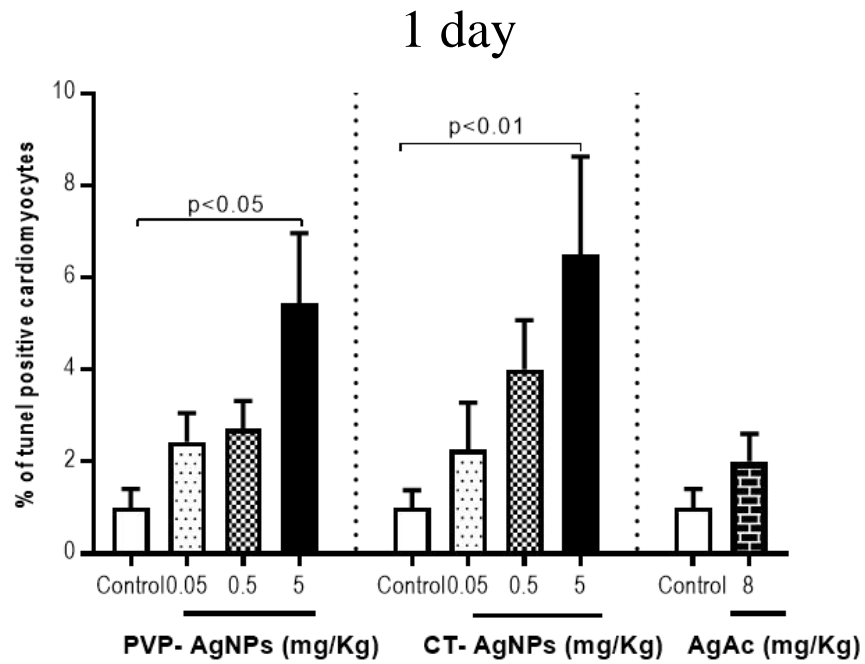


Figure 6: 8-hydroxy-2-deoxyguanosine (8-OH-dG, A, B) levels in heart tissues following 1 day and 7 days of intra-tracheal instillation of saline (control) or citrate 2 mM (control) or polyvinylpyrrolidone (PVP) or citrate (CT) silver nanoparticles (AgNPs) or silver acetate (AgAc) in mice. Data are mean \pm SEM ($n = 6-8$ in each group). Statistical analysis by one-way ANOVA followed by Holm-Sidak's multiple comparison test.

Measurement of cardiac cell apoptosis

Figure 7 represents percentage of tunel positive cardiomyocytes with the representative images for all particles and doses. A dose-dependent increase was observed, with significance being achieved at the highest dose; PVP- AgNPs ($P < 0.05$) and CT- AgNPs ($P < 0.01$) following 1-day exposure and only PVP-AgNPs ($P < 0.05$) after 7-days exposure. No significant effects were attained with Ag^+ ions.



1 day

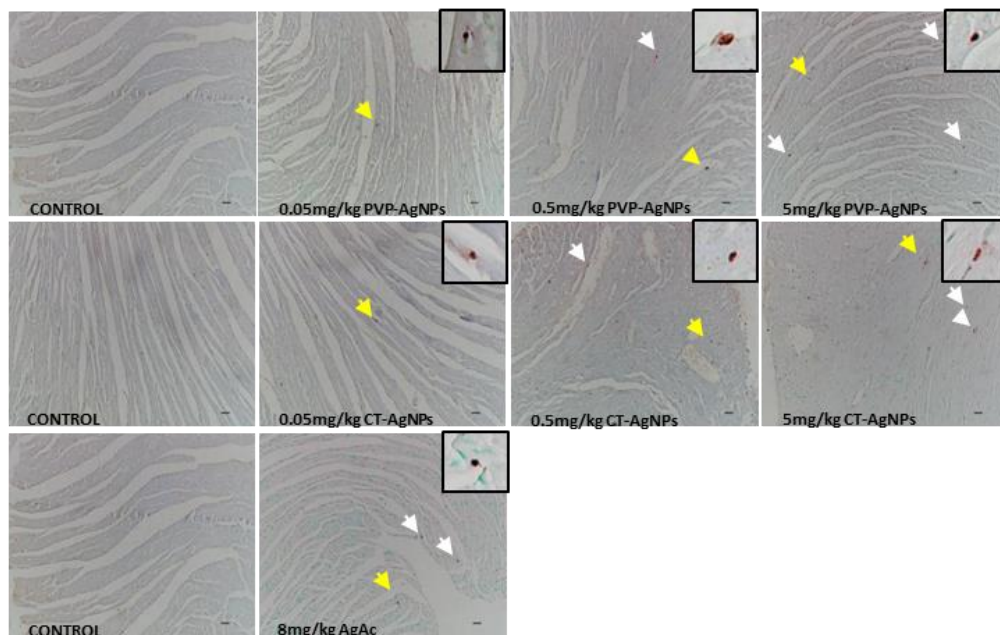
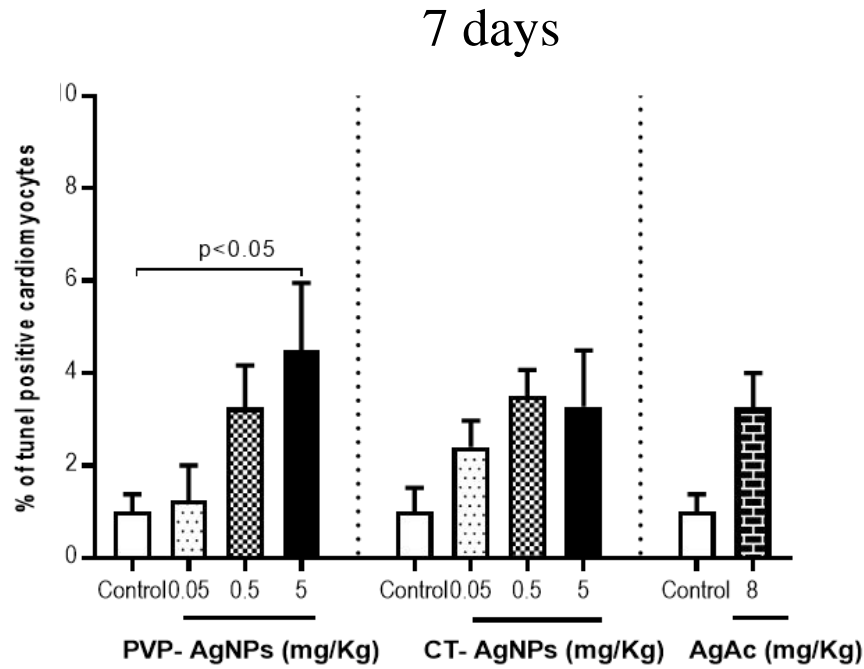


Figure 7: Estimation of apoptotic cells by an in situ TUNEL assay in heart sections and their representative images, following intra-tracheal instillation of saline (control) or citrate 2 mM (control) or polyvinylpyrrolidone (PVP) or citrate (CT) silver nanoparticles (AgNPs) or silver acetate (AgAc) in mice. The inset images are represented by yellow arrows. Counts of apoptotic cells were made in the sections (n=7-8 per group) at a final magnification of X200 and the average of apoptotic cell numbers in per group were calculated.



7 days

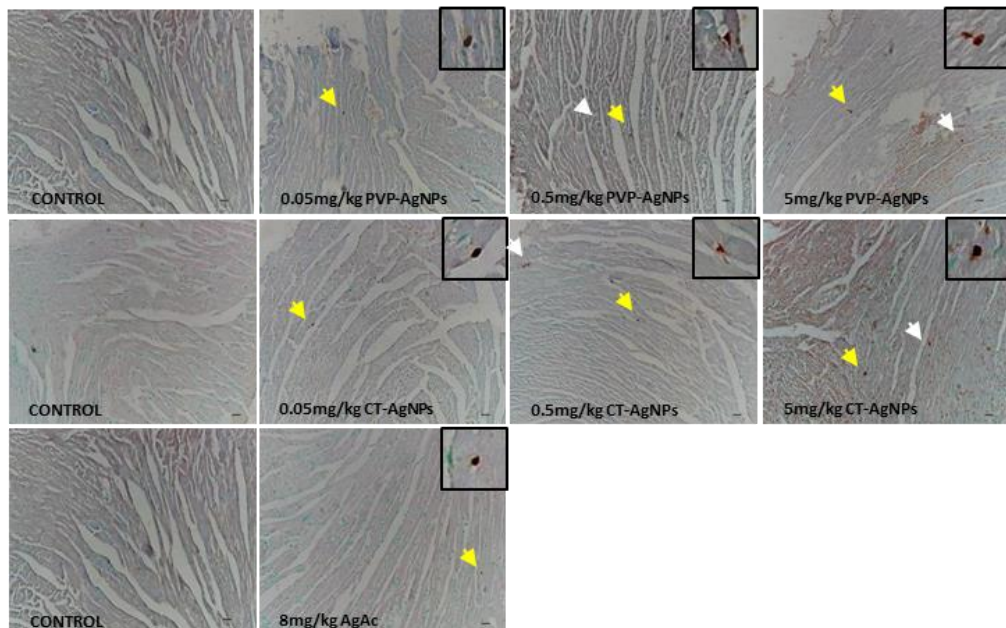


Figure 7: Estimation of apoptotic cells by an in situ TUNEL assay in heart sections and their representative images, following intra-tracheal instillation of saline (control) or citrate 2 mM (control) or polyvinylpyrrolidone (PVP) or citrate (CT) silver nanoparticles (AgNPs) or silver acetate (AgAc) in mice. The inset images are represented by yellow arrows. Counts of apoptotic cells were made in the sections (n=7-8 per group) at a final magnification of X200 and the average of apoptotic cell numbers in per group were calculated (cont'd).

Effect of AgNPs and Ag⁺ ions on fibrinogen and PAI-1 concentrations in plasma

Figure 8 represents the plasma concentration of fibrinogen and PAI-1. After 1-day of exposure, a significant increase in fibrinogen (Figure 8 A) was obtained at 0.05 mg/kg ($P < 0.01$), 0.5 mg/kg ($P < 0.01$) and 5 mg/kg ($P < 0.05$) for PVP- AgNPs. For CT- AgNPs the effect was significant at 0.5 mg/kg ($P < 0.01$) and 5 mg/kg ($P < 0.05$) compared with the control. The effect was significant for Ag⁺ ($P < 0.001$). Following 7-days exposure, there was an increase in fibrinogen for both type of AgNPs and Ag⁺ ions compared with their respective controls (Figure 8 B). However, the significance was achieved only for CT- AgNPs at 0.05 mg/kg ($P < 0.05$) and 5 mg/kg ($P = 0.001$).

PVP- AgNPs significantly increased PAI-1 at 0.05 mg/kg ($P < 0.001$), 0.5 mg/kg ($P = 0.05$) and 5 mg/kg ($P < 0.001$), post 1-day exposure (Figure 8 C). The significant effect for CT- AgNPs was seen at 0.05 mg/kg ($P < 0.05$) and 5 mg/kg ($P < 0.001$). At the 7-days time point (Figure 8 D), an increase of PAI-1 was observed in all doses; however, the significance was achieved for PVP- AgNPs at 0.5 mg/kg ($P < 0.01$) and 5 mg/kg ($P < 0.001$), and for Ag⁺ ($P < 0.001$).

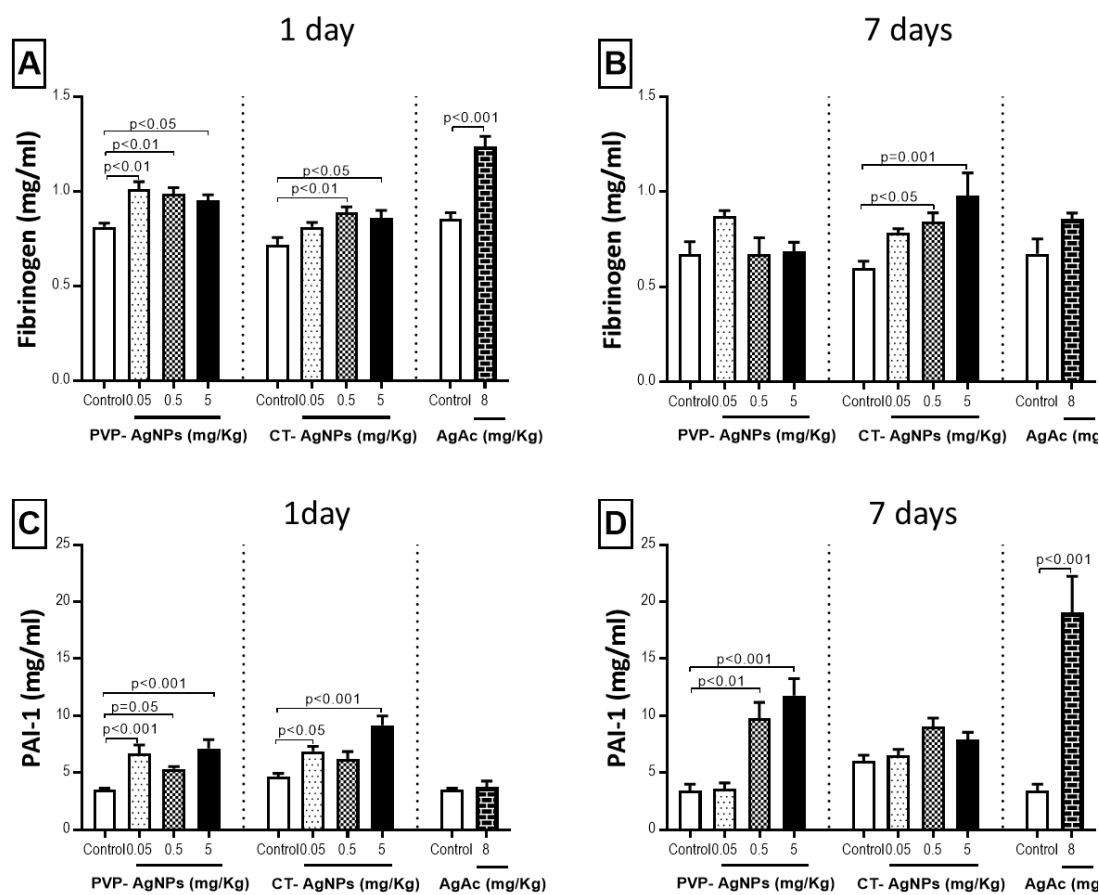


Figure 8: Fibrinogen (A, B) Plasminogen activator inhibitor-1 (PAI-1, C, D) concentrations in plasma, following 1-day and 7-days of intra-tracheal instillation of saline (control) or citrate 2 mM (control) or polyvinylpyrrolidone (PVP) or citrate (CT) silver nanoparticles (AgNPs) or silver acetate (AgAc) in mice. Data are mean \pm SEM (n = 6-8 in each group). Statistical analysis by one-way ANOVA followed by Holm-Sidak's multiple comparison test.

Effect of AgNPs and Ag⁺ ions on BNP concentrations in plasma

Figure 9 illustrates the plasma concentration of BNP following 1 and - days of i.t. instillation of either AgNPs or Ag⁺. Increase of BNP was observed for all particle types following 1-day exposure, though the significance was only attained at 5 mg/kg (P < 0.05) for PVP- AgNPs and at 0.5 mg/kg (P < 0.05) and 5 mg/kg (P < 0.05) for CT- AgNPs, compared with their respective controls (Figure 9 A). Post 7 days exposure, a significant increase (P < 0.05) was achieved at the highest dose for both

particle types compared with their respective controls (Figure 9 B). However, Ag⁺ ions did not increase BNP concentrations at these time points.

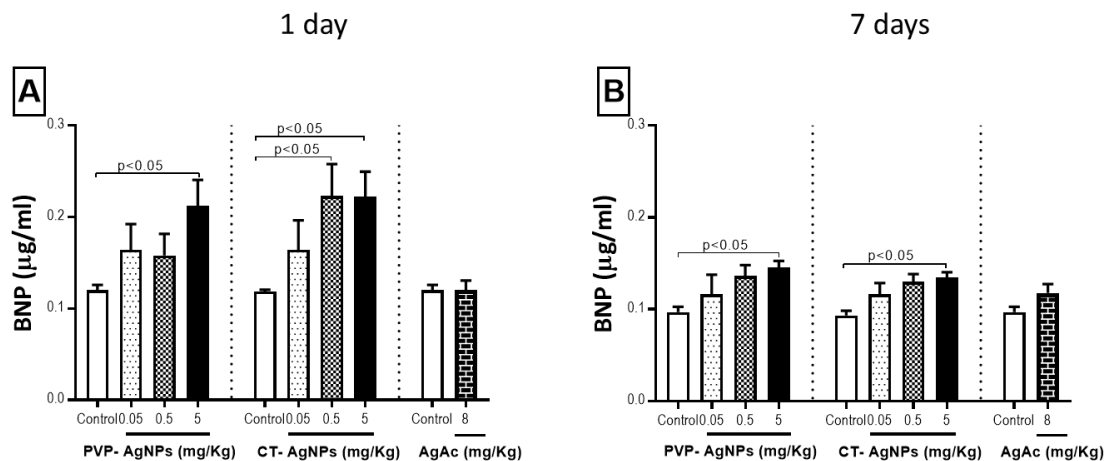


Figure 9: Plasma brain natriuretic peptide (BNP) (A, B) following 1-day and 7-days of intra-tracheal instillation of saline (control) or citrate 2 mM (control) or polyvinylpyrrolidone (PVP) or citrate (CT) silver nanoparticles (AgNPs) or silver acetate (AgAc) in mice. Data are mean \pm SEM (n = 6-8 in each group). Statistical analysis by one-way ANOVA followed by Holm-Sidak's multiple comparison test.

Effect of AgNPs and Ag⁺ ions on PT and aPTT in vitro

Figure 10 illustrates the PT and aPTT in PPP collected from mice treated with either AgNPs or Ag⁺ ions. Compared with the control group, a significant and dose-dependent reduction in PT was observed with both coating NPs, following 1-day exposure (Figure 10 A). For PVP-AgNPs, the effect was statistically significant at all concentration studied (P < 0.001). For CT-AgNPs the statistical significance was obtained at 0.05 mg/kg (P < 0.01), 0.5 mg/kg (P < 0.001) and 5 mg/kg (P < 0.001). The effect was also significant for Ag⁺ ions (P < 0.001). Post 7-days exposure (Figure 10 B), a significant reduction of PT was obtained in the PVP group at 0.05 mg/kg (P < 0.001), 0.5 (P < 0.001) and 5 mg/kg (P = 0.01) compared with the control. In the case of CT-AgNPs, the level of significance was achieved at 0.05 mg/kg (P < 0.001) and

5 mg/kg ($P < 0.05$). The effect was significant for Ag^+ ions ($P < 0.001$). After 1-day exposure (Figure 10 C), PVP- AgNPs induced a significant shortening of aPTT at all concentrations ($P < 0.001$). CT-AgNPs reduced the aPTT at 0.5 mg/kg ($P < 0.001$). Ag^+ ions also caused a reduction ($P < 0.001$) compared with the control. Following 7-days of i.t. instillation (Figure 10 D), a significant reduction of aPTT was achieved at 0.05 mg/kg ($P < 0.001$) for PVP- AgNPs and at 0.05 mg/kg ($P < 0.001$) and 0.5 mg/kg ($P < 0.001$) for CT- AgNPs, compared with their respective controls. Ag^+ also induced a significant effect ($P < 0.001$).

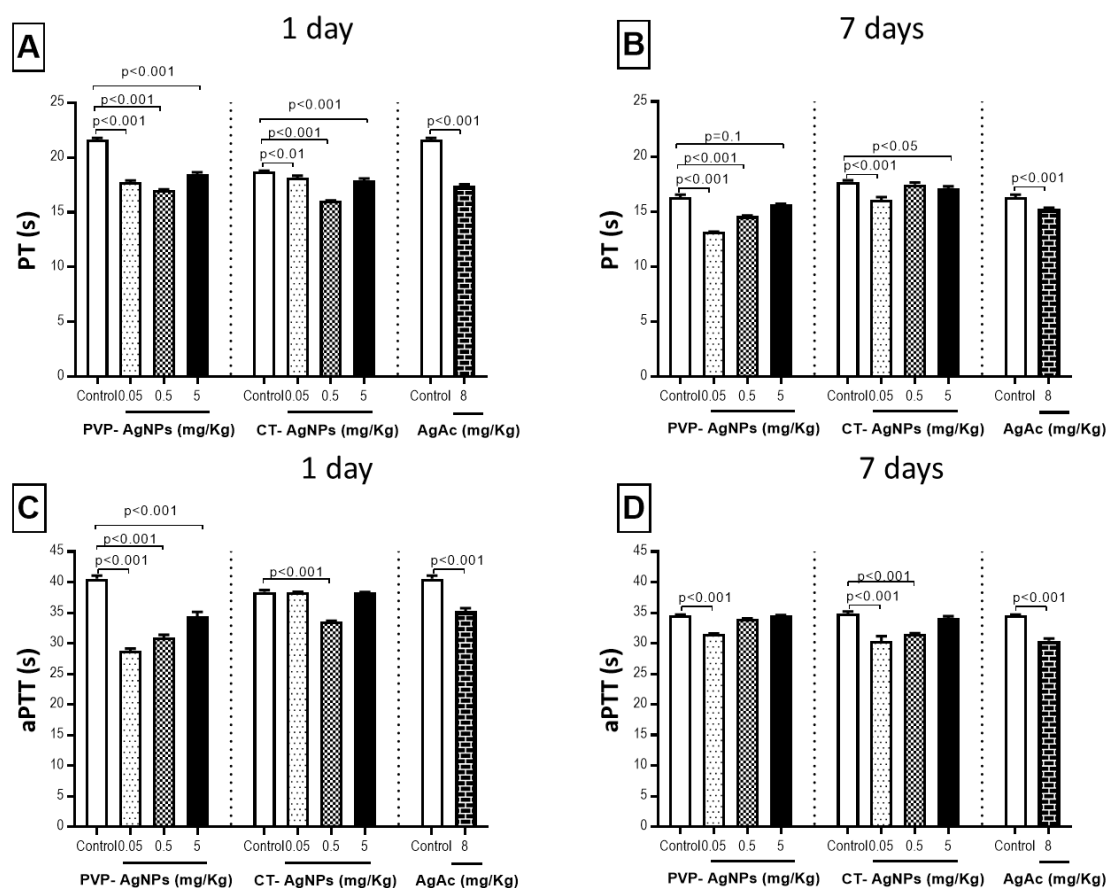


Figure 10: Prothrombin time (PT, A, B) and activated partial thromboplastin time (aPTT, C, D) measured following 1-day and 7-days of intra-tracheal instillation of saline (control) or citrate 2 mM (control) or polyvinylpyrrolidone (PVP) or citrate (CT) silver nanoparticles (AgNPs) or silver acetate (AgAc) in mice. Data are mean \pm SEM ($n = 6-8$ in each group). Statistical analysis by one-way ANOVA followed by Holm-Sidak's multiple comparison test.

Effect of AgNPs and Ag⁺ ions on photochemically-induced thrombosis in pial arterioles and venules of mouse in vivo

Figure 11 illustrates the effect of PVP- or CT- AgNPs, or Ag⁺ ions on thrombotic occlusion time. Both PVP- and CT- AgNPs induced significant dose-dependent shortening of the thrombotic occlusion time at both time points. In the case of arterioles, following 1-day exposure (Figure 11 A), the level of significance was achieved at all tested doses ($P < 0.001$) for PVP- AgNPs, and for CT- AgNPs the significance was obtained at 0.05 mg/kg ($P < 0.05$), 0.5 mg/kg ($P < 0.001$) and 5 mg/kg ($P < 0.001$) compared with their respective controls. In venules (Figure 11 B), the effect was significant for all concentrations ($P < 0.001$) of PVP- AgNPs compared with the control. In the case of CT- AgNPs, the effect was significant at 0.05 mg/kg ($P < 0.01$), 0.5 mg/kg ($P < 0.01$) and 5 mg/kg ($P < 0.001$) compared with the control. Following 7-days post i.t. instillation (Figure 11 C), a significant shortening of thrombotic occlusion time in the arterioles at doses of 0.05 mg/kg ($P < 0.05$), 0.5 mg/kg ($P < 0.01$) and 5 mg/kg ($P < 0.001$) was observed for PVP- AgNPs. For CT- AgNPs the effect was significant at 0.05 mg/kg ($P < 0.05$), 0.5 mg/kg ($P < 0.01$) and 5 mg/kg ($P < 0.001$). In venules (Figure 11 D), while for the PVP group the effect was significant at 0.05 mg/kg ($P < 0.01$), 0.5 mg/kg ($P < 0.01$) and 5 mg/kg ($P < 0.001$), the CT- AgNPs showed significance at 0.5 mg/kg ($P < 0.01$), 0.5 mg/kg ($P < 0.001$) and 5 mg/kg ($P < 0.001$) compared with their respective controls. Significant shortening was also achieved by Ag⁺ ions at 1 ($P < 0.001$) and 7 ($P < 0.05$) days respectively, compared with the control.

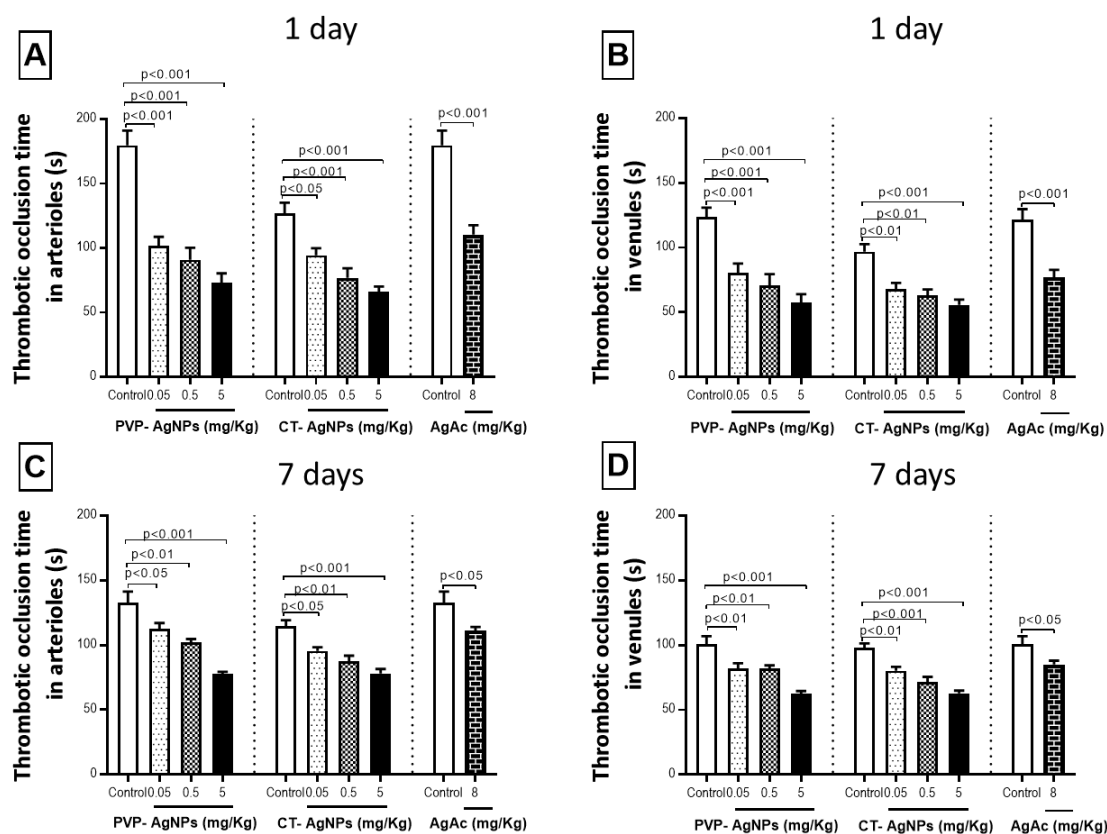


Figure 11: Thrombotic occlusion time in pial arterioles or venules following 1-day (A, B) and 7-days (C, D) of intra-tracheal instillation of saline (control) or citrate 2 mM (control) or polyvinylpyrrolidone (PVP) or citrate (CT) silver nanoparticles (AgNPs) or silver acetate (AgAc) in mice. Data are mean \pm SEM ($n = 6-8$ in each group). Statistical analysis by one-way ANOVA followed by Holm-Sidak's multiple comparison test.

Effect of AgNPs and Ag⁺ ions on platelet aggregation in whole blood in vitro

Figure 12 illustrates the effect of either AgNPs or Ag⁺ ions on platelet aggregation in whole blood. The *in vitro* treatment of whole blood from untreated mice with either PVP- or CT- AgNPs at various concentrations caused a significant dose-dependent reduction of platelet count compared with their respective controls. The effect was significant at 0.04 $\mu\text{g/mL}$ ($P < 0.05$), 0.2 $\mu\text{g/mL}$ ($P < 0.05$) and 1 $\mu\text{g/mL}$ ($P < 0.01$) for PVP- AgNPs compared with the control. Likewise, statistical

significance was also obtained for CT- AgNPs at 0.2 $\mu\text{g}/\text{mL}$ ($P < 0.05$) and 1 $\mu\text{g}/\text{mL}$ ($P < 0.05$) compared with the control. The effect was also significant for the whole blood treated with Ag^+ at 1.55 $\mu\text{g}/\text{mL}$ compared with the control.

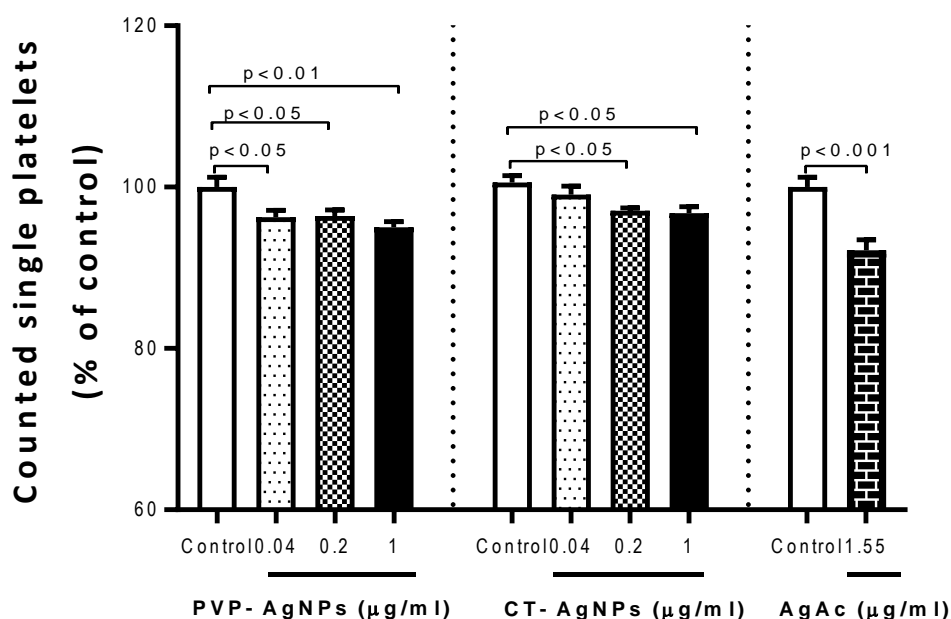


Figure 12: In vitro effect after the administration of saline (control) or citrate 2 mM (control) or polyvinylpyrrolidone (PVP) or citrate (CT) silver nanoparticles (AgNPs) or silver acetate (AgAc) on platelet aggregation in whole blood of untreated mice. Platelet aggregation in untreated whole blood 3 min after the addition of either saline or PVP- AgNPs or CT- AgNPs was assessed. The degree of platelet aggregation following AgNPs and AgAc exposure was expressed as a percent of control. Data are mean \pm SEM ($n = 4$). Statistical analysis by one-way ANOVA followed by Holm-Sidak's multiple comparison test.

3.3.4 Discussions

In this study, we evaluated the pathophysiological responses after single i.t. instillation of 10 nm AgNPs considering 2 different coatings (PVP and CT), three doses (*in vivo*: 0.05, 0.5 and 5 mg/kg BW, *in vitro*: 0.04, 0.2 and 1 $\mu\text{g}/\text{mL}$) and 2 time endpoints (1 and 7 days) in plasma and heart of BALB/C mice. Our findings showed

that AgNPs can induce acute dose-dependent cardiovascular effects including thrombosis, oxidative stress, inflammation, coagulation and apoptosis, with some of the effects being detected even after 7-days.

Characterization of test particles is a prerequisite to interpret scientific data. In the present study, besides the TEM, the size distribution and the zeta potential of the NPs were analyzed using Malvern zetasizer instrument. The TEM analysis showed individual particle size of ~10 nm and agglomerated clusters. The size distribution analysis revealed that both PVP- and CT-coated NPs showed agglomeration with a homogeneous size distribution of the agglomerates around 100 nm. This is in accordance with the TEM results. The PVP- AgNPs showed a zeta potential of -0.3 mV onto their surfaces, which indicates the charge close to neutrality of the AgNPs as depicted by the un-ionized PVP coating [219]. On the other hand, the negative values of CT- AgNPs (-36 mV) could be related to the presence of ionized carboxylate groups onto the surface of the Ag NPs [219].

NPs translocation to the systemic circulation after pulmonary exposure and their consequent effects on remote organs have been previously reported [166]. In this context, there is current literature evidence that pulmonary exposure to particulate matter and ENMs can lead to progression of cardiovascular dysfunction through pathways including inflammation and oxidative stress [175, 233]. In our study, we administered the AgNPs i.t., in order to ensure equivalent dosing for each animal. Compared with inhalation, which is a natural route of human exposure to consumer products, i.t. instillation is a preferred method of administration with the aim to address specific endpoints regarding the toxicity of nanomaterials [210, 211]. The size of the particle has been reported to play a critical role in NP-induced toxicity; size \leq 20 nm

AgNPs induces greater inflammatory response and increased cytotoxicity [41, 73, 128, 168, 173]. Hence, we presently assessed the impact of 10 nm AgNPs with 2 different coatings, namely PVP and CT.

Our histological data show that exposure to PVP- or CT- AgNPs or Ag⁺ ions triggered lung inflammation substantiated by interstitial infiltration of inflammatory cells consisting of neutrophils, lymphocytes and macrophages. All the observed effects persisted after 7 days of instillation and this corroborates the results of Silva *et al.* who demonstrated persistence of inflammatory infiltrates at 7 days post exposure of either PVP- or CT- AgNPs [173]. Similar to their findings, no differences were noted between animals administered AgNPs with different coatings. Compared with AgNPs, Ag⁺ ions produced a milder inflammatory response consisting mainly of neutrophil polymorphs and lymphocytes. Hence, the cardiovascular effects herein obtained by subsequent assays could be attributed to either the AgNPs themselves or inflammation induced or due to the release of Ag⁺ ions [234].

Our recent *in vitro* study on mouse erythrocytes demonstrated that AgNPs can induce hemolysis via mechanisms like oxidative stress and increase cytosolic Ca²⁺ [118]. Additionally, several previous data suggested a link between ENMs and cardiovascular events [235]; these effects were explained by the capacity of NPs to induce lung inflammation, subsequently causing systemic inflammation and oxidative stress, and/or the capacity of the NPs to translocate and enter the blood and affect cardiovascular endpoints [178, 236]. Nevertheless, the systemic effects of AgNPs following pulmonary exposure are not fully understood, particularly their possible impact on cardiovascular response. This study evaluated the cardiac effect of pulmonary exposed AgNPs by measuring markers of inflammation, oxidative stress

and DNA damage in heart. A direct correlation between inflammatory cytokines and myocardial injury has been previously reported in studies using silica, zinc oxide and TiO₂ NPs [237-239]. In this context, our study revealed a significant and a dose-dependent increase of two of the major pro-inflammatory cytokines, TNF- α and IL-6, following 1-day instillation of PVP- and CT- AgNPs. Increase in TNF- α and IL-6 have been reported to induce inflammation in cardiovascular system and cause cardiotoxicity in studies using various NPs including silica, zinc oxide and TiO₂ [240]. The treatment with an ionic form of Ag⁺ also resulted in significant increase of the TNF- α and IL-6, post 1-day exposure. Oxidative stress, characterized by the formation of a wide range of reactive oxygen species, is a key pathological process in a variety of disease conditions affecting various organs such as the lung, heart, kidney and liver. It subsequently results in DNA, protein, and lipid damage leading to cellular dysfunction and death [241]. Our data reveal that PVP- AgNPs cause more significant and dose dependent increase in total antioxidants and GSH compared with CT-AgNPs. The effect however declined 7-days post exposure, except for the highest dose of both AgNPs in the case of total antioxidants. Conversely, Ag⁺ ions caused a significant decrease of GSH post 7-days i.t. instillation indicating that the particulate and ionic form of silver may act by a different mechanism. Our data also show that exposure to AgNPs induced a significant increase of 8-isoprostane in the heart, a marker of lipid peroxidation. This derangement of oxidative biomarkers is in line with previous reports which showed that silver as well as other metallic NPs, including iron and silica, promoted cardiac oxidative stress [213, 239, 242, 243]. The effect of AgNPs on DNA damage in the heart has never been reported so far *in vivo*. In this case, we evaluated DNA damage in heart by measuring 8-OH-dG levels and apoptosis by TUNEL assay. 8-OH-dG is one of the predominant forms of free radical induced

oxidative lesions, and has therefore been widely used as a biomarker for oxidative damage to DNA [244]. Increase in 8-OH dG levels was reported in liver, brain, and kidney following administration of TiO₂, gold or iron oxide NPs [245-247]. Our work revealed an increase in 8-OH-dG in heart at the higher two doses of PVP and the highest dose of CT- AgNPs. The increase remained significant for PVP- AgNPs even after 7-days of exposure. However, Ag⁺ ions revealed no significant difference indicating that the oxidative DNA damage effect obtained could be NP dependent. TUNEL assay is one of the most widely used methods for detecting apoptotic cells in situ and is based on the ability of the enzyme terminal deoxynucleotidyl transferase to incorporate labelled dUTP into free 3'-hydroxyl termini generated by the fragmentation of DNA [248]. Our data show significant increase in tunel positive cardiomyocytes at the highest doses of PVP- and CT-AgNPs following 1-day after instillation and the results are relatable to our finding of 8-OH-dG level. However, Ag⁺ ions did not show any effect. Overall, PVP- and CT- AgNPs induced oxidative stress in heart evidenced by an increase of total antioxidants, GSH and 8-isoprostane, and caused cardiac DNA damage, thereby reinforcing the previously established mechanisms of DNA damage caused by reactive oxygen species and eventually resulting in cellular dysfunction and apoptosis [238, 249].

Further, we evaluated the impact of AgNPs on BNP concentration in the plasma and coagulation by measuring several endpoints, i.e., thrombosis in pial arterioles and venules *in vivo*, measurement of plasma concentrations of fibrinogen, PAI-1, PT, aPTT and *in vitro* platelet aggregation. Several studies demonstrated that exposure to ultrafine particles or diesel exhaust particles (DEPs) caused thrombotic complications and in this context, animal models of endothelial injury enables to understanding the mechanism by which particulate matter interact with the vascular

system [235, 250, 251]. To our knowledge, the effect of PVP- and CT- AgNPs on an animal model of thrombosis *in vivo* has not been reported so far. The data of the present study show that single i.t. administration of AgNPs (PVP or CT) induced a significant and a dose-dependent shortening of the thrombotic occlusion time in pial arterioles and venules, following 1 and 7-days, indicating that AgNPs possess prothrombotic effects, which persist even after a week of exposure. Along with thrombosis *in vivo*, a dose-dependent and significant increase in the concentrations of the coagulation factor, fibrinogen and PAI-1 in the plasma following 1-day i.t. instillation of AgNPs was found. Fibrinogen is an essential factor for clot formation [252]. PAI-1 is a potent endogenous serine proteinase inhibitor of fibrinolysis and its relationship with cardiovascular diseases is well established [253, 254]. Either one or both factors have been reported to increase following exposure to DEPs, silica NPs, carbon nanotubes and cerium oxide [228, 255, 256]. Interestingly, BNP that is normally present in low concentration in blood and a potential marker of cardiotoxicity [257, 258] also showed significant increase with the highest dose, for both coating NPs, at both the time points. Similar to AgNPs, Ag⁺ ions showed significant effect with respect to thrombosis and level of fibrinogen. Contrarily, with Ag⁺ ions, PAI-1 showed significant increase following post 7 days of exposure and there was no effect in the level of BNP. Based on the work on pulmonary toxicity of instilled AgNPs, Seiffert *et al.* suggested that surfactant interaction stabilized the surface conditions, preventing oxidation, which would otherwise lead to the release of Ag⁺ ions [179]. This might explain the dissimilar pattern of toxicity between AgNPs and Ag⁺ ions and also possibly suggest that the effect obtained in our study may be related primarily to AgNPs themselves rather than Ag⁺ ions. In order to determine which of the coagulation pathways, if any, could be affected, we evaluated the plasma PT and aPTT of treated animals. A significant

decrease of PT at almost all doses of PVP- and CT- AgNPs, as well as decrease of aPTT at some doses suggest both intrinsic and extrinsic pathways may be involved to cause prothrombotic effects *in vivo*. The results are in line with our earlier work with iron oxide nanoparticles that showed shortened PT and aPTT [242]. Our study also showed AgNPs are able to induce *in vitro* platelet aggregation and thereby significantly decrease platelet count even at doses much lower than anticipated to interact with systemic circulation after translocation of the highest instilled dose. These data are also in agreement with previous studies which demonstrated that NPs induced platelet aggregation *in vitro* [250, 259].

In the present study, the numbers of male and female mice used in each of the studied group were equally distributed and their age was comparable (8 to 10 weeks). However, we did not establish the stage of the estrous cycle of the experiments. The latter has been reported to have an impact on vascular function and circulatory factors [260]. Additional studies are required to clarify this point and to assess the AgNPs distribution in various organs following pulmonary exposure.

To conclude, with this study, the influence of two distinct AgNPs (size 10 nm), coating, concentration and two post exposure endpoints were comprehensively assessed in an *in vivo* model. We demonstrated that the acute toxic effect on plasma and heart after 1-day i.t instillation are dose- dependent and some of them persisted even after 7-days post exposure. Overall, the highest concentration resulted in more toxic effects for both PVP- and CT- AgNPs in heart and plasma, but the PVP- AgNPs tended to induce a more significant effects at all doses compared with CT- AgNPs. This suggests that application of AgNPs has to be carefully considered with respect to dose and coating. In comparison, Ag⁺ ions revealed a dissimilar pattern of toxicity

indicating that the *in vivo* effect of AgNPs may not only be attributed to release of Ag⁺ ions but also to the nanoparticulate form. The persistence of the cardiovascular effects following single i.t. administration reported in the present study, and the fact that occupational and consumer exposure to AgNPs are not time limited, additional studies are required to evaluate the chronic effect of AgNPs exposure.

3.4 Study two: Coating and time-dependent effect and biodistribution of pulmonary instilled silver nanoparticles in remote organs

3.4.1 Background

Previous studies have reported the translocation of AgNPs following various routes of exposure including inhalation, instillation, oral and dermal [22, 105, 113, 166]. The directly administered (intravenous) AgNPs or translocated particles, either in their ionic or nanoparticulate form, distributed to various organs and demonstrated variable effects largely dependent on their size, shape, coating, dose and duration of exposure [55, 73, 189]. Of all the potential routes, respiratory exposure of AgNPs is a recent concern of the researchers as inhalation of AgNPs can occur at nanosilver-manufacturing industries during particle synthesis, handling of dry powders, as well as during manufacturing of AgNPs containing products [88, 90, 99]. In this regard, studies evaluating workplace exposure and health hazard have reported that concentrations of AgNPs in the processes of manufacturing and integration of AgNPs into various consumer products can reach up to 1.35 $\mu\text{g}/\text{m}^3$ [90, 91]. Beside, use of nanotechnology based consumer sprays containing AgNPs, can lead to the generation of nanosized aerosols and the release of NPs near the human breathing zone [92, 93]. An occupational exposure limit of 0.19 $\mu\text{g}/\text{m}^3$ for AgNPs, have been proposed by Weldon BA *et al.* [97] based on subchronic rat inhalation toxicity study and taking in

consideration the human equivalent concentration with kinetics. Inhaled particles of ~20 nm mainly deposits in the alveolar region and have shown to interact with lung macrophages, epithelial cells and pulmonary surfactant [107, 167, 233]. Following pulmonary exposure, there is evidence showing that AgNPs may translocate from the lung to systemic circulation and eventually be deposited in remote organs causing toxicity [167]. However, compared to number of studies evaluating pulmonary toxicity to lung exposed AgNPs, there are much fewer investigations on the impact of pulmonary exposure on extra-pulmonary targets particularly heart, liver, spleen, kidney and brain [161, 168]. In this context, data from Holland *et al.* [174] showed exacerbation of cardiac ischemic-reperfusion injury following single i.t. instillation of 20 nm AgNPs in rats with cardiovascular injury. Lee *et al.* [165] found that a short term (14 days) nose only exposure of mice to 20 nm AgNPs at concentration of 1.91×10^7 particles/cm³ led to alterations in brain gene expression. Some studies also demonstrated silver accumulation in olfactory bulb, kidney and spleen, following pulmonary exposure [110, 167, 168]. However, yet a well understanding of the *in vivo* distribution, accumulation and effect of pulmonary exposed AgNPs, in major organs including liver, kidney, brain and spleen, is still lacking.

We recently studied the effect of pulmonary exposed 10 nm AgNPs, on cardiovascular homeostasis and showed AgNPs can induce time and dose-dependent cardiovascular effects including thrombosis, oxidative stress, inflammation, coagulation and apoptosis [176]. In order to further investigate the effect of these NPs on other major organs including liver, kidney, spleen and brain, we used the same type of particles from the same source and assessed markers of inflammation, oxidative stress, apoptosis and DNA damage. The latter effects were correlated with the biodistribution of silver in the studied organs.

3.4.2 Methods

Nanoparticles, silver acetate and vehicles

Suspensions of 10 nm polyvinylpyrrolidone (PVP) or citrate (CT) AgNPs (BioPure™) used in the present study were purchased from NanoComposix (San Diego, CA, USA) and all the particles were thoroughly characterized in our recent paper by techniques including transmission electron microscopy (TEM), size distribution analysis and zeta potential measurement [118]. The individual particle size of ~10 nm for both particle types were revealed in TEM. The size distribution analysis revealed agglomeration of both PVP- and CT- AgNPs and homogeneous size distribution of the agglomerates around 100 nm. The zeta potential for PVP- and CT- AgNPs were -0.305 ± 0.09 mV and -36.25 ± 1.2 , respectively [176]. Silver acetate (AgAc), as the source of Ag⁺ ions, was purchased from Sigma-Aldrich (#216674, St. Louis, MO, USA). While 0.9% NaCl was used as control vehicle and diluent for PVP- AgNPs and AgAc, 2 mM sodium citrate was used for CT- AgNPs group.

Animals and intratracheal (i.t.) administration of AgNPs

Both male and female BALB/C mice of age 8 -10 weeks (BW: 23 ± 2 g) (Taconic Farms Inc., Germantown, NY, USA) were housed in light (12 hrs light: 12 hrs dark cycle) and temperature-controlled ($22 \pm 1^\circ\text{C}$) rooms. They had free access to commercial laboratory chow and were provided tap water *ad libitum*.

Pulmonary exposure was achieved by single i.t. instillation of 100 μL of either PVP- or CT- AgNPs (5 mg/kg), or AgAc (8 mg/kg) or control vehicle by method previously described [176, 228]. For each group a sample size of 6-8 mice were used for histological, biomolecular and apoptotic studies. Another set of 5 animals for each

treated group were used to study silver distribution in various organs. All the endpoints were measured following 1 and 7-days of exposure. Immediately after the sacrifice, the lung, liver, kidney, spleen and whole brain were harvested, homogenized and supernatant collected for biochemical analysis. The total concentration of protein was determined using bicinchoninic acid assay, as described earlier [176].

This study was reviewed and approved by the Institutional Review Board of the United Arab Emirates University, College of Medicine and Health Sciences, and experiments were performed in accordance with protocols approved by the Institutional Animal Care and Research Advisory Committee.

Histology of tissues

Lungs, brain, kidney, spleen, liver and heart were excised immediately following sacrifice, washed with ice-cold saline, dissected, casseted and fixed in 10% neutral formalin for 24 hours. This was followed by dehydration in increasing concentrations of ethanol, cleared with xylene and embedded with paraffin. Three- μm sections of each tissue were prepared from paraffin blocks and stained with hematoxylin and eosin (H & E) [228]. The stained sections were evaluated using light microscopy by the histopathologist who participated in this project.

Measurement of tumor necrosis factor alpha (TNF- α) and interleukin 6 (IL-6) in tissue homogenates

TNF- α and IL-6 were measured using ELISA Kits (Duo Set, R & D systems, Minneapolis, MN, USA).

Oxidative stress and lipid peroxidation evaluation: Detection of reduced glutathione (GSH), total nitric oxide (NO) and 8-isoprostane in tissue homogenates

The concentration of GSH was measured using a commercially available kit (Sigma-Aldrich Fine Chemicals, St Louis, MO, USA). The determination of NO was performed with a total NO assay kit from R&D systems (Minneapolis, MN, USA) which measures the more stable NO metabolites [261]. 8-isoprostane concentrations were measured using ELISA Kit (Cayman Chemicals, Michigan, USA) [230].

Oxidative DNA damage evaluation by measurement of 8-hydroxy-2-deoxyguanosine (8-OH-dG) in tissue homogenates

8-OH-dG was quantified using an ELISA kit (Cayman, Ann Arbor, MI, USA) according to the manufacturer's instruction [231].

In situ detection of apoptosis in tissues

Apoptotic cells were detected by terminal deoxynucleotide transferase mediated dUTP nick end-labelling (TUNEL) assay, using a TACS® 2 TdT diaminobenzidine (DAB) kit (Trevigen, Gaithersburg, MD, USA) according to method previously described [176]. Briefly, 5 µm tissue sections were deparaffinized, rehydrated and incubated with proteinase K. Following quenching, the tissue sections were labelled with biotin labeled dUTP. The sections were then incubated with horseradish peroxidase-conjugated streptavidin, washed, stained with DAB solution, counterstained with methyl green and mounted. Negative and positive control of the TUNEL assay were prepared according to the instruction of kit. Preparations were observed and photographed using a light microscope. Cells with green nuclei after TUNEL staining using methyl green were considered normal, whereas cells with brown nuclei were considered apoptotic. Apoptotic (TUNEL positive) cells were counted in at least ten areas per tissue section, in eight individual sections from each animal, at 400X magnification.

Measurement of total silver content

Total silver concentrations were determined in organs by inductively coupled plasma mass spectrometer (ICP-MS), according to method previously described [73]. Briefly, the heart, lungs, liver, spleen, kidneys, and brain ($n = 4-5$) were collected, weighed and placed in acid washed tubes during necropsy. The organ tissues were then digested in a microwave after addition of 3 ml HNO₃ and 1 ml of H₂O₂. After cooling, the digests were diluted by adding 3 M HCL. Then, the content of Ag ($\mu\text{g/g}$) in organs was detected through ICP-MS (Optima 5300DV, America). Measurements were carried out on ¹⁰⁷Ag and ¹⁰³Rh, as internal standard, by the method of external calibration.

3.4.3 Results

Histopathological examination

Light microscopy analysis of the investigated tissue sections stained with H&E is shown in Figure 13. In the lung, compared with their respective controls (A, B, C, D), there was marked increase of inflammatory infiltrate in the sections of mice instilled with either PVP- or CT- AgNPs (E, F, G, H), at both endpoints (1 and 7-days). The intensity of infiltrate was higher after 7 days of exposure to 5 mg/kg PVP- and CT- AgNPs. The inflammatory infiltrate consisted of neutrophil polymorphs, macrophages, and lymphocytes. Likewise, compared with the control there was mild peribronchial inflammatory cells infiltration consisting of neutrophil polymorphs and lymphocytes, following 1 and 7-days of i.t. instillation of Ag⁺ ions (figure not shown). Figure 13 also shows that there were unremarkable morphologic changes in liver, kidney, spleen, brain and heart tissues of both control and treated groups.

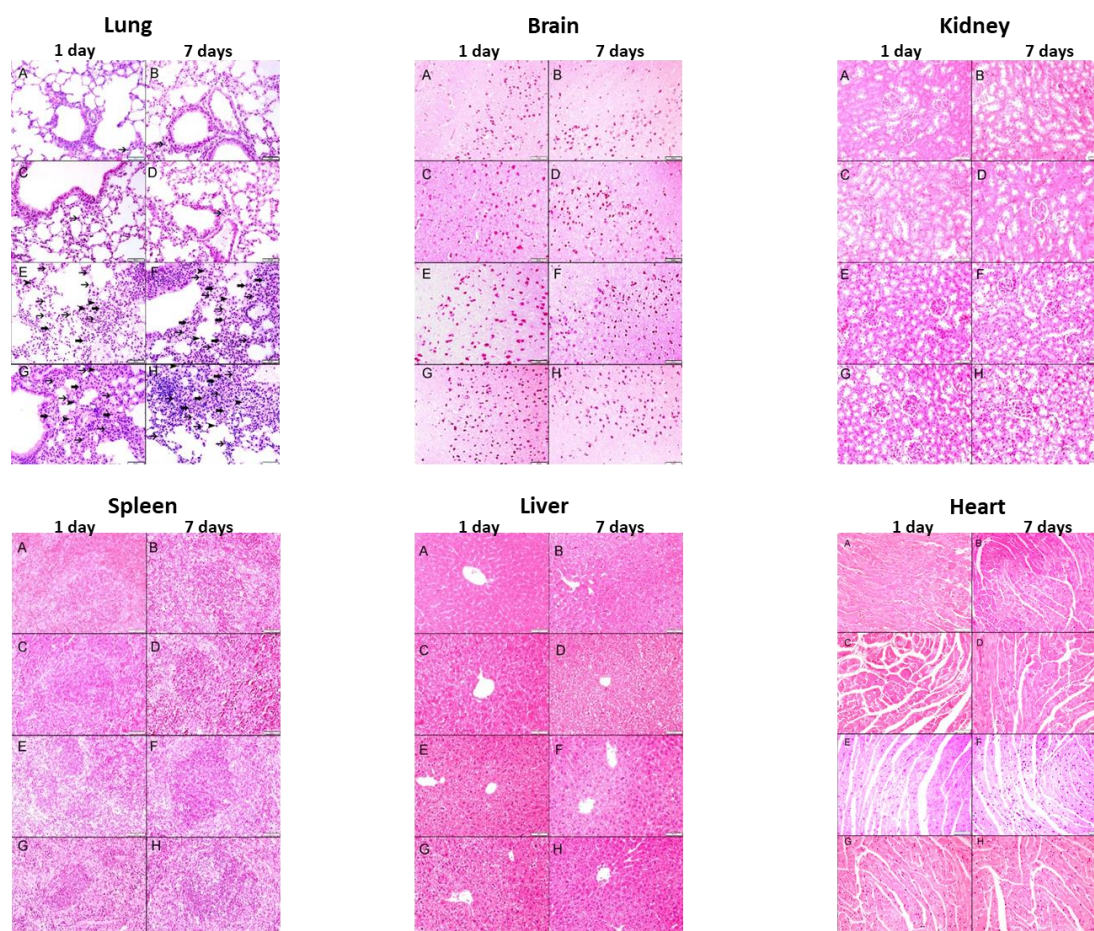


Figure 13: Representative light microscopy sections of lung, brain, kidney, spleen, liver and heart tissues of control mice (A,B) and those treated with polyvinylpyrrolidone (PVP) silver nanoparticles (AgNPs) at dose of 5 mg/kg, stained with H&E (E,F) and of control mice (C,D) and those treated with citrate (CT) silver nanoparticles (AgNPs) at dose 5 mg/kg, stained with H&E (G,H). All magnifications: 400X. The control group shows normal lung architecture and histology. PVP- and CT-AgNPs treated group shows increased interstitial inflammatory cells following 1-day and 7-days of intratracheal instillation in alveolar and bronchial walls. The inflammatory infiltrate consists of neutrophil polymorphs (arrowhead), macrophages (thick arrow) and lymphocytes (thin arrow).

Effect of AgNPs and Ag⁺ on cytokines concentrations in homogenates

Concentrations of TNF- α and IL-6 are shown in Figure 14 and Figure 15. After 1-day exposure, the administered CT-AgNPs caused significant increase in the levels of TNF- α in brain ($P < 0.05$) and liver ($P < 0.001$), compared with their respective control (Figure 14). The increase was statistically significant only in lung ($P < 0.01$) for the PVP group. Similarly, Ag⁺ significantly augmented the level of TNF- α in kidney ($P < 0.05$) and spleen ($P < 0.001$). Following 7-days of exposure, significant increase was observed with, PVP- AgNPs in lung ($P < 0.05$) and Ag⁺ in kidney ($P < 0.01$).

In comparison with the control group, CT- AgNPs caused significant increase of IL-6 in lung ($P < 0.05$), brain ($P < 0.01$) and liver ($P < 0.001$) following 1-day post exposure (Figure 15). However, PVP- AgNPs showed significant increase only in lung ($P < 0.001$). As for Ag⁺ significant increase was observed in lung ($P < 0.05$), kidney ($P < 0.01$) and spleen ($P < 0.01$). Interestingly, following 7 days of i.t. instillation, only Ag⁺ showed significant increase in kidney ($P < 0.05$).

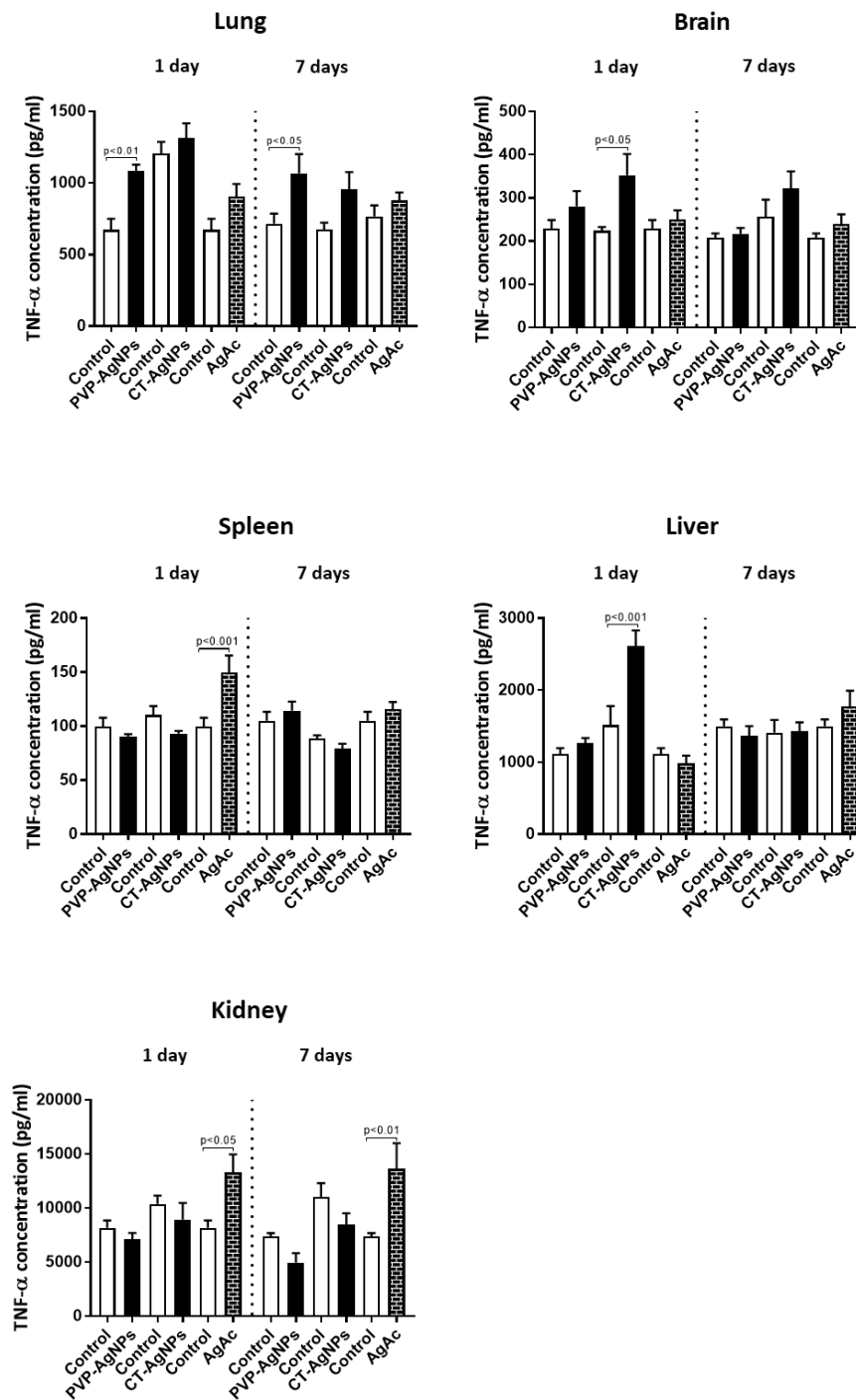


Figure 14: TNF- α concentrations in lung, brain, spleen, liver and kidney tissues following 1-day and 7-days of intra-tracheal instillation of saline (control) or citrate 2 mM (control) or polyvinylpyrrolidone (PVP) or citrate (CT) silver nanoparticles (AgNPs) or silver acetate (AgAc) in mice. Data are mean \pm SEM ($n = 6-8$ in each group). Statistical analysis by one-way ANOVA followed by Holm-Sidak's multiple comparison test.

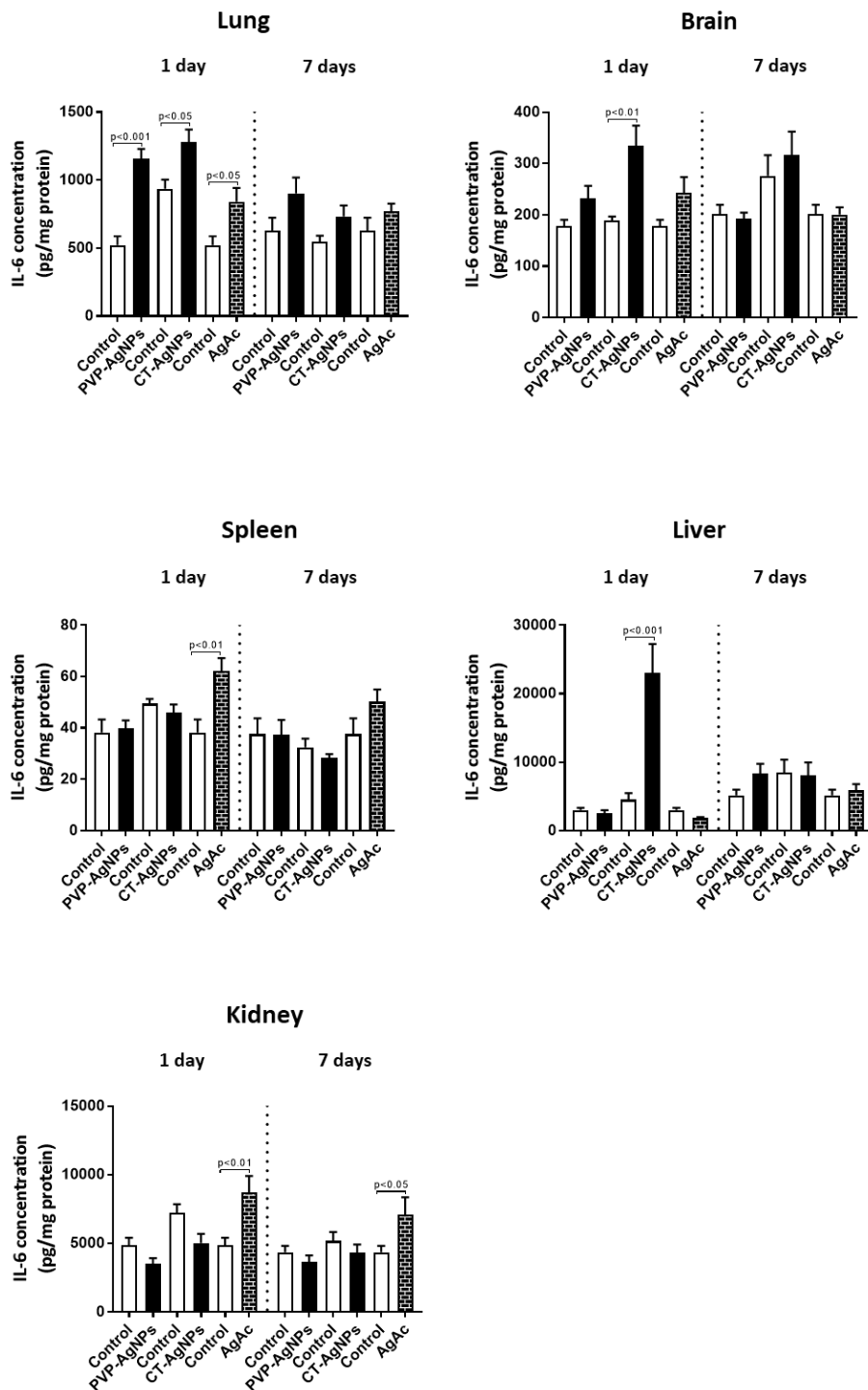


Figure 15: IL-6 concentrations in lung, brain, spleen, liver and kidney tissues following 1-day and 7-days of intra-tracheal instillation of saline (control) or citrate 2 mM (control) or polyvinylpyrrolidone (PVP) or citrate (CT) silver nanoparticles (AgNPs) or silver acetate (AgAc) in mice. Data are mean \pm SEM ($n = 6-8$ in each group). Statistical analysis by one-way ANOVA followed by Holm-Sidak's multiple comparison test.

Effect of AgNPs and Ag⁺ ions on oxidative stress markers and lipid peroxidation in tissue homogenates

The effects of PVP- and CT- AgNPs and Ag⁺ on the markers of oxidative stress (GSH) and nitrosative stress (NO) and lipid peroxidation (8-isoprostane) in the lung, liver, kidney, spleen, and brain are illustrated in Figures 16, 17 and 18. Following 1-day exposure the concentration of GSH was significantly increased for CT- AgNPs in lung (P < 0.001), brain (P < 0.05), kidney (P < 0.05) and spleen (P < 0.05) compared to the control (Figure 16). The PVP- AgNPs showed significant increase in kidney (P < 0.05) and liver (P < 0.001). Interestingly, a significant decrease was also observed for Ag⁺ ions (P < 0.05). After 7-days, no significant changes were observed in either PVP- or CT- AgNPs group. However, Ag⁺ showed significant increase of GSH in lung (P < 0.001) and decrease in spleen (P < 0.001) following 7-days of exposure.

As shown in Figure 17, post 1-day instillation, total NO was significantly increased for the CT- AgNPs in lung (P < 0.01), brain (P < 0.001) and kidney (P < 0.01), compared to the control. The increase was significant only in liver (P < 0.05) for the PVP- AgNPs. For the Ag⁺ treated animals significant increase was achieved in lung (P < 0.05) and kidney (P < 0.01). At 7-days, significant increase was observed with only CT- AgNPs in kidney (P < 0.01) and Ag⁺ in spleen (P < 0.01).

8-isoprostane was measured as marker of lipid peroxidation and the results are shown in Figure 18. Following 1-day post exposure, significant increase was observed in lung (P < 0.01) and brain (P < 0.05) for CT- AgNPs, in lung (P < 0.001) and liver (P < 0.01) for PVP-AgNPs, and in spleen (P < 0.01) and liver (P < 0.05) for Ag⁺, compared to their respective controls. No significant changes were observed following 7-days of instillation.

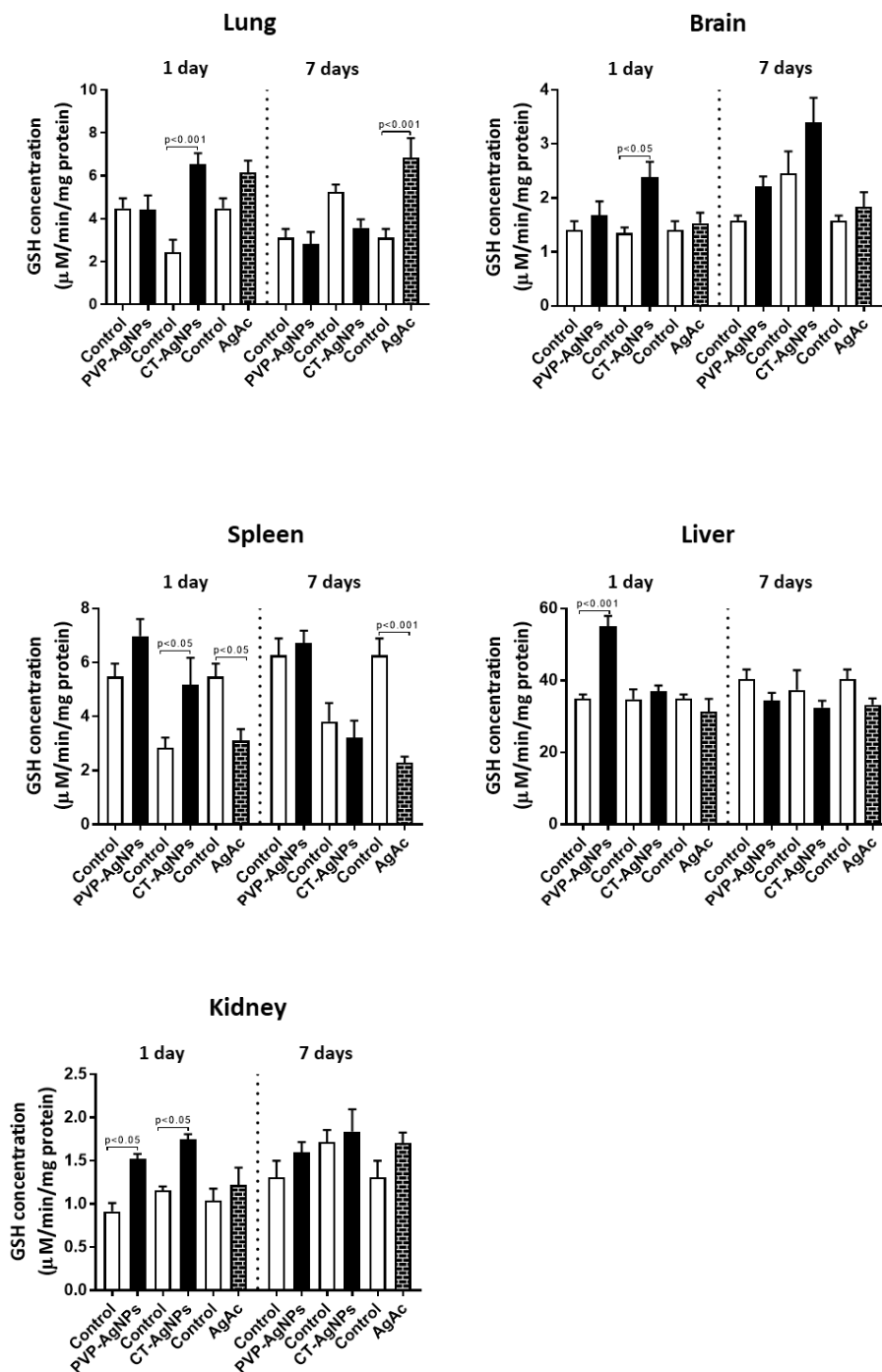


Figure 16: Reduced glutathione (GSH) levels in lung, brain, spleen, liver and kidney tissues following 1-day and 7-days of intra-tracheal instillation of saline (control) or citrate 2 mM (control) or polyvinylpyrrolidone (PVP) or citrate (CT) silver nanoparticles (AgNPs) or silver acetate (AgAc) in mice. Data are mean \pm SEM ($n = 6-8$ in each group). Statistical analysis by one-way ANOVA followed by Holm-Sidak's multiple comparison test.

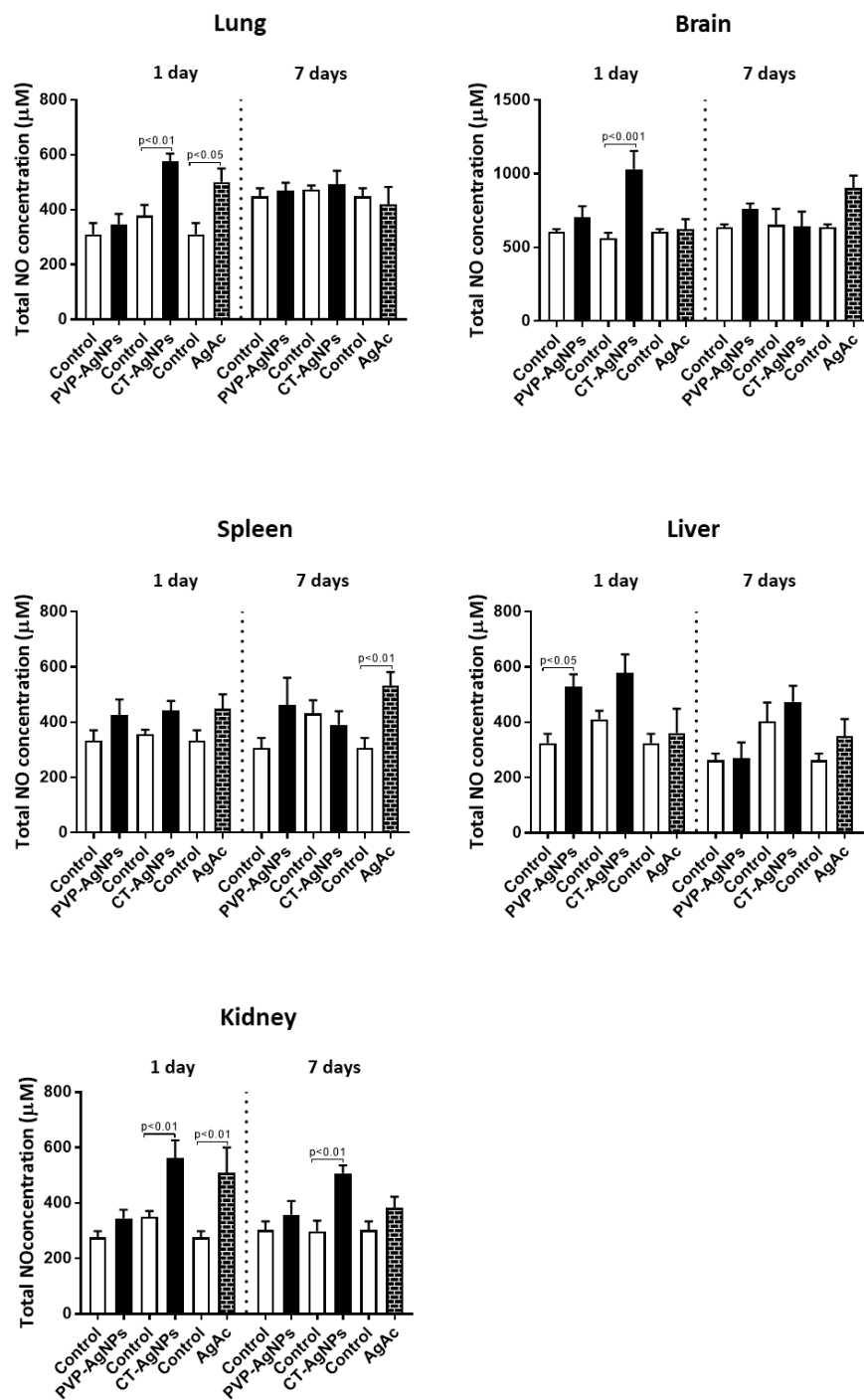


Figure 17: Total NO levels in lung, brain, spleen, liver and kidney tissues following 1-day and 7-days of intra-tracheal instillation of saline (control) or citrate 2 mM (control) or polyvinylpyrrolidone (PVP) or citrate (CT) silver nanoparticles (AgNPs) or silver acetate (AgAc) in mice. Data are mean \pm SEM ($n = 6-8$ in each group). Statistical analysis by one-way ANOVA followed by Holm-Sidak's multiple comparison test.

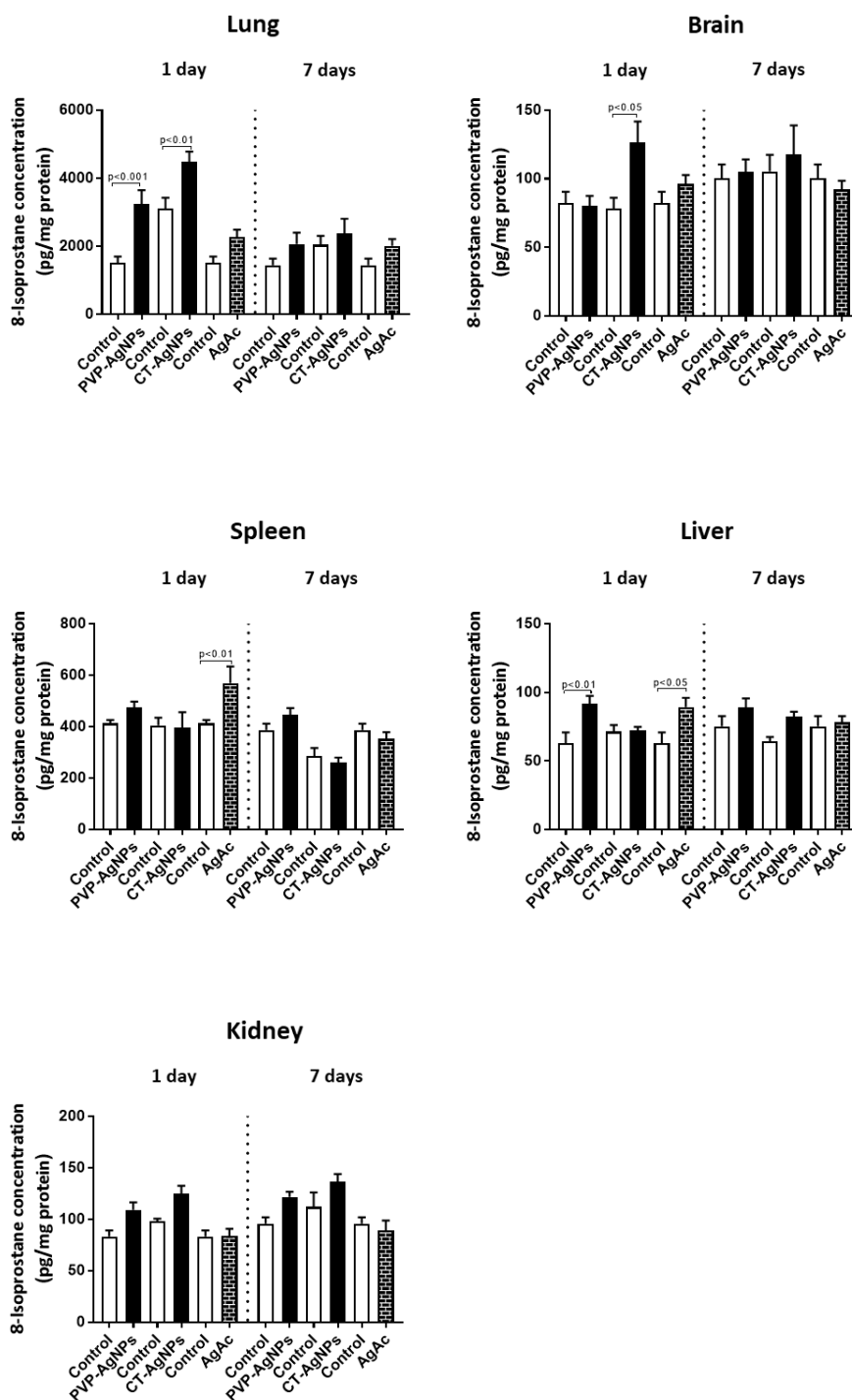


Figure 18: 8-isoprostane levels in lung, brain, spleen, liver and kidney tissues following 1-day and 7-days of intra-tracheal instillation of saline (control) or citrate 2 mM (control) or polyvinylpyrrolidone (PVP) or citrate (CT) silver nanoparticles (AgNPs) or silver acetate (AgAc) in mice. Data are mean \pm SEM ($n = 6-8$ in each group). Statistical analysis by one-way ANOVA followed by Holm-Sidak's multiple comparison test.

Effect of AgNPs and Ag⁺ ions on 8-OH-dG concentrations in tissue homogenates

Figure 19 shows the concentration of 8-OH-dG in lung, liver, kidney, spleen, and brain following 1 and 7-days of i.t. instillation of either AgNPs or Ag⁺. Following 1-day exposure, while the concentration of 8-OH-dG significantly increased for CT-AgNPs in lung ($P < 0.01$) and brain ($P < 0.05$), for PVP-AgNPs the increase was significant in lung ($P < 0.001$) and liver ($P < 0.05$) compared to their respective control. A significant increase was also observed with Ag⁺ in lung ($P < 0.05$) and liver ($P < 0.001$). No effect on 8-OH-dG was observed following 7-days of i.t. instillation of either AgNPs or Ag⁺.

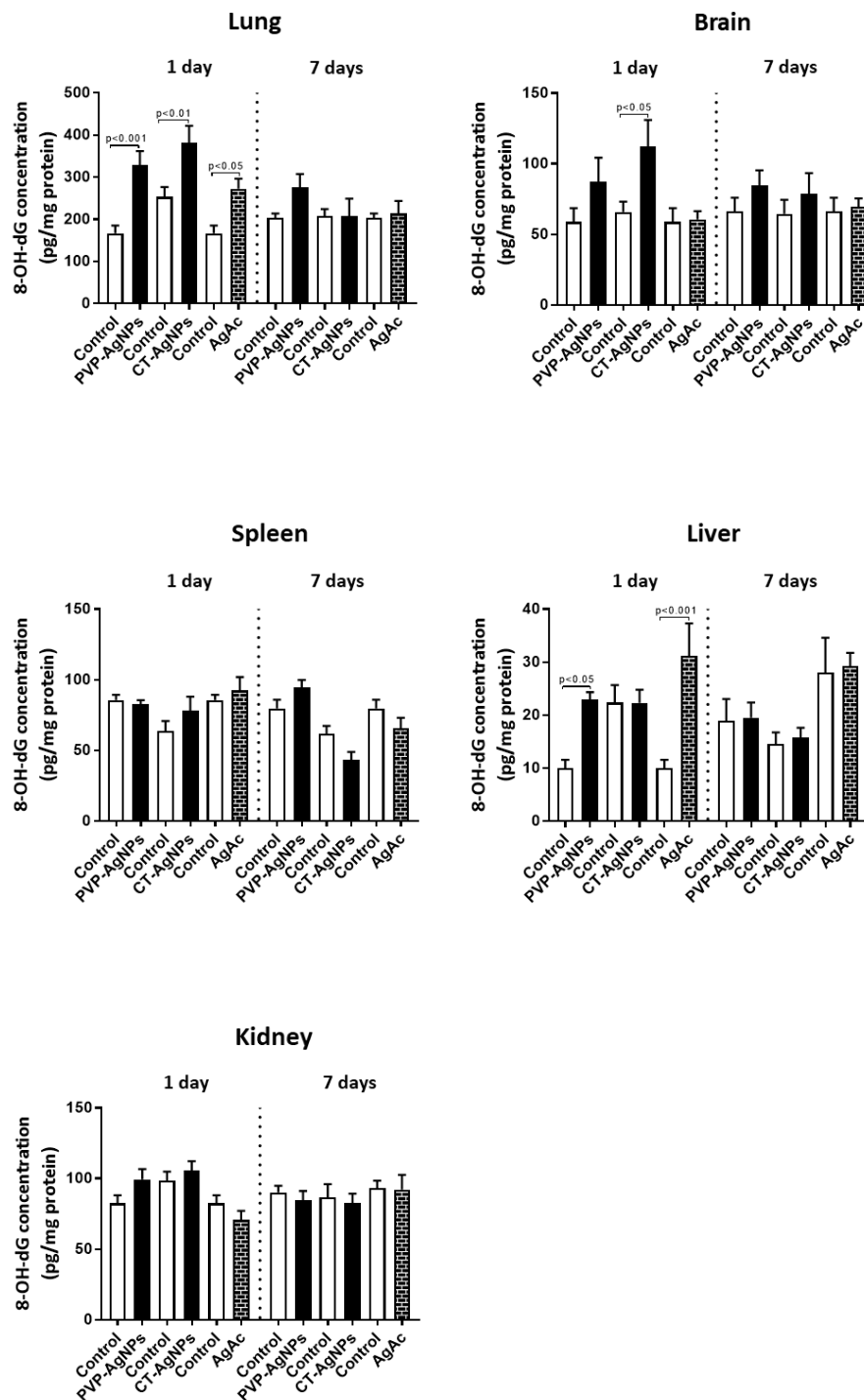


Figure 19: 8-hydroxy-2-deoxyguanosine (8-OH-dG) levels in lung, brain, spleen, liver and kidney tissues following 1-day and 7-days of intra-tracheal instillation of saline (control) or citrate 2 mM (control) or polyvinylpyrrolidone (PVP) or citrate (CT) silver nanoparticles (AgNPs) or silver acetate (AgAc) in mice. Data are mean \pm SEM ($n = 6-8$ in each group). Statistical analysis by one-way ANOVA followed by Holm-Sidak's multiple comparison test.

Measurement of apoptosis

Figure 20 represents percentage of tunel positive cells with the representative images for all particles in lung, brain and liver. Following 1-day post exposure, compared to the respective controls, a significant increase was observed with CT - AgNPs in lung ($P < 0.001$) and brain ($P < 0.001$), and PVP- AgNPs showed significant increase in lung ($P < 0.001$) and liver ($P < 0.001$). Ag^+ ions showed significant increase in liver ($P < 0.001$). No significant changes were observed post 7-days of instillation. No apoptosis has been detected in the kidney or spleen for either particles at any time point.

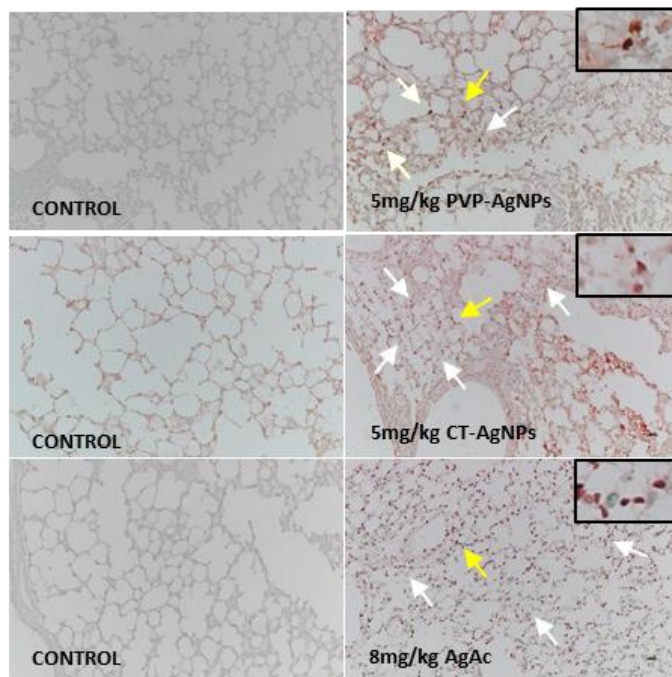
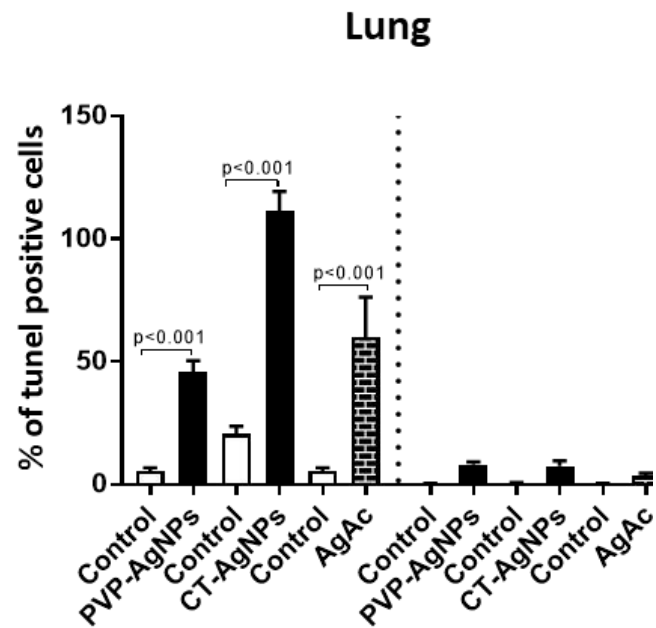


Figure 20: Estimation of apoptotic cells by an in situ TUNEL assay in tissue sections and their representative images, following 1-day and 7-days of intratracheal instillation of saline (control) or citrate 2 mM (control) or polyvinylpyrrolidone (PVP) or citrate (CT) silver nanoparticles (AgNPs) or silver acetate (AgAc) in mice. The inset images are represented by yellow arrows. Counts of apoptotic cells were made in the sections (n=7-8 per group) at a final magnification of X200 and the average of apoptotic cell numbers in per group were calculated.

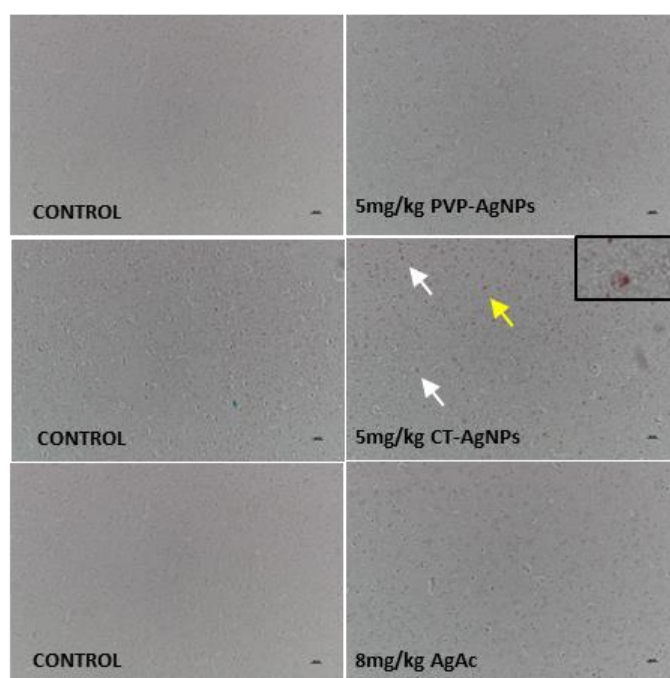
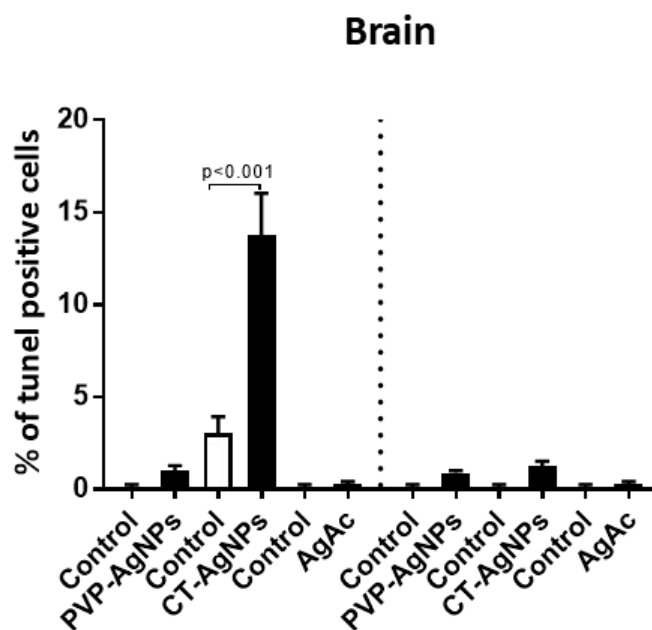


Figure 20: Estimation of apoptotic cells by an in situ TUNEL assay in tissue sections and their representative images, following 1-day and 7-days of intra-tracheal instillation of saline (control) or citrate 2 mM (control) or polyvinylpyrrolidone (PVP) or citrate (CT) silver nanoparticles (AgNPs) or silver acetate (AgAc) in mice. The inset images are represented by yellow arrows. Counts of apoptotic cells were made in the sections (n=7-8 per group) at a final magnification of X200 and the average of apoptotic cell numbers in per group were calculated (cont'd).

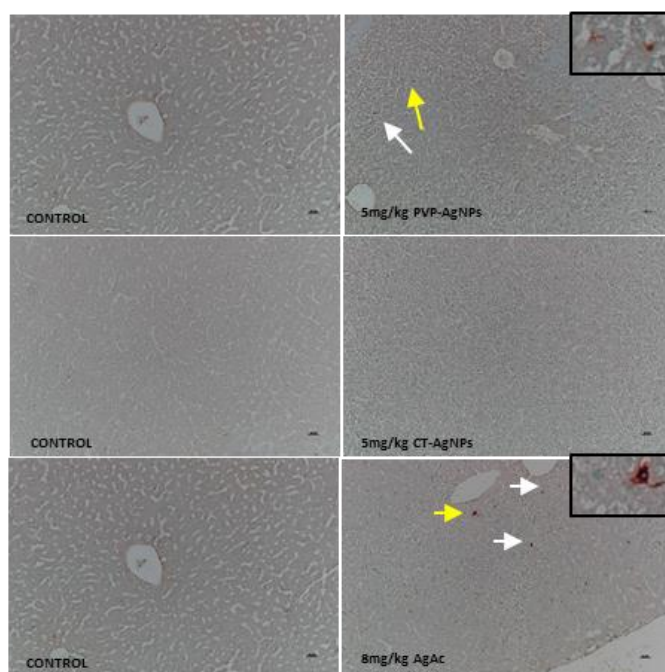
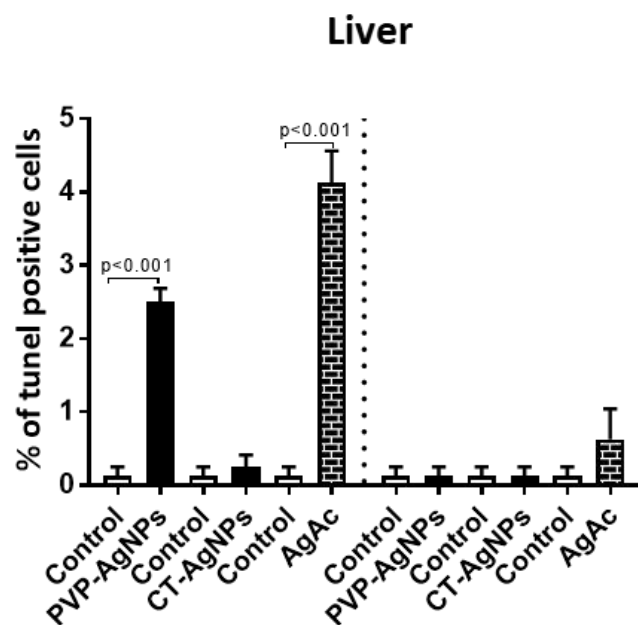


Figure 20: Estimation of apoptotic cells by an in situ TUNEL assay in tissue sections and their representative images, following 1-day and 7-days of intra-tracheal instillation of saline (control) or citrate 2 mM (control) or polyvinylpyrrolidone (PVP) or citrate (CT) silver nanoparticles (AgNPs) or silver acetate (AgAc) in mice. The inset images are represented by yellow arrows. Counts of apoptotic cells were made in the sections (n=7-8 per group) at a final magnification of X200 and the average of apoptotic cell numbers in per group were calculated (cont'd).

Measurement of total Ag content in tissues

Table 8 shows the distribution of Ag in lung, heart, liver, kidney, spleen and brain. Following 1-day of i.t. instillation, highest concentration of Ag was detected in spleen, liver, lung, heart, kidney and brain. For CT-AgNPs, the highest concentration was detected in lung followed by spleen, liver, heart, kidney and brain. For Ag⁺ ions the highest amount was detected in liver followed by lung, spleen, heart, kidney and brain. Post 7-days instillation, the amount of silver detected was reduced for all the particles used. However, Ag content was more some organs for the AgAc treated group compared with PVP- or CT- AgNPs treated group.

Table 8: Concentrations of Ag ($\mu\text{g/g}$) in lung, heart, brain, kidney, spleen and liver following 1-day and 7-days of intra-tracheal instillation of polyvinylpyrrolidone (PVP) or citrate (CT) silver nanoparticles (AgNPs) or silver acetate (AgAc) in mice.

Organs	Amount of Silver ($\mu\text{g/g}$ of tissue)					
	1 day			7 days		
	PVP-AgNPs	CT-AgNPs	AgAc	PVP-AGNPs	CT-AgNPs	AgAc
Lung	0.10 \pm 0.02	0.11 \pm 0.03	0.72 \pm 0.25	0.19 \pm 0.1	0.06 \pm 0.01	0.4 \pm 0.09
Heart	0.04 \pm 0.01	0.01 \pm 0.01	0.15 \pm 0.06	0.01 \pm 0.0	0.0 \pm 0.0	0.08 \pm 0.07
Brain	0.02 \pm 0.0	0.02 \pm 0.0	0.07 \pm 0.1	0.03 \pm 0.0	0.02 \pm 0.0	0.08 \pm 0.4
Kidney	0.02 \pm 0.01	0.01 \pm 0.0	0.13 \pm 0.04	0.0 \pm 0.0	0.0 \pm 0.0	0.28 \pm 0.27
Spleen	0.18 \pm 0.08	0.05 \pm 0.01	0.49 \pm 0.16	0.01 \pm 0.01	0.0 \pm 0.0	0.25 \pm 0.24
Liver	0.13 \pm 0.05	0.05 \pm 0.02	0.9 \pm 0.26	0.01 \pm 0.01	0.0 \pm 0.0	0.35 \pm 0.3

Data are mean \pm SEM ($n = 4-6$ in each group).

3.4.4 Discussions

Silver is one of the most frequently used nanomaterials for consumer products and respiratory exposure to AgNPs containing aerosolized products provides a potential route of interaction with human health. The effects to inhaled or instilled AgNPs have been discussed in several studies though there is discrepancies in their results. For instance, a 28-day inhalation toxicity study on rats showed no significant changes in the hematology and blood biochemistry in either the male or female rats following 11-14 nm AgNPs at concentration of $1.73 \times 10^4/\text{cm}^3$, $1.27 \times 10^5/\text{cm}^3$ and 1.32×10^6 particles/ cm^3 [161]. Likewise Hyun *et al.* [164] exposed rats to 12-15 nm AgNPs for similar duration and doses and showed no remarkable histopathological changes in the nasal cavity and lung of the exposed group compared to the control group. On the other hand, 14-days and 90-days exposure studies to 20 nm and 18 nm AgNPs respectively, demonstrated dose-dependent pulmonary inflammation, alterations in pulmonary functions and brain gene expression [163, 165].

Several studies not only reported the occurrence of lung inflammation and oxidative stress but also particle translocation and accumulation in secondary organs, such as the liver, following i.t. instillation or inhalation AgNPs [110, 161, 167, 168, 171]. In addition, few other researches also demonstrated the biodistribution of pulmonary exposed AgNPs to kidney, spleen, brain, olfactory bulb and placenta [110, 167-169]. However, the effects of AgNPs on these organs have not been clearly identified. Moreover, we have recently showed that pulmonary exposure to AgNPs induce time and dose-dependent cardiovascular effects [176]. The data in the latter study revealed significant effect of AgNPs on proinflammatory markers, oxidative stress, DNA damage and apoptosis in heart [176]. Consequently, we thought it was

important to assess the pathophysiological mechanisms and biodistribution of pulmonary exposure to AgNPs in other distant major organs including liver, brain, spleen and kidney. Thus, in the present study, we did not assess the impact of AgNPs on cardiac inflammation, oxidative stress and apoptosis because this has been recently reported by our group [176]. However, we have included the heart in the study related to the biodistribution of AgNPs.

The particles, route of administration (i.t.), and time points (1 day and 7-days) were chosen to be the same as that of our recent paper where we investigated the effect of i.t. instilled PVP- and CT- AgNPs in heart and plasma [176]. In the latter study, we used 3 doses (0.05, 0.5 and 5 mg/kg BW) and observed the effects in cardiovascular system were more prominent and significant at the dose of 5 mg/kg AgNPs and equivalent dose of 8 mg/kg AgAc. Hence, we chose the same dose to evaluate the pathophysiological responses in other major organs for the present study. As far as we are aware, no study has investigated systematically the biodistribution and the inflammation (TNF- α and IL-6), oxidative stress (GSH, total NO and 8-isoprostane), and DNA damage (8-OH-dG and TUNEL assay) in the lung and important secondary organs including liver, kidney, spleen, and brain.

Our histological data show that exposure to PVP- or CT- AgNPs or Ag⁺ ions triggered lung inflammation substantiated by interstitial infiltration of inflammatory cells consisting of neutrophils, lymphocytes and macrophages. All the observed effects persisted after 7-days of instillation and this corroborates the results of Silva *et al.* who demonstrated persistence of inflammatory infiltrates at 7-days post exposure of either PVP- or CT- AgNPs [173]. Interesting to note that, no significant difference were observed in the intensity of inflammation between the different coatings and different

particle used, AgNPs or Ag⁺ ions, which suggests that the extra-pulmonary effects observed herein by subsequent assays could be attributed to either the AgNPs themselves or inflammation induced or due to the release of Ag⁺ ions [234].

The present data further revealed that pulmonary exposure to AgNPs induced a significant augmentation in the concentrations of two of the major pro-inflammatory cytokines, TNF- α and IL-6. While PVP- AgNPs caused significant increase of TNF- α in lung, CT- AgNPs showed increase in brain and liver. As for IL-6, CT- AgNPs induced significant increase in lung, brain and liver, while PVP-AgNPs showed the increase only in lung. The Ag⁺ ions on the other hand induced these effects in kidney and spleen. None of these effects persisted after 7-days except for TNF- α in lung caused by PVP-AgNPs, and TNF- α and IL-6 in kidneys caused by Ag⁺ ions. Interestingly, a significant increase of TNF- α and IL-6 have also been observed in heart post 1-day exposure to PVP- and CT- AgNPs in our recent study [176]. Oxidative stress, characterized by the formation of a wide range of reactive oxygen species, is a key pathological process in a variety of disease conditions affecting various organs such as the lung, heart, kidney and liver. It subsequently results in DNA, protein, and lipid damage leading to cellular dysfunction and death [241]. Beside measuring markers of inflammation, we also provide evidence that both coating AgNPs cause significant increase in oxidative stress. While CT- AgNPs showed increase in GSH in lung, brain, kidney and spleen, PVP- AgNPs increased GSH in kidney and liver and Ag⁺ ions in spleen, following 1-day exposure. An increase of total NO was also observed with CT- AgNPS in lung, brain and kidney; PVP- AgNPs in liver; and Ag ions in lung and kidney. These effects however declined 7-days post exposure except for effect CT- AgNPs in kidney. Our present data also show that exposure to AgNPs induced a significant increase of 8-isoprostane, a marker of lipid

peroxidation, in the lungs and brain (for CT coating), in lung and liver (for PVP-coating) and in spleen and liver for Ag⁺ ions. Augmentation of oxidative stress markers including GSH, total antioxidants and 8-isoprostane were also observed in heart of PVP- and CT- AgNPs exposed mice [176]. This derangement of oxidative biomarkers is in line with other previous reports and indicate that either parenteral or oral administration of AgNPs promoted inflammatory reactions and oxidative stress in lung, liver, and brain [159, 187, 193, 207]. Even though the release of markers investigated in this study varied between the particle type used and the investigated organs, at least one or more than one marker of inflammation and oxidative stress augmented in each studied organ, showing the occurrence of inflammation and oxidative stress after i.t. instillation of AgNPs.or Ag⁺ ions.

The effect of AgNPs on DNA damage in the remote organs following pulmonary exposure to AgNPs have never been reported so far *in vivo*. In the present study, we evaluated DNA damage in lung, brain, kidney, spleen and liver by measuring 8-OH-dG levels and apoptosis by TUNEL assay. 8-OH-dG is one of the predominant forms of free radical induced oxidative lesions, and has therefore been widely used as a biomarker for oxidative damage to DNA [244]. Increase in 8-OH-dG levels was reported in liver, brain, and kidney following administration of TiO₂, gold or iron oxide NPs [245-247]. Our present data showed that post 1-day exposure, CT-AgNPs significantly increased 8-OH-dG in lung and brain, PVP- AgNPs and Ag⁺ ions in lung and liver. TUNEL assay is one of the most widely used methods for detecting apoptotic cells in situ and is based on the ability of the enzyme terminal deoxynucleotidyl transferase to incorporate labelled dUTP into free 3'-hydroxyl termini generated by the fragmentation of DNA [248]. Apoptosis is a distinctive mode of programmed cell death and occurs as a defense mechanism when cells are damaged beyond repair,

particularly when disease or toxicant mediated damage affects cellular DNA, and cellular repair mechanisms are unable to deal with the injury [262]. Our data show significant increase in tunel positive cells in lung, brain and liver with CT- AgNPs in lung and brain; PVP- AgNPs in lung and liver and with Ag⁺ ions in lung and liver following 1 day after instillation and the results are relatable to our finding of 8-OH-dG level. Moreover, our recent paper evaluating the cardiovascular effect also showed significant increase in 8-OH-dG in heart and tunel positive cardiomyocytes following 1-day post instillation of PVP- and CT- AgNPs at concentration of 5 mg/kg [176]. Overall, pulmonary exposed PVP- and CT- AgNPs induced pro-inflammatory cells and oxidative stress in major organs including lung, heart, liver, kidney and brain, evidenced by an increase of TNF- α , IL-6, GSH, NO and 8-isoprostane, and caused DNA damage, thereby reinforcing the previously established mechanisms of DNA damage caused by reactive oxygen species and eventually resulting in cellular dysfunction and apoptosis [238, 249].

Distribution of silver in the different organs, 1 day and 7 days after i.t. exposure to CT- and PVP-coated AgNPs and Ag⁺ ions were evaluated using ICP-MS. Our present data revealed accumulation of silver, post 1 day of i.t. instillation, in all the organs examined with the highest in lung, spleen and liver, similar to previous respiratory exposed AgNPs studies [110, 161, 167, 169]. Interestingly, particles administered intravenously or intraperitoneally also showed liver, spleen and kidney to be the major target organs for Ag accumulation [40, 73, 112]. Ag was also detected in organs following 7-days post exposure to Ag⁺ ions, with some of the organs showing more than that treated with AgNPs, Furthermore, the findings in our study suggest that lung exposed 10 nm AgNPs were translocated either in nanoparticulate or ionic form

and distributed to the different tissues during the 1st day as well as 7th day post exposure.

To conclude, with this study, the influence of two distinct AgNPs (size 10 nm), coating, and two post exposure endpoints (1 and 7 days) were comprehensively assessed in an *in vivo* model. We demonstrated acute toxic effect of AgNPs as well as Ag⁺ ions at the site of administration i.e. lung, as well as in the remote organs including brain, kidney, spleen and liver. It is of utmost significance that particle deposited in lung are not only ably to translocate and accumulate in various organs, but also induce pathophysiological effect in the same. More importantly these particles were able induce DNA damage and apoptosis in brain. In this regard, Lee *et al.* [165] also demonstrated alteration in brain gene expression caused by short term pulmonary exposure of 20 nm AgNPs, in mice. These results suggest that application of AgNPs has to be carefully considered with respect to size, dose, coating and duration of exposure. It is also important to highlight that Ag⁺ ions revealed a dissimilar pattern of toxicity emphasizing the fact that, the *in vivo* effect of AgNPs observed, may not only be attributed to release of Ag⁺ ions but also to the nanoparticulate form. The persistence of these pathophysiological effects following single i.t. administration reported in the present study, and the fact that occupational and consumer exposure to AgNPs are not time limited, additional studies are warranted to evaluate the chronic effect of AgNPs exposure.

3.5 Study three: The *in vitro* effect of polyvinylpyrrolidone and citrate coated silver nanoparticles on erythrocytic oxidative damage and eryptosis

3.5.1 Background

Extensive increase in the use of AgNPs has raised serious concerns about their potential adverse effects and toxicity on human health [24, 25]. There are several mechanisms through which AgNPs can enter the human body and interact with blood components, either directly, or indirectly. The respiratory system provides a major portal for AgNPs used extensively in healthcare and hygiene sprays [263]. In this context, several animal and human studies have demonstrated significant alveolar-capillary translocation of inhaled nanoparticles via endocytosis or transcytosis [263-265]. In addition, penetration into hair follicles of NPs has been previously reported [266]. In fact, close contact with AgNPs used as coatings in surgical dressings may allow AgNPs to penetrate the skin barrier and enter the capillaries [263]. AgNPs are also used widely as food preservatives and water disinfectants [267]. Hence, the gastrointestinal system provides another route for AgNPs entry to human body [263]. Other potential route of AgNPs in case of biomedical applications includes parenteral administration, where AgNPs are able to directly interact with blood components [268], including erythrocytes and may potentially induce pathophysiological effects.

Previous studies using diesel exhaust particle (DEP), silica nanoparticles (SiNPs) and lead nanoparticles (PbNPs) have demonstrated significant hemolysis and oxidative stress on human, rat and mouse erythrocytes [269, 270]. In addition, studies using human erythrocytes have investigated the effects of AgNPs on hemolysis, morphology and their uptake [139, 141]. Nevertheless, the mechanism underlying the

pathophysiological effects of AgNPs on erythrocytes physiology is not fully understood.

Several physiochemical properties determine the toxicity of AgNPs including their size, shape and surface chemistry [74]. In addition, coating has been reported to play an important role in NPs toxicity. In this context, *in vivo* studies have reported that polyvinylpyrrolidone (PVP) and citrate (CT) coated AgNPs induce tissue specific toxicity and aggravate cardiac ischemic reperfusion injury [73, 175]. Moreover, a previous *in vitro* study has shown that PVP- and CT- AgNPs induce toxicity in J774A.1 macrophage and HT29 epithelial cells [47]. Also, Huang *et al* [145] have investigated the hemolytic effect of PVP- and CT- AgNPs on human erythrocytes. However, to our knowledge, no study has comprehensively evaluated the effect of PVP- and CT- AgNPs on hemolysis, oxidative stress, calcium homeostasis and eryptosis. Hence, the aim of our study was to investigate the mechanism underlying the effect of PVP- and CT- AgNPs, at various concentrations (2.5, 10 and 40 $\mu\text{g/ml}$), on hemolysis, uptake of AgNPs by erythrocytes, oxidative stress, intracellular calcium, annexin V, caspase 3 and calpain.

3.5.2 Materials and Methods

Particles

Suspensions of silver nanoparticles of 10 nm (BioPure™), coated with either PVP or CT were purchased from NanoComposix (San Diego, CA, USA). The provided stock concentrations were 1.0 mg/ml with endotoxin level <5 EU/ml and silver purity of 99.99%. The zeta potential of PVP- and CT- AgNPs were -26 mV and -33 mV, respectively, and the surface areas were 53.5 m²/g and 59.0 m²/g, respectively.

The pH of both the suspensions was 7.4. The suspending solvents of PVP- and CT-AgNPs were 0.9% NaCl and 2.0 mM sodium citrate, respectively. To minimize aggregation, the stock particle suspensions were always sonicated for 15 min and vortexed for 30 sec before their dilution, or before incubation with erythrocytes.

Transmission electron microscopy (TEM) of AgNPs

We analyzed the nanoparticle suspension used in our study by TEM. The suspensions were primarily subjected to sonication at room temperature for 15 min prior to processing for TEM. A drop of PVP- and CT- AgNPs suspensions were deposited on a 200 mesh Formvar/Carbon coated copper grid and allowed to dry for 1 hr at room temperature. Then the grids were examined and photographed at different magnifications using FEI Tecnai Biotwin Spirit G2 TEM (FEI, Eindhoven, Netherlands).

Animal handling and blood collection

Balb/C mice were housed in light (12 hrs light:12 hrs dark cycle) and temperature controlled ($22 \pm 1^\circ\text{C}$) rooms. They had free access to water and standard pallet diet ad libitum. All experimental procedures were in accordance with protocols of the Institutional Animal Care and Research Advisory Committee and the project approved by Institutional Review Board of United Arab Emirates University.

Animals were anesthetized intraperitoneally with sodium pentobarbital 30 mg/kg, and then blood was drawn from the inferior vena-cava with syringe prewetted with 4% sodium citrate and collected in ethylenediamine tetraacetic acid (4%) containing tubes. The blood sample was then processed according to the type of experiment conducted.

Preparation of erythrocytes

The method for preparation of erythrocytes used in the present study has been previously described [271, 272]. Briefly, collected mouse blood was mixed by gentle inversion of tube and centrifuged at 1200 g for 15 min. The plasma supernatant was discarded, and the erythrocytes were washed 4 times by suspending them in 0.9% NaCl followed by centrifugation at 1200 g for 10 mins. The final suspension consisted of 5% by volume of erythrocyte in saline. Flat bottom well plates were used to incubate 840 μ l of erythrocyte with 160 μ l of PVP- and CT- coated AgNP suspensions (2.5, 10 and 40 μ g/ml). Negative control consisted of 0.9% NaCl and 2 mM Citrate respectively. Positive control consisted of 0.1% Triton X 100. The plates were incubated for 4 h at room temperature under shaded light, shaking gently on an orbital plate shaker. After incubation the samples were transferred to 1.5 ml eppendorf tube and were centrifuged at 1200 g for 5 min. The resulting supernatant was collected for hemolysis assay, annexin V and oxidative markers assays. The deposited erythrocytes were fixed with Karnovsky's fixative (2% paraformaldehyde and 2.5% glutaraldehyde in 0.1 M phosphate buffer at 7.2 pH) for TEM.

Hemolysis assay

The hemolysis assay was performed according to previously reported technique [269, 273]. Briefly, erythrocytes incubated with PVP- and CT- AgNPs was centrifuged as described above. After that, 90 μ l of the supernatant was added in a 96 well plate and the amount of hemoglobin released was determined spectrophotometrically at a wavelength of 540 nm. The percent hemolysis was calculated using the linear equation $y = mx + c$ where %hemolysis (x) = [(sample

optical density (y) – negative control optical density (c))/ (positive control optical density – negative control optical density) (m)] * 100 [271, 272].

Erythrocyte analysis by TEM

Fixed cells were processed according to method described previously [269]. Briefly, the cells were washed with 0.1 M phosphate buffer and for 1 hr at room temperature on rotamixer and post fixed with 1% osmium tetroxide in 100 mM cacodylate buffer. After that cells were dehydrated in a series of graded ethanol concentration, infiltrated with Agar 100 epoxy resin, embedded into resin filled molds and polymerized at 65°C for 24 hrs. Blocks were trimmed and ultrathin sections were obtained by an ultra-microtome (Leica, Mikrosysteme GmbH, Wien, Austria). Ultrathin sections were collected on 200 mesh Cu grids and were contrasted with uranyl acetate and followed by lead citrate double stain. The grids were examined and photographed at variable magnification by TEM [269, 274].

Measurements of oxidative stress markers

Supernatants were collected after incubation of erythrocytes with PVP- and CT- AgNP (2.5, 10 and 40 µg/ml) by the process described above and was subjected to oxidative stress marker assay. The erythrocytes treated with 0.9% NaCl and 2 mM citrate were taken as control. Erythrocyte malondialdehyde (MDA) was quantified colorimetrically following its controlled reaction with thiobarbituric acid [275] with a commercially available kit (Cayman chemicals, Ann Arbor, MI, USA). Reduced glutathione (GSH) concentration (Sigma Chemicals, St Louis, MO, USA) and catalase (CAT) activity (Activity kit, Cayman chemicals, Ann Arbor, MI, USA) were analyzed spectrophotometrically according to methods described by the manufacturers.

Measurement of intracellular calcium

Intracellular Ca^{2+} was measured in incubated medium of erythrocytes treated with either vehicle or various concentrations of PVP- and CT- AgNPs according to a previously described technique [276]. Briefly, erythrocytes were washed with saline (0.9% NaCl) four times followed by centrifugation for 10 min at 1200 g. The erythrocytes were then resuspended in 1 mM Ringers solution. The final suspension consisted of 0.5% hematocrit of erythrocyte in 1 mM Ringers solution. The cells were then incubated in a flat bottom plate with the AgNPs at 37°C for 4 hrs. After that the incubated cell suspensions were collected in eppendorf tube and centrifuged for 5 min at 1200 g. The supernatant was discarded, and the cells resuspended in 5 mM Ringers solution to which 5 μl of Fura 2AM (Calbiochem; La Jolla, CA, USA) was added and incubated for 15 min at 37°C in dark on a shaker. After that, the cell suspensions were centrifuged at 1200 g for 5 min. The Fura 2AM loaded erythrocytes were resuspended in 1 mM Ringers solution and incubated for 30 min at 37°C in dark on a shaker. Finally Ca^{2+} - dependent fluorescence intensity was then monitored with a fluorometer (model SFM 25, Kontron; Zurich, Switzerland) set at 340 nm excitation and 510 nm emission [277].

Assessment of Annexin V

Annexin V bound to exposed phosphatidylserine was measured in incubated medium of erythrocytes using mouse ANXA5 ELISA kit according to manufacturer's instruction (Elabscience, Texas, USA).

Caspase 3 analysis

The activity of caspase 3 was determined in incubated medium of erythrocytes using a caspase 3 activity fluorometric assay kit according to manufacturer's instruction (BD Biosciences, San Jose, CA)

Moreover, caspase 3 expression was analysed by Western blot analysis according to previously described technique [278]. Freshly isolated erythrocytes that were incubated with either vehicle or various concentrations of PVP- or CT- AgNPs, were washed twice in PBS and lysed in 250 μ l of radioimmunoprecipitation assay (RIPA) buffer (25 mM Tris-HCl pH 7.6, 150 mM NaCl, 1% NP-40, 1% sodium deoxycholate, 0.1% SDS) containing protease and phosphatase inhibitor. Insolubilized material was removed by centrifugation at 14000 g for 15 min. The supernatants were immediately removed and used for protein estimation using a Pierce bicinchoninic acid protein assay kit (Thermo Scientific, Waltham, MA, USA). A 100 μ g of protein/ lane was electrophoretically resolved by 12% sodium dodecyl sulfate polyacrylamide gel electrophoresis (SDS-PAGE) and then transferred onto polyvinylidene difluoride membranes. The immunoblots were blocked for 2 hrs, with 5% nonfat dry milk in 1X Tris-buffered saline containing Tween 20 (1%, v/v) (TBST) and subsequently incubated overnight at 4°C with rabbit polyclonal caspase-3 antibody (1:1000 dilution, Cell Signalling Technology, Danvers, MA, USA) in 5% w/v nonfat dry milk. The blots were then incubated with goat anti-rabbit IgG horseradish peroxidase (HRP) conjugated secondary antibody (1:5000 dilution, Abcam), for 2 hrs, at room temperature, and developed using Pierce enhanced chemiluminescent plus Western blotting substrate Kit (Thermo Scientific). The densitometric analysis of the protein bands was performed for caspase-3 with Typhoon FLA 9500 (GE Healthcare Bio-

Sciences AB, Uppsala, Sweden). Blots were then re-probed with mouse monoclonal β -actin HRP conjugated antibody (1:1000 dilution, Santa Cruz Biotechnology, Dallas, Texas, U.S.A) and used as a loading control.

Measurement of calpain activity

The activated calpain in cytosol of incubated erythrocytes was flurometrically determined using a calpain activity assay kit according to manufacturer's instruction (Genway Biotech, San Diego, USA).

Statistics

All statistical analyses were performed with GraphPad Prism Software version 7 (San Diego, CA, USA) and the data and figures were reported as mean \pm SEM. Comparisons between groups were performed by one-way analysis variance (ANOVA) followed by Dunnett's multiple range test. P-values < 0.05 were considered as significant.

3.5.3 Results

Characterization of PVP- and CT- AgNPs

The morphology and particle size of PVP- and CT- AgNPs were determined by TEM are shown in Figure 21. TEM analysis of PVP- and CT- AgNPs revealed homogenous particle size of approximately 10 nm in diameter and this corroborates the size provided by the manufacturer. Both types of AgNPs were spherical in shape.

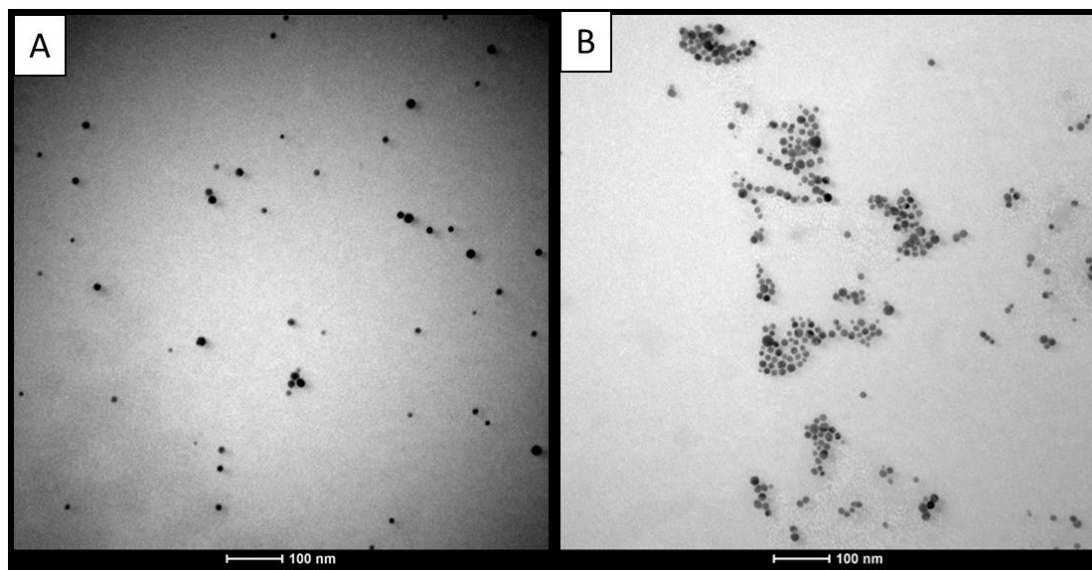


Figure 21: Transmission electron microscope analysis of polyvinylpyrrolidone (A) or citrate (B) coated silver nanoparticles.

Effect of AgNPs on erythrocyte hemolysis

Figure 22 shows the hemolytic effect of AgNPs on erythrocytes. Incubation of erythrocytes with AgNPs caused a dose-dependent hemolysis. The effects were significant at concentrations of 10 $\mu\text{g/ml}$ ($P < 0.001$) and 40 $\mu\text{g/ml}$ ($P < 0.001$) for PVP- AgNPs and at a concentration of 40 $\mu\text{g/ml}$ ($P < 0.001$) for CT- AgNPs compared with their respective controls. The degree of hemolysis observed at concentration of 2.5, 10 and 40 $\mu\text{g/ml}$ for PVP- AgNPs were 0.99%, 3.96% and 16.34% and those observed for CT- AgNPs were 2.43%, 2.67% and 16.67% respectively.

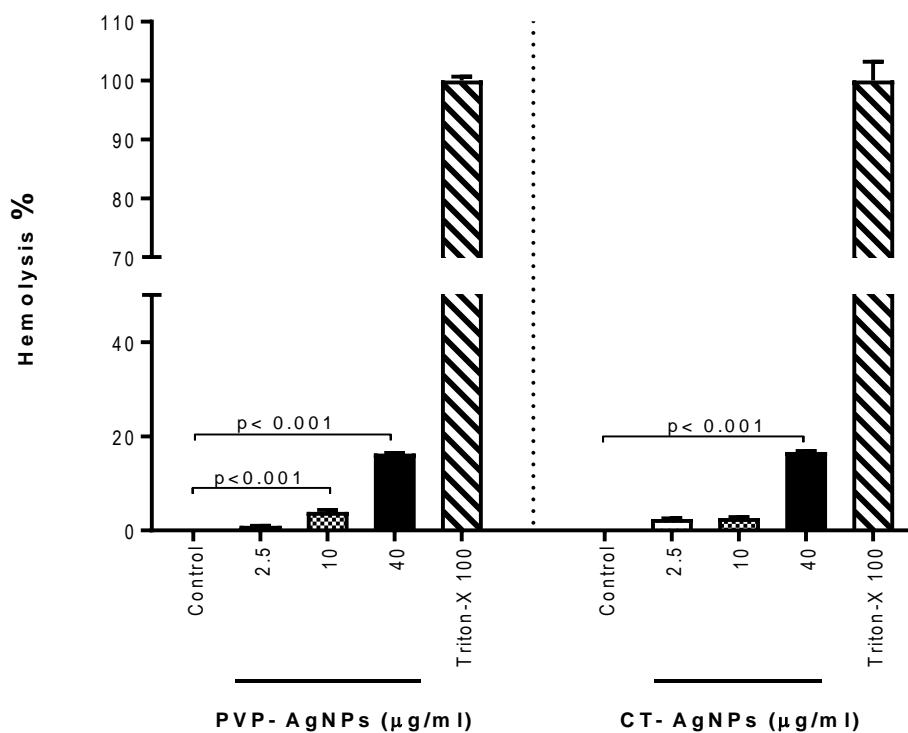


Figure 22: Hemolytic effect of polyvinylpyrrolidone (PVP) and citrate (CT) silver nanoparticles (AgNPs) on mouse erythrocytes.

Erythrocyte analysis by EM

TEM images of erythrocytes incubated with PVP- and CT- AgNPs at concentration of 2.5, 10 and 40 µg/ml are shown in Figure 23. Both types of AgNPs were found to be taken up by erythrocytes at all tested concentrations. In the erythrocytes the AgNPs were located both within as well as on the margins.

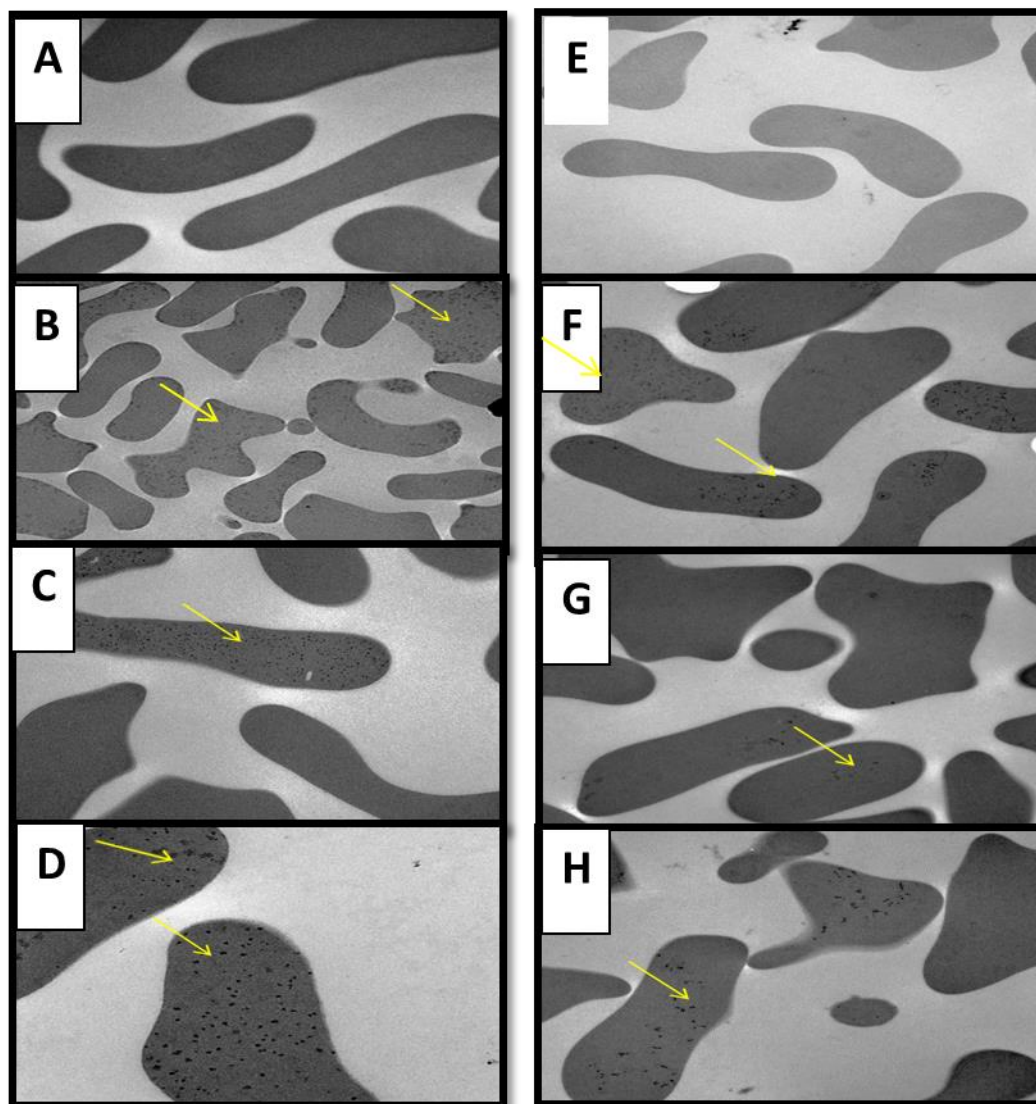


Figure 23: Transmission electron microscope (TEM) analysis of erythrocytes after in vitro incubation with saline (control, A), polyvinylpyrrolidone (PVP) silver nanoparticles (AgNPs) 2.5, 10, 40 $\mu\text{g/ml}$ (B, C, D respectively), 2 mM citrate (control, E) or citrate (CT) coated AgNPs 2.5, 10, 40 $\mu\text{g/ml}$ (F, G, H respectively). AgNPs are localized within (thin arrows) as well as on the margins (thick arrows) of the erythrocytes.

Effect of AgNPs on concentrations of MDA and GSH and CAT activity

Concentrations of MDA, GSH and measurement of CAT activity are shown in Figure 24. MDA was used to assess the susceptibility of erythrocytes lipid peroxidation *in vitro*. Compared with their respective controls, the MDA concentration

was dose-dependently increased by the incubation of erythrocytes with various concentrations of PVP- and CT- AgNPs (Fig. 24 A). However, the level of significance was only achieved at highest tested concentration, i.e. 40 $\mu\text{g/ml}$ ($P < 0.001$) for both PVP- and CT- AgNPs. Figure 24 B shows the effect of AgNPs on concentration of GSH. Compared with control, the concentration of GSH was significantly decreased. The level of significance was achieved at all studied concentrations ($P < 0.001$) for both PVP- and CT- AgNPs. Likewise, compared with their respective controls, there was a significant decrease of catalase activity in erythrocytes incubated with PVP and CT- AgNPs at all tested concentrations ($P < 0.001$) as shown in Figure 24 C.

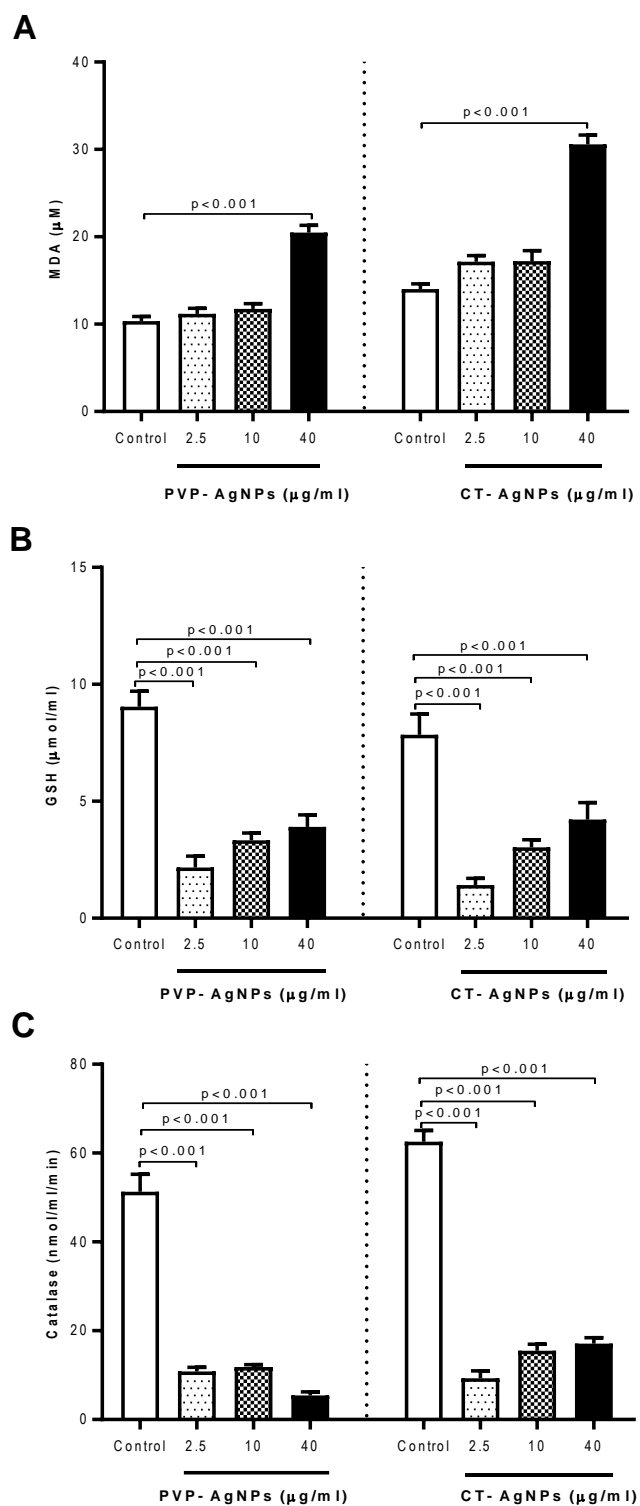


Figure 24: Effect of polyvinylpyrrolidone (PVP) and citrate (CT) silver nanoparticles (AgNPs) on concentration of malonaldehyde (MDA, A), reduced glutathione (GSH, B) and catalase activity (C) measured in the incubation medium of erythrocytes. Data are mean \pm SEM (n=8 in each group). Statistical analysis by one-way anova followed by Dunnett's multiple range test.

Effect of AgNPs on intracellular calcium

Figure 25 illustrates the effect of various concentrations of PVP- and CT-AgNPs on cytosolic calcium concentration from Fluro3 fluorescence. The incubation of erythrocytes with AgNPs caused a dose-dependent increase in cytosolic calcium concentration compared with control. While the level of significance was achieved at 10 and 40 $\mu\text{g/ml}$ ($P < 0.001$) for PVP- AgNPs, the CT- AgNPs showed increased cytosolic calcium concentration at all tested dose, i.e. 2.5, 10, and 40 $\mu\text{g/ml}$ ($P < 0.001$).

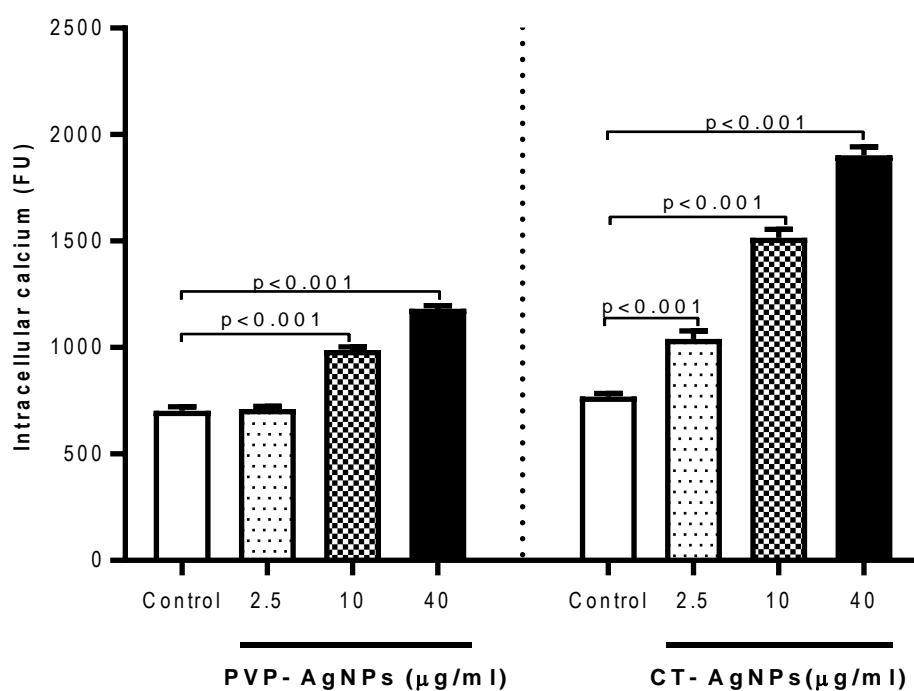


Figure 25: Effect of polyvinylpyrrolidone (PVP) and citrate (CT) silver nanoparticles (AgNPs) on intracellular calcium concentration measured in incubated erythrocytes. Data are mean \pm SEM ($n=8$ in each group). Statistical analysis by one-way anova followed by Dunnett's multiple range test.

Effect of AgNPs on annexin V-binding

Exposure of phosphatidylserine at the cell surface was estimated from bound annexin V. Incubation of erythrocyte with PVP- and CT- AgNPs triggered annexin V binding as shown in Figure 26. The effect was significant at concentration of 2.5 $\mu\text{g/ml}$ ($P < 0.05$), 10 $\mu\text{g/ml}$ ($P < 0.001$) and 40 $\mu\text{g/ml}$ ($P < 0.001$) of PVP- AgNPs. The effect of CT- AgNPs was also significant at all concentrations used, i.e. 2.5, 10 and 40 $\mu\text{g/ml}$ ($P < 0.001$).

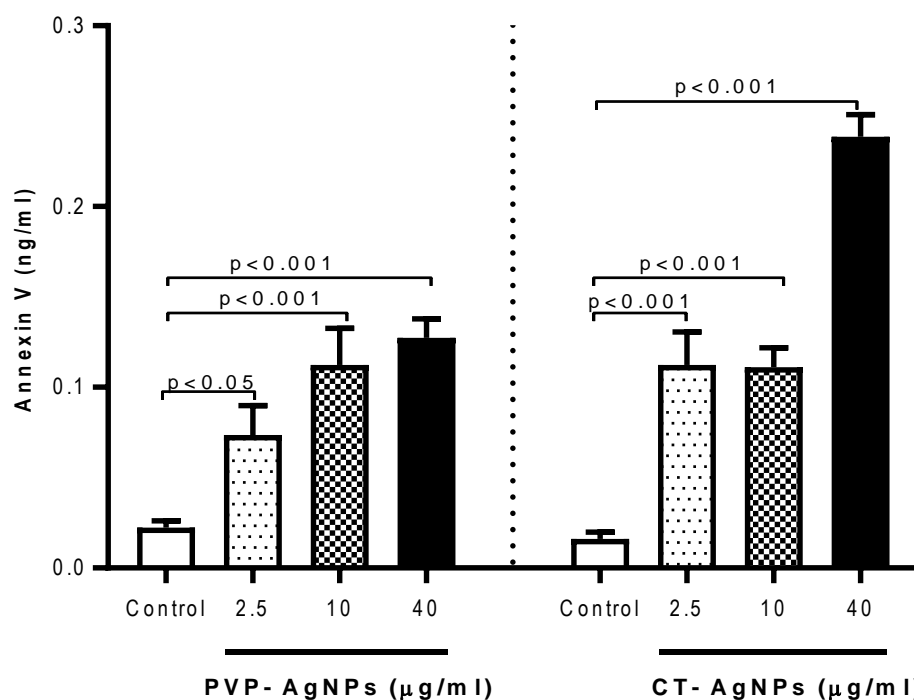


Figure 26: Effect of polyvinylpyrrolidone (PVP) and citrate (CT) silver nanoparticles (AgNPs) on the concentration of bound Annexin V in the incubation medium of erythrocytes. Data are mean \pm SEM ($n=8$ in each group). Statistical analysis by one-way anova followed by Dunnett's multiple range test.

Effect of AgNPs on caspase 3 activity and expression

The assessments of caspase 3 activity and expression in erythrocytes following exposure to various concentrations of PVP- or CT- AgNPs are represented in Figure 27. Overall, there was no effect of both PVP- and CT- AgNPs on caspase activity in incubated erythrocytes. Compared with the control group, only CT- AgNPs showed a significant increase at a dose 10 $\mu\text{g/ml}$ ($P < 0.05$). Likewise, compared with the control group, the western blot analysis showed no statistically significant effect of various concentrations of PVP- or CT- AgNPs on total caspase 3 expression in erythrocytes.

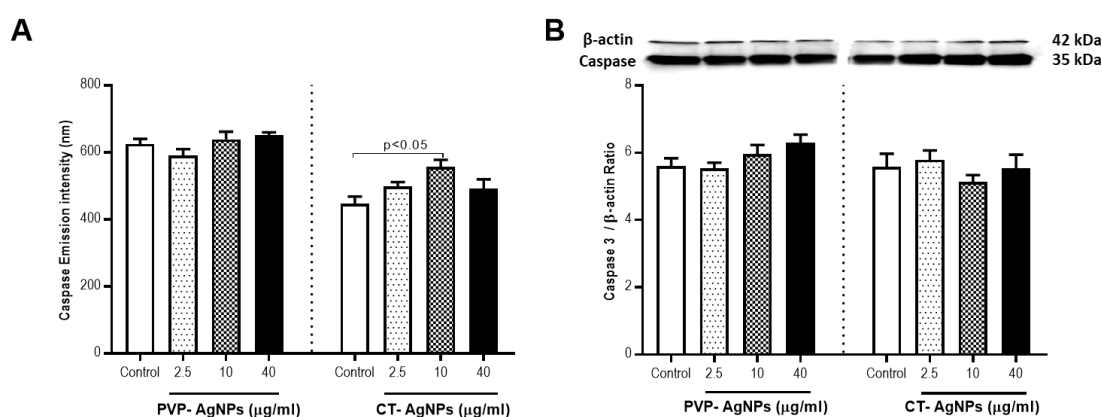


Figure 27: Effect of polyvinylpyrrolidone (PVP) and citrate (CT) silver nanoparticles (AgNPs) on erythrocyte caspase 3 activity (A) and caspase 3 expression assessed by western blotting (B). Data are mean \pm SEM ($n=7-8$ in each group). Statistical analysis by one-way anova followed by Dunnett's multiple range test.

Effect of AgNPs on calpain activity

Detection of activated calpain in cytosol upon incubation of erythrocytes with PVP- and CT- AgNPs is shown in Figure 28. Compared with the control, the incubation of erythrocytes with PVP- AgNPs caused a significant increase in calpain

activity at dose 40 $\mu\text{g/ml}$ ($P < 0.01$), and incubation with CT- AgNPs caused a significant increase in calpain activity at all concentrations used, i.e. 2.5, 10 and 40 $\mu\text{g/ml}$ ($P < 0.001$).

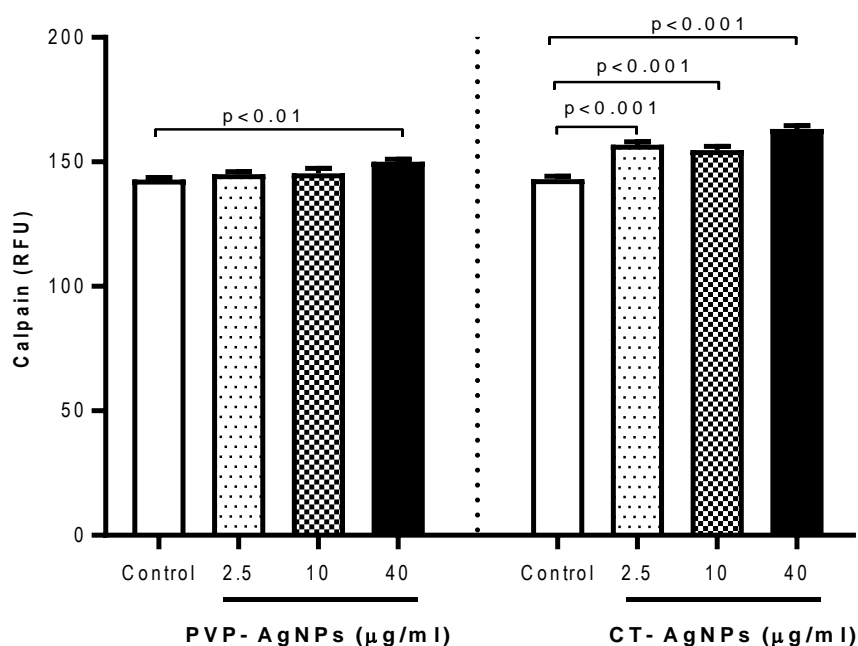


Figure 28: Effect of polyvinylpyrrolidone (PVP) and citrate (CT) silver nanoparticles (AgNPs) on calpain activity measured in incubated erythrocytes. Data are mean \pm SEM ($n=8$ in each group). Statistical analysis by one-way anova followed by Dunnett's multiple range test.

3.5.4 Discussions

In this work, we assessed the *in vitro* effects of PVP- and CT- AgNPs on mouse erythrocytes and showed that AgNPs can induce hemolysis, oxidative stress and increase cytosolic Ca^{2+} , annexin V binding and calpain activity.

Our *in vitro* erythrocyte study is relevant to previous *in vivo* studies which demonstrated that exposure to AgNPs is associated with cardiovascular dysfunction in

addition to cytotoxicity and oxidative stress [73, 175]. We incubated the erythrocytes with vehicle or PVP- or CT- AgNPs for 4 h; a time point similar to previous *in vitro* studies [139, 279]. The various concentrations of PVP- and CT- AgNPs (2.5, 10 and 40 $\mu\text{g/ml}$) used in our study are also similar to previous studies evaluating nanotoxicity and blood compatibility of erythrocytes incubated with AgNPs [141, 145]. Our concentrations are comparable with previous studies using AgNPs on human, mouse and fish erythrocytes and the highest dose of 40 $\mu\text{g/ml}$, is much lower than the optimal dose of AgNPs (200 $\mu\text{g/ml}$) that has been reported to induce hemolysis in human erythrocytes [139, 141, 145, 280-282]. In fact, in humans following oral exposure, *in vivo* serum concentration of AgNPs of up to 10 $\mu\text{g/ml}$ has been reported [283, 284]. The latter is within the range of concentrations of AgNPs that we used in our present study. Both particle size and coating have been reported to play critical role in NP-induced toxicity; size <50 nm AgNPs induces greater hemolysis and increased uptake by erythrocytes [47, 141, 145, 282]. Hence, we presently assessed the impact of 10 nm AgNPs with 2 different coating, namely PVP and CT.

Our hemolytic assay results show that both 10 nm PVP- and CT- AgNPs cause a dose-dependent hemolysis. Similar results were obtained when fish and human erythrocytes were incubated with various sizes of AgNPs (15-100 nm); the highest hemolytic activity being observed with size <50 nm AgNPs [139, 141]. Huang *et al.* [145], in a study using human erythrocytes demonstrated that PVP- AgNPs (20 nm) caused ~19% hemolysis while CT- AgNPs (20 nm) caused ~10% hemolysis at the concentration of 40 $\mu\text{g/ml}$. Research focusing on TiO_2 also showed evidence of hemolysis in rabbit erythrocytes [285]. Our previous studies on interaction of erythrocytes with DEP and amorphous SiNPs demonstrated significant dose-dependent hemolysis [269, 271]. Besides using Triton X 100 as a positive control, we

have also assessed the hemolytic effects of a positive control particle, namely amorphous SiNPs (50 nm), at a dose of 25 $\mu\text{g/ml}$ [269]. The latter results confirmed the hemolytic effect of SiNPs (data not shown). The hemolytic activity of SiNPs exposed erythrocytes has been demonstrated to be dependent on presence of negatively charged silanol groups [286]. However, the mechanism by which AgNPs may induce hemolysis is not fully understood. There is a strong body of evidence suggesting interaction of RBC with AgNPs itself can induce hemolysis, rather than released silver ion mediated cellular toxicity [139, 141]. It has been also stated that AgNPs can bind to thiol groups within proteins or phospholipids of membrane with high affinity and thereby promote denaturation [287]. Moreover, interaction of negatively charged silver surface with cations in membrane of RBC may also contribute to hemolysis [287].

To obtain more information about the possible uptake and localization of AgNPs within RBCs, TEM analysis has been performed following incubation of erythrocytes with various concentrations of AgNPs. Interestingly, both 10 nm PVP- and CT- AgNPs were observed within the erythrocytes even at our lowest concentration of AgNPs that is 2.5 $\mu\text{g/ml}$. The optimal size for uptake of AgNPs by fish erythrocytes was reported to be ~ 50 nm [141]. However, despite the presence of AgNPs in the erythrocytes the degree of hemolysis observed was relatively slight for the concentrations of 2.5 $\mu\text{g/ml}$ and 10 $\mu\text{g/ml}$ for CT- AgNPs and concentration of 2.5 $\mu\text{g/ml}$ for PVP- AgNPs. This could probably suggest that the hemolytic effect is both coating and dose dependent. Our previous studies showed that DEP and SiNPs are taken up by erythrocytes [269, 271]. Geiser *et al.* [288], in studies of TiO_2 NPs on lung cells and erythrocytes showed that particle uptake in cells was by diffusion or adhesive interactions rather than endocytosis. However, it is well established that RBC's lack

endocytic machinery and there is no actin myosin system [289], and therefore the mechanism underlying the uptake of nanoparticle by erythrocytes may be different from other phagocytic cells. Though our study does not clearly define the mechanism of entry of AgNPs into the cell it could be possible that, given their very small size, the 10 nm AgNPs were able to enter the erythrocytes via diffusion as suggested before [74]. Further studies are required to clarify this particular point.

To further clarify the possible mechanism related to hemolytic effect of PVP- and CT- AgNPs, we assessed biomarkers of oxidative stress including MDA, GSH concentration and CAT activity. MDA is one of the final products of polyunsaturated fatty acid peroxidation in the cells and is used as a marker of cell membrane injury as its production is increased with increase in free radicals [275]. Our data showed a dose-dependent increase of MDA with significance at the highest concentration 40 $\mu\text{g/ml}$ for both PVP- and CT-AgNPs. Previous *in vitro* hemolytic studies also demonstrated significant and dose-dependent increase in MDA in fish erythrocyte incubated with AgNPs (15-100 nm) at various concentrations (1.25-20 $\mu\text{g/ml}$) [141]. However, our previous study of interaction of DEP with erythrocytes demonstrated no significant changes of MDA in mouse erythrocytes at 100 $\mu\text{g/ml}$ [271]. In contrast, our other study on interaction of erythrocytes with SiNPs showed significant MDA increase even at 25 $\mu\text{g/ml}$ [269]. These results collectively indicate that the overproduction of MDA in erythrocytes is particle and dose-dependent and that both studied coating (PVP and CT) induce lipid peroxidation of RBC. Oxidative stress results from imbalance between reactive oxygen species (ROS) and the antioxidant defense system. Erythrocyte antioxidant enzymes are major circulating antioxidant enzymes in the oxidative stress defense system [290]. GSH and CAT are major enzymes that control the biological effect of ROS [290]. While GSH quenches the free radicals by serving

as electron donor, CAT converts hydrogen peroxide to water and oxygen [291]. Our data show, incubation with AgNPs results in significant decrease in GSH concentration and CAT activity compared to control. The decrease of antioxidants in the present study can be attributed to the increase of their consumption due to increase in ROS. The activity of CAT has been shown to be decreased, and the concentrations of GSH and MDA increased in trout hepatocytes incubated with selenomethionine [292]. The data of our previous study showed a significant and dose - dependent increase in CAT activity and GSH concentrations in erythrocytes treated with SiNPs [269]. The latter effect has been explained by an adaptive response that counterbalances the potentially damaging activity of free oxygen radicals by antioxidant defense mechanism [269]. Overall, these results indicate the relation between AgNPs interaction and alteration in oxidative stress and antioxidant enzymes activities.

Mature erythrocytes are highly specialized cells that lack normal cell organelles, such as nucleus and mitochondria, which are vital for the regulation of apoptosis, an innate mechanism of cell clearance [293]. The senescence involved in mature erythrocytes, is characterized by distinct changes in shape and plasma membrane with translocation of phosphatidylserine from the inner leaflet of cell membrane, and is termed as eryptosis [294, 295]. The later has been evaluated using various techniques including cytofluorometric analysis [296]. However, unlike apoptosis of erythroblast that is caspase - dependent, the mature erythrocyte is driven into eryptosis by increase in intracellular calcium which in turn triggers activation of calpain [295]. Apoptosis mediated cell death via AgNPs exposure has previously been demonstrated in various cell line including normal human lung fibroblast, glioblastoma and osteoblastic cells [297]. However, little is known about the mechanism of cell death in AgNPs - treated erythrocytes. Our data shows significant

and dose dependent increase of intracellular calcium and Annexin V binding for both PVP- and CT- AgNPs. It has been shown that increased calcium activity is due to activation of Ca^{2+} permeable cation channels which is, in turn, triggered by erythrocyte injury including oxidative stress [294]. Additionally, typical features of eryptosis including cell shrinkage, membrane blebbing, phosphatidylserine externalization has been reported in erythrocytes exposed to Ca^{2+} ionophore ionomycin or A23187 [298, 299]. Annexin V is a Ca^{2+} dependent cellular protein that has the ability to bind with phosphatidylserine and used as an apoptotic marker when exposed on outer leaflet of cell membrane [298, 300]. Our present findings also corroborates our previous study that demonstrated increased erythrocyte cytosolic calcium and annexin V binding following incubation with SiNPs [269]. However, unlike the previous study, there were no significant changes in caspase 3 activity compared to control except for CT- AgNPs at concentration of 10 $\mu\text{g/ml}$. The discrepancy between the present and the previous study could be related to type of NPs (PVP- and CT- AgNPs versus SiNPs) and/or size of NPs (10 nm versus 50 nm). The caspase activity results were further confirmed by western blot analysis, which also showed no significant changes in expression of the total caspase 3 in erythrocytes exposed to various concentration of PVP- or CT- AgNPs, compared with controls. Caspase members contain a cysteine residue and exists as zymogens that needs to undergo proteolytic cleavage before inducing its initiator or effector function in apoptosis [301]. Though the presence of caspase is well established in erythrocyte, their role in eryptosis is not clearly defined [293]. Berg *et al.* [302] suggested that the inability of caspase activation in erythrocyte might be due to presence of novel inhibitor or lack of other elements of apoptotic machinery like Apaf1 and cytochrome C. Similar to caspases, another calcium dependent cysteine protease, calpains, exists as proenzymes and is reported to play a role

in eryptosis [303]. Our data show that the incubation of erythrocytes with PVP- or CT- AgNPs, results in significant increase in calpain activity compared with control, and this increase could be attributed to the increase in cytosolic calcium. Our findings corroborates with a previous study which demonstrated that changes in intracellular calcium led to the activation of calpain [302].

To conclude, the interaction of two differently coated AgNPs was comprehensively investigated in an *in vitro* model of mouse erythrocytes. We observed that both PVP- and CT- AgNPs caused hemolysis and were taken up by the erythrocytes at all tested concentrations. We also demonstrated that PVP- and CT- AgNPs induced oxidative stress and increased cytosolic calcium, annexin V binding and calpain activity which may explain the cause of hemolysis and mechanism by which eryptosis may be triggered. More studies are required to further investigate the mechanism underlying pathophysiological effects of AgNPs on eryptosis.

Chapter 4: Conclusions, Limitations of study and Future directions

4.1 Conclusions

Owing to their antimicrobial properties AgNPs have become one of the most popular types of NMs today. Like all NMs, AgNPs may pose a pulmonary and systemic toxicity hazard should their level increase in air and translocate from the lung to systemic circulation and various distant organs, a threat that has received inadequate attention and that is the focus of our study. Collectively, this study investigated local and systemic effects of pulmonary exposed 10 nm AgNPs of 2 coatings (PVP and CT), 3 doses (0.05, 0.5 and 5 mg/kg) and at 2 different time points (1 day and 7-days) in Balb/C mice. We initially evaluated the cardiac effect of pulmonary exposed AgNPs by measuring markers of inflammation, oxidative stress, DNA damage and apoptosis in heart. Next, we evaluated the impact of AgNPs on coagulation by measuring several endpoints, i.e., thrombosis in pial arterioles and venules *in vivo*, measurement of plasma concentrations of fibrinogen, PAI-1, PT, aPTT and *in vitro* platelet aggregation. Finding significant cardiovascular effects, we further studied the biodistribution and pathophysiological effect of pulmonary exposed AgNPs on other major organs including lung, liver, kidney, spleen and brain, by quantifying silver and measuring markers of inflammation, oxidative stress, DNA damage and apoptosis. Following translocation, a major component of systemic circulation with which NPs may potentially interact with, is the erythrocytes. Hence, we also investigated *in vitro* effect of 10 nm AgNPs of both coating (PVP and CT) and at 3 concentration (2.5, 10 and 40 $\mu\text{g/ml}$) on mouse erythrocytes. All the effects of AgNPs were compared with control which are the diluents (0.9% NaCl and 2 mM citrate) used in our study as well as Ag ions.

The major findings in this thesis related to the studies described above are as follows:

4.1.1 *In vivo* studies: Pulmonary exposure to AgNPs and pathophysiological effects

4.1.1.1 *Effect of coating*

- Both AgNPs, (PVP and CT) induced lung inflammation substantiated by interstitial infiltration of inflammatory cells consisting of neutrophils, lymphocytes and macrophages and the observed effects persisted after 7-days of instillation.
- PVP-AgNPs caused significant increase of TNF- α in lung and heart, CT-AgNPs showed increase in heart, brain and liver. As for IL-6, CT-AgNPs induced significant increase in lung, heart, brain and liver, while PVP-AgNPs showed the increase in lung and heart. PVP- AgNPs caused more significant increase in total antioxidants and GSH compared with CT-AgNPs in heart. As for the other organs investigated, while CT-AgNPs showed increase of GSH in lung, brain, kidney and spleen, PVP- AgNPs increased GSH in kidney and liver following 1-day exposure. An increase of total NO was also observed with CT-AgNPs in lung, brain and kidney, and PVP-AgNPs in liver. In case of marker of lipid peroxidation, 8-isoprostane, CT- AgNPs induced a significant increase in the lungs, heart and brain and PVP- AgNPs caused increase in lungs, heart and liver.
- With regard to markers of DNA damage and apoptosis measured, while CT-AgNPs significantly increased 8-OH-dG in lung, heart and brain, PVP-AgNPs increased in lung, heart and liver. Relatable to finding of 8-OH-dG level,

significant increases of tunel positive cells were found in lung, heart and brain with CT-AgNPs, and in lung, heart and liver with PVP-AgNPs.

- Both coating AgNPs induced a significant shortening of the thrombotic occlusion time in pial arterioles and venules, significant increase in the concentrations of the coagulation factor, fibrinogen, PAI-1 and BNP in the plasma. A significant shortening of PT and aPTT with both PVP- and CT-AgNPs was observed suggesting that both intrinsic and extrinsic pathways may be involved in the prothrombotic effects observed *in vivo*.
- Both AgNPs induced *in vitro* platelet aggregation and thereby significantly decreased platelet count at a dose of 1 µg/ml, which corresponds to 0.02% of the highest instilled dose (5 mg/kg) *in vivo*.
- Accumulation of silver post 1-day of i.t. instillation was observed in all the organs examined with the highest in spleen and liver.

4.1.1.2 Effect of time

- Inflammatory effects observed in H&E of lung post 1-day exposure persisted after 7-days of instillation for both PVP and CT AgNPs. In case of pro-inflammatory markers, TNF- α in lung induced by PVP-AgNPs, persisted post 7-days of exposure. The oxidative stress effect declined 7-days post exposure, except for total antioxidants in heart for both AgNPs type and NO in kidney for CT- AgNPs. The increase of 8-OH-dG and tunel positive cells in heart remained significant for PVP – AgNPs even after 7 days of exposure.
- Significant shortening of the thrombotic occlusion time in pial arterioles and venules were observed post 7-days of i.t. instillation, indicating that prothrombotic effect of AgNPs persisted even after a week of exposure. The

rise in BNP and decrease of PT and aPTT also persisted after 7 days of exposure.

4.1.1.3 Effect of dose

- Both PVP- and CT- AgNPs caused significant dose-dependent increase of proinflammatory markers, oxidative stress, DNA damage and apoptosis and significant dose dependent shortening of the thrombotic occlusion time in pial arterioles and venules. However, the highest dose (5 mg/kg) resulted in more toxic effects for both PVP- and CT- AgNPs in heart and plasma. Nevertheless, some of the effects were significant at the lowest dose indicating that no effect level could be much lower.

4.1.1.4 Distinct effect of Ag ions (ionic control)

- Compared with histological findings of AgNPs, Ag⁺ ions produced a milder inflammatory response in lungs consisting mainly of neutrophil polymorphs and lymphocytes.
- Unlike AgNPs, Ag⁺ ions induced significant increase of TNF- α and IL-6 in kidney and spleen. While Ag⁺ ions increased GSH in spleen post 1-day exposure, the ions significantly decreased GSH in heart post 7-days i.t. instillation.
- Ag⁺ ions caused significant increase of NO in lung and kidney, an increase of 8-isoprostane in spleen and liver; and an increase of 8-OH-dG and tunel positive cells in lung and liver following 1 day after instillation.
- Similar to AgNPs, Ag⁺ ions showed significant effect with respect to thrombosis and concentration of fibrinogen. Contrarily to AgNPs, with Ag⁺ ions, PAI-1 showed significant increase at 7-days of exposure.

- With respect to Ag distribution, Ag⁺ ions were also distributed in different tissues after single i.t. instillation.

4.1.2 *In vitro* studies: Effect of AgNPs on incubated mouse erythrocytes

- Both PVP- and CT- AgNPs caused a significant concentration-dependent hemolysis and were taken up by erythrocytes.
- Both coating AgNPs induced oxidative stress as shown by significantly increased MDA and decreased GSH and CAT activity.
- Both PVP- and CT- AgNPs caused significant and dose dependent increase of intracellular calcium, Annexin V binding and calpain activity which may explain the cause of hemolysis and mechanism of eryptosis.
- However, the degree of hemolysis varied between concentration (2.5, 10 and 40 µg/ml) and coatings of AgNPs.

To conclude, the influence of AgNPs (size 10 nm) with two distinct coating (PVP and CT), three doses (0.05, 0.5 and 5 mg/dl) and two post exposure time points (1 and 7-days) were comprehensively assessed in an *in vivo* model. Pulmonary exposed PVP- and CT- AgNPs induced pro-inflammatory response and oxidative stress in major organs including lung, heart, liver, kidney and brain, evidenced by an increase of TNF- α , IL-6, GSH, total antioxidant, NO and 8-isoprostane, and caused DNA damage, thereby reinforcing the previously established mechanisms of DNA damage caused by reactive oxygen species and eventually resulting in cellular dysfunction and apoptosis. The findings in our study indicate that lung exposed 10nm AgNPs were translocated and distributed to the different tissues during the 1st day of exposure either in the particle or ionic form. The overall pathophysiological effects obtained herein by subsequent assays could be attributed to either the AgNPs

themselves at the site of exposure or inflammation and oxidative stress induced in lungs (site of deposition of AgNPs) or translocated AgNPs and markers of inflammation and oxidative from the lung to the blood which subsequently can affect distant organs (heart, liver, kidney, spleen and brain) or due to the release of Ag⁺ ions or the combination of all the aforementioned mechanisms. Even though the release of various markers investigated in this study varied between the particle types used and the investigated organs, at least one or more than one marker of inflammation and oxidative stress augmented in each studied organ, showing the occurrence of inflammation and oxidative stress after single i.t. instillation of AgNPs. Some of the acute effects observed persisted even after 7 days of instillation suggesting continuing effect of AgNPs. The pattern of toxicity observed between AgNPs and Ag⁺ ions were dissimilar possibly indicating that the effect obtained in our study may be related primarily to AgNPs themselves rather than Ag⁺ ions. The difference observed in pathophysiological effect in various organs also indicate that the particulate and ionic form of silver may act by a different mechanism. With regard to dose, both particle types showed a dose- dependent effect for some of the parameters measured. However, PVP- AgNPs tended to induce a more significant effects at all doses compared with CT- AgNPs. This study further revealed that these particles are able to induce DNA damage and apoptosis in the brain possibly by crossing the blood-brain barrier in particulate or ionic form after dissolution. Moreover, our *in vitro* study demonstrated significant hemolysis and eryptosis by both PVP- and CT- AgNPs.

Overall, our results in this study suggest that application of AgNPs has to be carefully considered with respect to size, dose, coating and duration of exposure. The persistence of the pathophysiological effects following single i.t. administration and

the fact that occupational and consumer exposure to AgNPs are not time limited, necessitate the evaluation of the chronic effects of AgNPs exposure by inhalation.

4.2 Limitations of study

There were some limitations in our study including the use of both male and female Balb/C mice for our work. Estrous cycle of female has been reported to have an impact on vascular function and circulatory factors and we have not established the stage during our *in vivo* experiments [260]. Moreover, our work did not differentiate the effects observed between male and female, where gender difference in distribution and toxicity of AgNPs have been reported previously [177, 204]. Moreover, although our study characterized the particles thoroughly using TEM, zeta potential and size distribution measurement, additional techniques can be applied to further characterize AgNPs such as dynamic light scattering and UV-visible spectroscopy that provide hydrodynamic diameter and intrinsic feature of possible aggregates of the particles, respectively. Our work also lacked to evaluate the dissolution rates of AgNPs *in vivo* as it is an important parameter needed for risk assessment [304]. Beside not having appropriate evidence of the AgNPs like TEM within the organs where significant pathophysiological effects were achieved, we were unable to conclude if the effect observed were due to the particle itself or the Ag ions after dissolution.

4.3 Future directions

In this study, we were able to demonstrate that pulmonary exposed AgNPs, either in particulate or ionic form, can induce pulmonary toxicity and cause pathophysiological effect on vascular and distant organs including heart, liver, kidney, spleen and brain. Data generated in our work added more to the growing evidence of induced acute and remote toxicity following respiratory exposure to NPs based

products. The persistence of the cardiovascular as well as other investigated organ effects following single i.t. administration, and the fact that occupational and consumer exposure to AgNPs are not time limited to 1-day, further researches are required to evaluate the chronic effect of AgNPs exposure. The i.t. instillation used in the present work has been shown to be a reliable, convenient and valid for certain objectives, though admittedly not physiologically perfect, mode of administration of foreign compounds into the airways. Additional studies using inhalation exposures are needed to confirm our findings. Furthermore, it is well established that the impact of particulate air pollution is aggravated in patients with pre-existing cardiorespiratory diseases, for e.g., asthma, chronic respiratory diseases such as chronic obstructive pulmonary disease, hypertension and ischemic heart diseases [305]. In this regard, the impeding pathophysiological effects of AgNPs on susceptible populations can be investigated in future studies using animal models of increased susceptibility, such as, asthma, hypertension etc.

References

- [1] A. Keiper, "The nanotechnology revolution," *The New Atlantis*, no. 2, pp. 17-34, 2003.
- [2] I. Khan, K. Saeed, and I. Khan, "Nanoparticles: Properties, applications and toxicities," *Arabian Journal of Chemistry*, pp. 908-993, 2017.
- [3] S. Bakand and A. Hayes, "Toxicological considerations, toxicity assessment, and risk management of inhaled nanoparticles," *International Journal of Molecular Sciences*, vol. 17, no. 6, pp. 929-946, 2016.
- [4] J. Jeevanandam, A. Barhoum, Y. S. Chan, A. Dufresne, and M. K. Danquah, "Review on nanoparticles and nanostructured materials: history, sources, toxicity and regulations," *Beilstein Journal of Nanotechnology*, vol. 9, no. 1, pp. 1050-1074, 2018.
- [5] Z. Li, H. Cong, Z. Yan, A. Liu, and B. Yu, "The Potential Human Health and Environmental Issues of Nanomaterials," in *Handbook of Nanomaterials for Industrial Applications*: Elsevier, pp. 1049-1054, 2018.
- [6] M. Korani, E. Ghazizadeh, S. Korani, Z. Hami, and A. Mohammadi-Bardbori, "Effects of silver nanoparticles on human health," *European Journal of Nanomedicine*, vol. 7, no. 1, pp. 51-62, 2015.
- [7] M. E. Vance *et al.*, "Nanotechnology in the real world: Redeveloping the nanomaterial consumer products inventory," *Beilstein Journal of Nanotechnology*, vol. 6, no. 1, pp. 1769-1780, 2015.
- [8] A. Syafiuddin, M. R. Salim, A. Beng Hong Kueh, T. Hadibarata, and H. Nur, "A review of silver nanoparticles: Research trends, global consumption, synthesis, properties, and future challenges," *Journal of the Chinese Chemical Society*, vol. 64, no. 7, pp. 732-756, 2017.
- [9] X.-F. Zhang, Z.-G. Liu, W. Shen, and S. Gurunathan, "Silver nanoparticles: synthesis, characterization, properties, applications, and therapeutic approaches," *International Journal of Molecular Sciences*, vol. 17, no. 9, pp. 1534-1568, 2016.
- [10] D. R. Boverhof *et al.*, "Comparative assessment of nanomaterial definitions and safety evaluation considerations," *Regulatory Toxicology and Pharmacology*, vol. 73, no. 1, pp. 137-150, 2015.
- [11] W.-K. Shin, J. Cho, A. G. Kannan, Y.-S. Lee, and D.-W. Kim, "Cross-linked composite gel polymer electrolyte using mesoporous methacrylate-functionalized SiO₂ nanoparticles for lithium-ion polymer batteries," *Scientific reports*, vol. 6, pp. 26332-26342, 2016.

- [12] D. Hristozov and I. Malsch, "Hazards and risks of engineered nanoparticles for the environment and human health," *Sustainability*, vol. 1, no. 4, pp. 1161-1194, 2009.
- [13] J. N. Tiwari, R. N. Tiwari, and K. S. Kim, "Zero-dimensional, one-dimensional, two-dimensional and three-dimensional nanostructured materials for advanced electrochemical energy devices," *Progress in Materials Science*, vol. 57, no. 4, pp. 724-803, 2012.
- [14] S. Bhatia, "Nanoparticles Types, Classification, Characterization, Fabrication Methods and Drug Delivery Applications," in *Natural Polymer Drug Delivery Systems*: Springer, pp. 33-93, 2016.
- [15] A. K. Singh, *Engineered Nanoparticles: Structure, Properties and Mechanisms of toxicity*. Academic Press, pp. 1-8, 2015.
- [16] F. Zivic, N. Grujovic, S. Mitrovic, I. U. Ahad, and D. Brabazon, "Characteristics and applications of silver nanoparticles," in *Commercialization of Nanotechnologies—A Case Study Approach*: Springer, pp. 227-273, 2018.
- [17] A. Ali, M. Z. Hira Zafar, I. ul Haq, A. R. Phull, J. S. Ali, and A. Hussain, "Synthesis, characterization, applications, and challenges of iron oxide nanoparticles," *Nanotechnology, Science and Applications*, vol. 9, pp. 49-68, 2016.
- [18] M. F. L. De Volder, S. H. Tawfick, R. H. Baughman, and A. J. Hart, "Carbon nanotubes: present and future commercial applications," *Science*, vol. 339, no. 6119, pp. 535-539, 2013.
- [19] Z. F. Yin, L. Wu, H. G. Yang, and Y. H. Su, "Recent progress in biomedical applications of titanium dioxide," *Physical Chemistry Chemical Physics*, vol. 15, no. 14, pp. 4844-4858, 2013.
- [20] H. O. Pierson, *Handbook of Carbon, Graphite, Diamonds and Fullerenes: Processing, Properties and Applications*. William Andrew, pp. 2-6, 2012.
- [21] X. Zhang, "Gold nanoparticles: recent advances in the biomedical applications," *Cell Biochemistry and Biophysics*, vol. 72, no. 3, pp. 771-775, 2015.
- [22] V. De Matteis, "Exposure to inorganic nanoparticles: routes of entry, immune response, biodistribution and in vitro/in vivo toxicity evaluation," *Toxics*, vol. 5, no. 4, pp. 29-50, 2017.
- [23] L. Gate *et al.*, "Biopersistence and translocation to extrapulmonary organs of titanium dioxide nanoparticles after subacute inhalation exposure to aerosol in adult and elderly rats," *Toxicology Letters*, vol. 265, pp. 61-69, 2017.

- [24] Q. H. Tran, V. Quy Nguyen, and A.-T. Le, "Silver nanoparticles: synthesis, properties, toxicology, applications and perspectives," *Advances in Natural Sciences: Nanoscience and Nanotechnology*, vol. 4, no. 3, pp. 1-23, 2013.
- [25] J. Natsuki, T. Natsuki, and Y. Hashimoto, "A review of silver nanoparticles: synthesis methods, properties and applications," *International Journal Material Science and Applications*, vol. 4, pp. 325-332, 2015.
- [26] J. Rumble, *CRC Handbook of Chemistry and Physics*. CRC press, pp. 6-26, 2017.
- [27] M. Ahamed, M. S. AlSalhi, and M. K. J. Siddiqui, "Silver nanoparticle applications and human health," *Clinica Chimica Acta*, vol. 411, no. 23-24, pp. 1841-1848, 2010.
- [28] K. S. Siddiqi, A. Husen, and R. A. K. Rao, "A review on biosynthesis of silver nanoparticles and their biocidal properties," *Journal of Nanobiotechnology*, vol. 16, no. 1, pp. 14-42, 2018.
- [29] D. C. Tien *et al.*, "Novel technique for preparing a nano-silver water suspension by the arc-discharge method," *Reviews of Advanced Material Science*, vol. 18, pp. 750-756, 2008.
- [30] S.-J. Shih and I. C. Chien, "Preparation and characterization of nanostructured silver particles by one-step spray pyrolysis," *Powder Technology*, vol. 237, pp. 436-441, 2013.
- [31] S. Iravani, H. Korbekandi, S. V. Mirmohammadi, and B. Zolfaghari, "Synthesis of silver nanoparticles: chemical, physical and biological methods," *Research in Pharmaceutical Sciences*, vol. 9, no. 6, pp. 385-406, 2014.
- [32] K. Gudikandula and S. Charya Maringanti, "Synthesis of silver nanoparticles by chemical and biological methods and their antimicrobial properties," *Journal of Experimental Nanoscience*, vol. 11, no. 9, pp. 714-721, 2016.
- [33] D. H. Kim, J. C. Park, G. E. Jeon, C. S. Kim, and J. H. Seo, "Effect of the size and shape of silver nanoparticles on bacterial growth and metabolism by monitoring optical density and fluorescence intensity," *Biotechnology and Bioprocess Engineering*, vol. 22, no. 2, pp. 210-217, 2017.
- [34] A. R. Gliga, S. Skoglund, I. O. Wallinder, B. Fadeel, and H. L. Karlsson, "Size-dependent cytotoxicity of silver nanoparticles in human lung cells: the role of cellular uptake, agglomeration and Ag release," *Particle and Fibre Toxicology*, vol. 11, no. 1, pp. 11-28, 2014.
- [35] K. Loza *et al.*, "The dissolution and biological effects of silver nanoparticles in biological media," *Journal of Materials Chemistry B*, vol. 2, no. 12, pp. 1634-1643, 2014.

- [36] L. Wei, J. Lu, H. Xu, A. Patel, Z.-S. Chen, and G. Chen, "Silver nanoparticles: synthesis, properties, and therapeutic applications," *Drug Discovery Today*, vol. 20, no. 5, pp. 595-601, 2015.
- [37] P.-C. Lin, S. Lin, P. C. Wang, and R. Sridhar, "Techniques for physicochemical characterization of nanomaterials," *Biotechnology advances*, vol. 32, no. 4, pp. 711-726, 2014.
- [38] R. J. Vandebriel *et al.*, "Immunotoxicity of silver nanoparticles in an intravenous 28-day repeated-dose toxicity study in rats," *Particle and Fibre Toxicology*, vol. 11, no. 1, pp. 21-30, 2014.
- [39] M. D. Boudreau *et al.*, "Differential effects of silver nanoparticles and silver ions on tissue accumulation, distribution, and toxicity in the Sprague Dawley rat following daily oral gavage administration for 13 weeks," *Toxicological Sciences*, vol. 150, no. 1, pp. 131-160, 2016.
- [40] W. H. De Jong *et al.*, "Systemic and immunotoxicity of silver nanoparticles in an intravenous 28 days repeated dose toxicity study in rats," *Biomaterials*, vol. 34, no. 33, pp. 8333-43, 2013.
- [41] Y.-M. Cho, Y. Mizuta, J.-i. Akagi, T. Toyoda, M. Sone, and K. Ogawa, "Size-dependent acute toxicity of silver nanoparticles in mice," *Journal of Toxicologic Pathology*, vol. 31, no. 1, pp. 73-80, 2018.
- [42] M. H. Gherkholagh, Z. Alizadeh, M. J. Asari, and M. Sohrabi, "In Vivo Induced Nephrotoxicity of Silver Nanoparticles in Rat after Oral Administration," *Journal of Research in Medical and Dental Science*, vol. 6, no. 1, pp. 43-51, 2018.
- [43] T. M. Tolaymat, A. M. El Badawy, A. Genaidy, K. G. Scheckel, T. P. Luxton, and M. Suidan, "An evidence-based environmental perspective of manufactured silver nanoparticle in syntheses and applications: a systematic review and critical appraisal of peer-reviewed scientific papers," *Science of the Total Environment*, vol. 408, no. 5, pp. 999-1006, 2010.
- [44] Z. Lu, K. Rong, J. Li, H. Yang, and R. Chen, "Size-dependent antibacterial activities of silver nanoparticles against oral anaerobic pathogenic bacteria," *Journal of Materials Science: Materials in Medicine*, vol. 24, no. 6, pp. 1465-1471, 2013.
- [45] Y. Jeong, D. W. Lim, and J. Choi, "Assessment of size-dependent antimicrobial and cytotoxic properties of silver nanoparticles," *Advances in Materials Science and Engineering*, vol. 2014, pp. 1-6, 2014.
- [46] V. K. Sharma, K. M. Siskova, R. Zboril, and J. L. Gardea-Torresdey, "Organic-coated silver nanoparticles in biological and environmental conditions: fate, stability and toxicity," *Advances in Colloid and Interface science*, vol. 204, pp. 15-34, 2014.

- [47] K. C. Nguyen *et al.*, "Comparison of toxicity of uncoated and coated silver nanoparticles," vol. 429: IOP Publishing, 1 ed., pp. 012025-012041, 2013.
- [48] D. D. Jurašin *et al.*, "Surface coating affects behavior of metallic nanoparticles in a biological environment," *Beilstein Journal of Nanotechnology*, vol. 7, no. 1, pp. 246-262, 2016.
- [49] X. Hong, J. Wen, X. Xiong, and Y. Hu, "Shape effect on the antibacterial activity of silver nanoparticles synthesized via a microwave-assisted method," *Environmental Science and Pollution Research*, vol. 23, no. 5, pp. 4489-4497, 2016.
- [50] S. Pal, Y. K. Tak, and J. M. Song, "Does the antibacterial activity of silver nanoparticles depend on the shape of the nanoparticle? A study of the gram-negative bacterium *Escherichia coli*," *Applied Environmental Microbiology*, vol. 73, no. 6, pp. 1712-1720, 2007.
- [51] L. Actis, A. Srinivasan, J. L. Lopez-Ribot, A. K. Ramasubramanian, and J. L. Ong, "Effect of silver nanoparticle geometry on methicillin susceptible and resistant *Staphylococcus aureus*, and osteoblast viability," *Journal of Materials Science: Materials in Medicine*, vol. 26, no. 7, pp. 215-222, 2015.
- [52] A. Lankoff *et al.*, "The effect of agglomeration state of silver and titanium dioxide nanoparticles on cellular response of HepG2, A549 and THP-1 cells," *Toxicology Letters*, vol. 208, no. 3, pp. 197-213, 2012.
- [53] S. Argentiére, C. Cella, M. Cesaria, P. Milani, and C. Lenardi, "Silver nanoparticles in complex biological media: assessment of colloidal stability and protein corona formation," *Journal of Nanoparticle Research*, vol. 18, no. 8, pp. 253-283, 2016.
- [54] E. Bae, B.-C. Lee, Y. Kim, K. Choi, and J. Yi, "Effect of agglomeration of silver nanoparticle on nanotoxicity depression," *Korean Journal of Chemical Engineering*, vol. 30, no. 2, pp. 364-368, 2013.
- [55] M. Akter *et al.*, "A systematic review on silver nanoparticles-induced cytotoxicity: Physicochemical properties and perspectives," *Journal of Advanced Research*, vol. 9, pp. 1-16, 2018.
- [56] N. Durán, C. P. Silveira, M. Durán, and D. S. T. Martinez, "Silver nanoparticle protein corona and toxicity: a mini-review," *Journal of Nanobiotechnology*, vol. 13, no. 1, pp. 55-72, 2015.
- [57] P. Mathur, S. Jha, S. Ramteke, and N. K. Jain, "Pharmaceutical aspects of silver nanoparticles," *Artificial Cells, Nanomedicine, and Biotechnology*, vol. 46, no. sup1, pp. 115-126, 2018.
- [58] P. K. Jha, R. K. Jha, D. Rout, S. Gnanasekar, S. V. S. Rana, and M. Hossain, "Potential targetability of multi-walled carbon nanotube loaded with silver nanoparticles photosynthesized from *Ocimum tenuiflorum* (tulsi extract) in

- fertility diagnosis," *Journal of Drug Targeting*, vol. 25, no. 7, pp. 616-625, 2017.
- [59] M. Bilal, T. Rasheed, H. M. N. Iqbal, C. Li, H. Hu, and X. Zhang, "Development of silver nanoparticles loaded chitosan-alginate constructs with biomedical potentialities," *International Journal of Biological Macromolecules*, vol. 105, pp. 393-400, 2017.
- [60] M. Azizi, H. Ghourchian, F. Yazdian, S. Bagherifam, S. Bekhradnia, and B. Nyström, "Anti-cancerous effect of albumin coated silver nanoparticles on MDA-MB 231 human breast cancer cell line," *Scientific Reports*, vol. 7, no. 1, pp. 5178-5196, 2017.
- [61] G. Nam, B. Purushothaman, S. Rangasamy, and J. M. Song, "Investigating the versatility of multifunctional silver nanoparticles: preparation and inspection of their potential as wound treatment agents," *International Nano Letters*, vol. 6, no. 1, pp. 51-63, 2016.
- [62] M. J. Firdhouse and P. Lalitha, "Biosynthesis of silver nanoparticles and its applications," *Journal of Nanotechnology*, vol. 2015, pp. 1-18, 2015.
- [63] M. Catauro, M. G. Raucci, F. De Gaetano, and A. Marotta, "Antibacterial and bioactive silver-containing Na₂O·CaO·2SiO₂ glass prepared by sol-gel method," *Journal of Materials Science: Materials in Medicine*, vol. 15, no. 7, pp. 831-837, 2004.
- [64] J. H. Crabtree, R. J. Burchette, R. A. Siddiqi, I. T. Huen, L. L. Hadnott, and A. Fishman, "The efficacy of silver-ion implanted catheters in reducing peritoneal dialysis-related infections," *Peritoneal Dialysis International*, vol. 23, no. 4, pp. 368-374, 2003.
- [65] J. Tian *et al.*, "Topical delivery of silver nanoparticles promotes wound healing," *ChemMedChem: Chemistry Enabling Drug Discovery*, vol. 2, no. 1, pp. 129-136, 2007.
- [66] D. Roe, B. Karandikar, N. Bonn-Savage, B. Gibbins, and J.-B. Roullet, "Antimicrobial surface functionalization of plastic catheters by silver nanoparticles," *Journal of Antimicrobial Chemotherapy*, vol. 61, no. 4, pp. 869-876, 2008.
- [67] L. C. Yun'an Qing *et al.*, "Potential antibacterial mechanism of silver nanoparticles and the optimization of orthopedic implants by advanced modification technologies," *International Journal of Nanomedicine*, vol. 13, pp. 3311-3327, 2018.
- [68] B. Le Ouay and F. Stellacci, "Antibacterial activity of silver nanoparticles: a surface science insight," *Nano Today*, vol. 10, no. 3, pp. 339-354, 2015.
- [69] S. H. Lee and B.-H. Jun, "Silver nanoparticles: synthesis and application for nanomedicine," *International Journal of Molecular Sciences*, vol. 20, no. 4, pp. 865-889, 2019.

- [70] M. Seong and D. G. Lee, "Silver nanoparticles against *Salmonella enterica* serotype typhimurium: role of inner membrane dysfunction," *Current Microbiology*, vol. 74, no. 6, pp. 661-670, 2017.
- [71] R. Das, S. Gang, and S. S. Nath, "Preparation and antibacterial activity of silver nanoparticles," *Journal of Biomaterials and nanobiotechnology*, vol. 2, no. 04, pp. 472-482, 2011.
- [72] A. Abbaszadegan *et al.*, "The effect of charge at the surface of silver nanoparticles on antimicrobial activity against gram-positive and gram-negative bacteria: a preliminary study," *Journal of Nanomaterials*, vol. 16, no. 1, pp. 53-61, 2015.
- [73] C. Recordati *et al.*, "Tissue distribution and acute toxicity of silver after single intravenous administration in mice: nano-specific and size-dependent effects," *Particle and Fibre Toxicology*, vol. 13, no. 1, pp. 12-29, 2016.
- [74] L. Shang, K. Nienhaus, and G. U. Nienhaus, "Engineered nanoparticles interacting with cells: size matters," *Journal of Nanobiotechnology*, vol. 12, no. 1, pp. 5-16, 2014.
- [75] M. Raza, Z. Kanwal, A. Rauf, A. Sabri, S. Riaz, and S. Naseem, "Size- and shape-dependent antibacterial studies of silver nanoparticles synthesized by wet chemical routes," *Nanomaterials*, vol. 6, no. 4, pp. 74-89, 2016.
- [76] S. K. Kailasa, T.-J. Park, J. V. Rohit, and J. R. Koduru, "Antimicrobial activity of silver nanoparticles," in *Nanoparticles in Pharmacotherapy*: Elsevier, pp. 461-484, 2019.
- [77] L. L. Maurer and J. N. Meyer, "A systematic review of evidence for silver nanoparticle-induced mitochondrial toxicity," *Environmental Science: Nano*, vol. 3, no. 2, pp. 311-322, 2016.
- [78] Y.-M. Long *et al.*, "Surface ligand controls silver ion release of nanosilver and its antibacterial activity against *Escherichia coli*," *International Journal of Nanomedicine*, vol. 12, pp. 3193-3206, 2017.
- [79] S. W. Kim, J. H. Jung, K. Lamsal, Y. S. Kim, J. S. Min, and Y. S. Lee, "Antifungal effects of silver nanoparticles (AgNPs) against various plant pathogenic fungi," *Mycobiology*, vol. 40, no. 1, pp. 53-58, 2012.
- [80] A. M. Elgorban *et al.*, "Antifungal silver nanoparticles: synthesis, characterization and biological evaluation," *Biotechnology & Biotechnological Equipment*, vol. 30, no. 1, pp. 56-62, 2016.
- [81] H. H. Lara, N. V. Ayala-Nuñez, L. Ixtepan-Turrent, and C. Rodriguez-Padilla, "Mode of antiviral action of silver nanoparticles against HIV-1," *Journal of Nanobiotechnology*, vol. 8, no. 1, pp. 1-10, 2010.

- [82] S. Gaikwad *et al.*, "Antiviral activity of mycosynthesized silver nanoparticles against herpes simplex virus and human parainfluenza virus type 3," *International Journal of Nanomedicine*, vol. 8, pp. 4303-4314, 2013.
- [83] N. Khandelwal *et al.*, "Silver nanoparticles impair Peste des petits ruminants virus replication," *Virus Research*, vol. 190, pp. 1-7, 2014.
- [84] E. K. F. Elbeshehy, A. M. Elazzazy, and G. Aggelis, "Silver nanoparticles synthesis mediated by new isolates of *Bacillus* spp., nanoparticle characterization and their activity against Bean Yellow Mosaic Virus and human pathogens," *Frontiers in Microbiology*, vol. 6, pp. 453-466, 2015.
- [85] L. Lu *et al.*, "Silver nanoparticles inhibit hepatitis B virus replication," *Antiviral Therapy*, vol. 13, no. 2, pp. 253-263, 2008.
- [86] L. David *et al.*, "Green synthesis, characterization and anti-inflammatory activity of silver nanoparticles using European black elderberry fruits extract," *Colloids and Surfaces B: Biointerfaces*, vol. 122, pp. 767-777, 2014.
- [87] A. Hebeish, M. H. El-Rafie, M. A. El-Sheikh, A. A. Seleem, and M. E. El-Naggar, "Antimicrobial wound dressing and anti-inflammatory efficacy of silver nanoparticles," *International Journal of Biological Macromolecules*, vol. 65, pp. 509-515, 2014.
- [88] H. Qiao, W. Liu, H. Gu, D. Wang, and Y. Wang, "The transport and deposition of nanoparticles in respiratory system by inhalation," *Journal of Nanomaterials*, vol. 2015, pp. 2-10, 2015.
- [89] J. Park *et al.*, "Characterization of exposure to silver nanoparticles in a manufacturing facility," *Journal of Nanoparticle Research*, vol. 11, no. 7, pp. 1705-1712, 2009.
- [90] J. H. Lee, J. Mun, J. D. Park, and I. J. Yu, "A health surveillance case study on workers who manufacture silver nanomaterials," *Nanotoxicology*, vol. 6, no. 6, pp. 667-669, 2012.
- [91] J. H. Lee *et al.*, "Exposure assessment of workplaces manufacturing nanosized TiO₂ and silver," *Inhalation Toxicology*, vol. 23, no. 4, pp. 226-236, 2011.
- [92] Y. Nazarenko, T. W. Han, P. J. Liroy, and G. Mainelis, "Potential for exposure to engineered nanoparticles from nanotechnology-based consumer spray products," *Journal of Exposure Science and Environmental Epidemiology*, vol. 21, no. 5, pp. 515-528, 2011.
- [93] C. Lorenz *et al.*, "Nanosized aerosols from consumer sprays: experimental analysis and exposure modeling for four commercial products," *Journal of Nanoparticle Research*, vol. 13, no. 8, pp. 3377-3391, 2011.

- [94] D. M. Mitrano, E. Rimmelé, A. Wichser, R. Erni, M. Height, and B. Nowack, "Presence of nanoparticles in wash water from conventional silver and nano-silver textiles," *ACS Nano*, vol. 8, no. 7, pp. 7208-7219, 2014.
- [95] J. Farkas *et al.*, "Characterization of the effluent from a nanosilver producing washing machine," *Environment International*, vol. 37, no. 6, pp. 1057-1062, 2011.
- [96] R. Kaegi *et al.*, "Release of silver nanoparticles from outdoor facades," *Environmental Pollution*, vol. 158, no. 9, pp. 2900-2905, 2010.
- [97] B. A. Weldon *et al.*, "Occupational exposure limit for silver nanoparticles: considerations on the derivation of a general health-based value," *Nanotoxicology*, vol. 10, no. 7, pp. 945-956, 2016.
- [98] Q. Deng, L. Deng, Y. Miao, X. Guo, and Y. Li, "Particle deposition in the human lung: Health implications of particulate matter from different sources," *Environmental Research*, vol. 169, pp. 237-245, 2019.
- [99] I. G. Theodorou, M. P. Ryan, T. D. Tetley, and A. E. Porter, "Inhalation of silver nanomaterials—seeing the risks," *International Journal of Molecular Sciences*, vol. 15, no. 12, pp. 23936-23974, 2014.
- [100] S. Gaillet and J.-M. Rouanet, "Silver nanoparticles: their potential toxic effects after oral exposure and underlying mechanisms—a review," *Food and Chemical Toxicology*, vol. 77, pp. 58-63, 2015.
- [101] C. Gambardella *et al.*, "Effect of silver nanoparticles on marine organisms belonging to different trophic levels," *Marine Environmental Research*, vol. 111, pp. 41-49, 2015.
- [102] J. I. Choi *et al.*, "Potential silver nanoparticles migration from commercially available polymeric baby products into food simulants," *Food Additives & Contaminants: Part A*, vol. 35, no. 5, pp. 996-1005, 2018.
- [103] A. Mackevica, M. E. Olsson, and S. F. Hansen, "Silver nanoparticle release from commercially available plastic food containers into food simulants," *Journal of Nanoparticle Research*, vol. 18, no. 1, pp. 5-30, 2016.
- [104] J. L. Axson *et al.*, "Rapid kinetics of size and pH-dependent dissolution and aggregation of silver nanoparticles in simulated gastric fluid," *The Journal of Physical Chemistry C*, vol. 119, no. 35, pp. 20632-20641, 2015.
- [105] L.-p. Wang and J.-y. Wang, "Skin penetration of inorganic and metallic nanoparticles," *Journal of Shanghai Jiaotong University Science*, vol. 19, no. 6, pp. 691-697, 2014.
- [106] R. George, S. Merten, T. T. Wang, P. Kennedy, and P. Maitz, "In vivo analysis of dermal and systemic absorption of silver nanoparticles through healthy human skin," *Australasian Journal of Dermatology*, vol. 55, no. 3, pp. 185-190, 2014.

- [107] F. Alessandrini *et al.*, "Pro-inflammatory versus immunomodulatory effects of silver nanoparticles in the lung: The critical role of dose, size and surface modification," *Nanomaterials*, vol. 7, no. 10, pp. 300-317, 2017.
- [108] Y. S. Kim *et al.*, "Twenty-eight-day oral toxicity, genotoxicity, and gender-related tissue distribution of silver nanoparticles in Sprague-Dawley rats," *Inhalation Toxicology*, vol. 20, no. 6, pp. 575-583, 2008.
- [109] Y. S. Kim *et al.*, "Subchronic oral toxicity of silver nanoparticles," *Particle and Fibre Toxicology*, vol. 7, no. 1, pp. 20-31, 2010.
- [110] J. H. Sung *et al.*, "Subchronic inhalation toxicity of silver nanoparticles," *Toxicological Sciences*, vol. 108, no. 2, pp. 452-461, 2008.
- [111] K. S. Song *et al.*, "Recovery from silver-nanoparticle-exposure-induced lung inflammation and lung function changes in Sprague Dawley rats," *Nanotoxicology*, vol. 7, no. 2, pp. 169-180, 2013.
- [112] D. P. K. Lankveld *et al.*, "The kinetics of the tissue distribution of silver nanoparticles of different sizes," *Biomaterials*, vol. 31, no. 32, pp. 8350-8361, 2010.
- [113] M. van der Zande *et al.*, "Distribution, elimination, and toxicity of silver nanoparticles and silver ions in rats after 28-day oral exposure," *ACS Nano*, vol. 6, no. 8, pp. 7427-7442, 2012.
- [114] J. H. Lee *et al.*, "Biopersistence of silver nanoparticles in tissues from Sprague–Dawley rats," *Particle and Fibre Toxicology*, vol. 10, no. 1, pp. 36-50, 2013.
- [115] X. Jiang *et al.*, "Nanotoxicity of silver nanoparticles on HEK293T cells: A combined study using biomechanical and biological techniques," *ACS Omega*, vol. 3, no. 6, pp. 6770-6778, 2018.
- [116] J. Carrola *et al.*, "Metabolomics of silver nanoparticles toxicity in HaCaT cells: structure–activity relationships and role of ionic silver and oxidative stress," *Nanotoxicology*, vol. 10, no. 8, pp. 1105-1117, 2016.
- [117] S. C. Sahu *et al.*, "Comparative cytotoxicity of nanosilver in human liver HepG2 and colon Caco2 cells in culture," *Journal of Applied Toxicology*, vol. 34, no. 11, pp. 1155-1166, 2014.
- [118] Z. Ferdous, S. Beegam, S. Tariq, B. H. Ali, and A. Nemmar, "The in Vitro Effect of Polyvinylpyrrolidone and Citrate Coated Silver Nanoparticles on Erythrocytic Oxidative Damage and Eryptosis," *Cellular Physiology and Biochemistry*, vol. 49, no. 4, pp. 1577-1588, 2018.
- [119] L. Xin *et al.*, "Oxidative stress and mitochondrial injury-mediated cytotoxicity induced by silver nanoparticles in human A549 and HepG2 cells," *Environmental Toxicology*, vol. 31, no. 12, pp. 1691-1699, 2016.

- [120] M. Milić *et al.*, "Cellular uptake and toxicity effects of silver nanoparticles in mammalian kidney cells," *Journal of Applied Toxicology*, vol. 35, no. 6, pp. 581-592, 2015.
- [121] K. L. Lategan, C. R. Walters, and E. J. Pool, "The effects of silver nanoparticles on RAW 264.7. Macrophages and human whole blood cell cultures," *Frontiers in Bioscience*, vol. 24, pp. 347-365, 2019.
- [122] V. Galbiati *et al.*, "In vitro assessment of silver nanoparticles immunotoxicity," *Food and Chemical Toxicology*, vol. 112, pp. 363-374, 2018.
- [123] A. R. Gliga, S. Di Bucchianico, J. Lindvall, B. Fadeel, and H. L. Karlsson, "RNA-sequencing reveals long-term effects of silver nanoparticles on human lung cells," *Scientific Reports*, vol. 8, pp. 6668-6682, 2018.
- [124] A. Abdal Dayem, S. Lee, H. Choi, and S.-G. Cho, "Silver Nanoparticles: Two-Faced Neuronal Differentiation-Inducing Material in Neuroblastoma (SH-SY5Y) Cells," *International Journal of Molecular Sciences*, vol. 19, no. 5, pp. 1470-1489, 2018.
- [125] Y. S. Lee *et al.*, "Silver nanoparticles induce apoptosis and G2/M arrest via PKC ζ -dependent signaling in A549 lung cells," *Archives of Toxicology*, vol. 85, no. 12, pp. 1529-1540, 2011.
- [126] V. De Matteis *et al.*, "Negligible particle-specific toxicity mechanism of silver nanoparticles: the role of Ag⁺ ion release in the cytosol," *Nanomedicine: Nanotechnology, Biology and Medicine*, vol. 11, no. 3, pp. 731-739, 2015.
- [127] C. Carlson *et al.*, "Unique cellular interaction of silver nanoparticles: size-dependent generation of reactive oxygen species," *The Journal of Physical Chemistry B*, vol. 112, no. 43, pp. 13608-13619, 2008.
- [128] X. Wang *et al.*, "Use of coated silver nanoparticles to understand the relationship of particle dissolution and bioavailability to cell and lung toxicological potential," *Small*, vol. 10, no. 2, pp. 385-398, 2014.
- [129] V. Bastos, I. F. Duarte, C. Santos, and H. Oliveira, "A study of the effects of citrate-coated silver nanoparticles on RAW 264.7 cells using a toolbox of cytotoxic endpoints," *Journal of Nanoparticle Research*, vol. 19, no. 5, pp. 163-180, 2017.
- [130] B. K. Gaiser *et al.*, "Effects of silver nanoparticles on the liver and hepatocytes in vitro," *Toxicological Sciences*, vol. 131, no. 2, pp. 537-547, 2012.
- [131] F. Faedmaleki, F. H. Shirazi, A.-A. Salarian, H. A. Ashtiani, and H. Rastegar, "Toxicity effect of silver nanoparticles on mice liver primary cell culture and HepG2 cell line," *Iranian Journal of Pharmaceutical Research: IJPR*, vol. 13, no. 1, pp. 235-242, 2014.

- [132] Y. Xue, T. Zhang, B. Zhang, F. Gong, Y. Huang, and M. Tang, "Cytotoxicity and apoptosis induced by silver nanoparticles in human liver HepG2 cells in different dispersion media," *Journal of Applied Toxicology*, vol. 36, no. 3, pp. 352-360, 2016.
- [133] I. V. Vrček *et al.*, "Comparison of in vitro toxicity of silver ions and silver nanoparticles on human hepatoma cells," *Environmental Toxicology*, vol. 31, no. 6, pp. 679-692, 2016.
- [134] J.-P. Kaiser, M. Roesslein, L. Diener, and P. Wick, "Human health risk of ingested nanoparticles that are added as multifunctional agents to paints: an in vitro study," *PLoS One*, vol. 8, no. 12, pp. e83215-e83226, 2013.
- [135] L. Böhmert *et al.*, "Analytically monitored digestion of silver nanoparticles and their toxicity on human intestinal cells," *Nanotoxicology*, vol. 8, no. 6, pp. 631-642, 2014.
- [136] M. E. Samberg, S. J. Oldenburg, and N. A. Monteiro-Riviere, "Evaluation of silver nanoparticle toxicity in skin in vivo and keratinocytes in vitro," *Environmental Health Perspectives*, vol. 118, no. 3, pp. 407-413, 2009.
- [137] C. Bianco *et al.*, "In vitro percutaneous penetration and characterization of silver from silver-containing textiles," *International journal of nanomedicine*, vol. 10, pp. 1899-1908, 2015.
- [138] J. Tang *et al.*, "Distribution, translocation and accumulation of silver nanoparticles in rats," *Journal of Nanoscience and Nanotechnology*, vol. 9, no. 8, pp. 4924-4932, 2009.
- [139] M. J. Kim and S. Shin, "Toxic effects of silver nanoparticles and nanowires on erythrocyte rheology," *Food and Chemical Toxicology*, vol. 67, pp. 80-86, 2014.
- [140] R. Gupta and H. Xie, "Nanoparticles in Daily Life: Applications, Toxicity and Regulations," *Journal of Environmental Pathology, Toxicology and Oncology*, vol. 37, no. 3, pp. 209-230, 2018.
- [141] L. Q. Chen, L. Fang, J. Ling, C. Z. Ding, B. Kang, and C. Z. Huang, "Nanotoxicity of silver nanoparticles to red blood cells: size dependent adsorption, uptake, and hemolytic activity," *Chemical Research in Toxicology*, vol. 28, no. 3, pp. 501-509, 2015.
- [142] S. Shrivastava, T. Bera, S. K. Singh, G. Singh, P. Ramachandrarao, and D. Dash, "Characterization of antiplatelet properties of silver nanoparticles," *ACS nano*, vol. 3, no. 6, pp. 1357-1364, 2009.
- [143] Y. Bian *et al.*, "Silver nanoparticles promote procoagulant activity of red blood cells: a potential risk of thrombosis in susceptible population," *Particle and Fibre Toxicology*, vol. 16, no. 1, pp. 9-22, 2019.

- [144] E.-A. Jun *et al.*, "Silver nanoparticles enhance thrombus formation through increased platelet aggregation and procoagulant activity," *Nanotoxicology*, vol. 5, no. 2, pp. 157-167, 2011.
- [145] H. Huang *et al.*, "An evaluation of blood compatibility of silver nanoparticles," *Scientific Reports*, vol. 6, pp. 1-15, 2016.
- [146] C.-X. Lin, S.-Y. Yang, J.-L. Gu, J. Meng, H.-Y. Xu, and J.-M. Cao, "The acute toxic effects of silver nanoparticles on myocardial transmembrane potential, I Na and I K1 channels and heart rhythm in mice," *Nanotoxicology*, vol. 11, no. 6, pp. 827-837, 2017.
- [147] C. Greulich, S. Kittler, M. Epple, G. Muhr, and M. Köller, "Studies on the biocompatibility and the interaction of silver nanoparticles with human mesenchymal stem cells (hMSCs)," *Langenbeck's Archives of Surgery*, vol. 394, no. 3, pp. 495-502, 2009.
- [148] W. He, X. Liu, A. Kienzle, W. E. G. Müller, and Q. Feng, "In vitro uptake of silver nanoparticles and their toxicity in human mesenchymal stem cells derived from bone marrow," *Journal of Nanoscience and Nanotechnology*, vol. 16, no. 1, pp. 219-228, 2016.
- [149] L. Braydich-Stolle, S. Hussain, J. J. Schlager, and M.-C. Hofmann, "In vitro cytotoxicity of nanoparticles in mammalian germline stem cells," *Toxicological Sciences*, vol. 88, no. 2, pp. 412-419, 2005.
- [150] C. Sun *et al.*, "Silver nanoparticles induced neurotoxicity through oxidative stress in rat cerebral astrocytes is distinct from the effects of silver ions," *Neurotoxicology*, vol. 52, pp. 210-221, 2016.
- [151] C. Liao, Y. Li, and S. C. Tjong, "Bactericidal and Cytotoxic Properties of Silver Nanoparticles," *International Journal of Molecular Sciences*, vol. 20, no. 2, pp. 449-496, 2019.
- [152] K. S. Butler, D. J. Peeler, B. J. Casey, B. J. Dair, and R. K. Elespuru, "Silver nanoparticles: correlating nanoparticle size and cellular uptake with genotoxicity," *Mutagenesis*, vol. 30, no. 4, pp. 577-591, 2015.
- [153] A. Abdal Dayem *et al.*, "The role of reactive oxygen species (ROS) in the biological activities of metallic nanoparticles," *International Journal of Molecular Sciences*, vol. 18, no. 1, pp. 120-141, 2017.
- [154] M. Ahamed *et al.*, "DNA damage response to different surface chemistry of silver nanoparticles in mammalian cells," *Toxicology and Applied pharmacology*, vol. 233, no. 3, pp. 404-410, 2008.
- [155] M. Ahamed, R. Posgai, T. J. Gorey, M. Nielsen, S. M. Hussain, and J. J. Rowe, "Silver nanoparticles induced heat shock protein 70, oxidative stress and apoptosis in *Drosophila melanogaster*," *Toxicology and Applied Pharmacology*, vol. 242, no. 3, pp. 263-269, 2010.

- [156] S. Hackenberg *et al.*, "Silver nanoparticles: evaluation of DNA damage, toxicity and functional impairment in human mesenchymal stem cells," *Toxicology Letters*, vol. 201, no. 1, pp. 27-33, 2011.
- [157] L. Yang, H. Kuang, W. Zhang, Z. P. Aguilar, H. Wei, and H. Xu, "Comparisons of the biodistribution and toxicological examinations after repeated intravenous administration of silver and gold nanoparticles in mice," *Scientific Reports*, vol. 7, no. 1, pp. 3303-3315, 2017.
- [158] K. Dziendzikowska *et al.*, "Time-dependent biodistribution and excretion of silver nanoparticles in male Wistar rats," *Journal of Applied Toxicology*, vol. 32, no. 11, pp. 920-928, 2012.
- [159] J. Blanco *et al.*, "Oral exposure to silver nanoparticles increases oxidative stress markers in the liver of male rats and deregulates the insulin signalling pathway and p53 and cleaved caspase 3 protein expression," *Food and Chemical Toxicology*, vol. 115, pp. 398-404, 2018.
- [160] J. H. Sung *et al.*, "Acute inhalation toxicity of silver nanoparticles," *Toxicology and Industrial Health*, vol. 27, no. 2, pp. 149-154, 2011.
- [161] J. H. Ji *et al.*, "Twenty-eight-day inhalation toxicity study of silver nanoparticles in Sprague-Dawley rats," *Inhalation Toxicology*, vol. 19, no. 10, pp. 857-871, 2007.
- [162] L. V. Stebounova *et al.*, "Nanosilver induces minimal lung toxicity or inflammation in a subacute murine inhalation model," *Particle and Fibre Toxicology*, vol. 8, no. 1, pp. 5-17, 2011.
- [163] J. H. Sung *et al.*, "Lung function changes in Sprague-Dawley rats after prolonged inhalation exposure to silver nanoparticles," *Inhalation Toxicology*, vol. 20, no. 6, pp. 567-574, 2008.
- [164] J.-S. Hyun, B. S. Lee, H. Y. Ryu, J. H. Sung, K. H. Chung, and I. J. Yu, "Effects of repeated silver nanoparticles exposure on the histological structure and mucins of nasal respiratory mucosa in rats," *Toxicology Letters*, vol. 182, no. 1-3, pp. 24-28, 2008.
- [165] H.-Y. Lee *et al.*, "Genomics-based screening of differentially expressed genes in the brains of mice exposed to silver nanoparticles via inhalation," *Journal of Nanoparticle Research*, vol. 12, no. 5, pp. 1567-1578, 2010.
- [166] S. Takenaka *et al.*, "Pulmonary and systemic distribution of inhaled ultrafine silver particles in rats," *Environmental Health Perspectives*, vol. 109, no. Suppl 4, pp. 547-552, 2001.
- [167] M. Wiemann, A. Vennemann, F. Blaske, M. Sperling, and U. Karst, "Silver Nanoparticles in the Lung: Toxic Effects and Focal Accumulation of Silver in Remote Organs," *Nanomaterials*, vol. 7, no. 12, pp. 441-467, 2017.

- [168] H. M. Braakhuis *et al.*, "Particle size dependent deposition and pulmonary inflammation after short-term inhalation of silver nanoparticles," *Particle and Fibre Toxicology*, vol. 11, no. 1, pp. 49-65, 2014.
- [169] L. Campagnolo *et al.*, "Silver nanoparticles inhaled during pregnancy reach and affect the placenta and the foetus," *Nanotoxicology*, vol. 11, no. 5, pp. 687-698, 2017.
- [170] J. Seiffert *et al.*, "Pulmonary effects of inhalation of spark-generated silver nanoparticles in Brown-Norway and Sprague–Dawley rats," *Respiratory Research*, vol. 17, no. 1, pp. 85-100, 2016.
- [171] R. M. Silva *et al.*, "Aerosolized silver nanoparticles in the rat lung and pulmonary responses over time," *Toxicologic Pathology*, vol. 44, no. 5, pp. 673-686, 2016.
- [172] D. S. Anderson *et al.*, "Persistence of silver nanoparticles in the rat lung: Influence of dose, size, and chemical composition," *Nanotoxicology*, vol. 9, no. 5, pp. 591-602, 2015.
- [173] R. M. Silva *et al.*, "Pulmonary effects of silver nanoparticle size, coating, and dose over time upon intratracheal instillation," *Toxicological Sciences*, vol. 144, no. 1, pp. 151-162, 2015.
- [174] N. A. Holland *et al.*, "Cardiac ischemia reperfusion injury following instillation of 20 nm citrate-capped nanosilver," *Journal of Nanomedicine & Nanotechnology*, vol. 6, no. Suppl 6, pp. 1-28, 2015.
- [175] N. A. Holland *et al.*, "Impact of pulmonary exposure to gold core silver nanoparticles of different size and capping agents on cardiovascular injury," *Particle and Fibre Toxicology*, vol. 13, no. 1, pp. 48-69, 2016.
- [176] Z. Ferdous, S. Al-Salam, Y. E. Greish, B. H. Ali, and A. Nemmar, "Pulmonary exposure to silver nanoparticles impairs cardiovascular homeostasis: Effects of coating, dose and time," *Toxicology and Applied Pharmacology*, pp. 36-50, 2019.
- [177] W.-Y. Kim, J. Kim, J. D. Park, H. Y. Ryu, and I. J. Yu, "Histological study of gender differences in accumulation of silver nanoparticles in kidneys of Fischer 344 rats," *Journal of Toxicology and Environmental Health, Part A*, vol. 72, no. 21-22, pp. 1279-1284, 2009.
- [178] A. Nemmar, J. A. Holme, I. Rosas, P. E. Schwarze, and E. Alfaro-Moreno, "Recent advances in particulate matter and nanoparticle toxicology: a review of the in vivo and in vitro studies," *BioMed Research International*, vol. 2013, pp. 1-22, 2013.
- [179] J. Seiffert *et al.*, "Pulmonary toxicity of instilled silver nanoparticles: influence of size, coating and rat strain," *PloS One*, vol. 10, no. 3, pp. e0119726-e119743, 2015.

- [180] K. Loeschner *et al.*, "Distribution of silver in rats following 28 days of repeated oral exposure to silver nanoparticles or silver acetate," *Particle and Fibre Toxicology*, vol. 8, no. 1, pp. 18-32, 2011.
- [181] G. N. Jeong, U. B. Jo, H. Y. Ryu, Y. S. Kim, K. S. Song, and I. J. Yu, "Histochemical study of intestinal mucins after administration of silver nanoparticles in Sprague–Dawley rats," *Archives of Toxicology*, vol. 84, no. 1, pp. 63-83, 2010.
- [182] B. Shahare, M. Yashpal, and Gajendra, "Toxic effects of repeated oral exposure of silver nanoparticles on small intestine mucosa of mice," *Toxicology Mechanisms and Methods*, vol. 23, no. 3, pp. 161-167, 2013.
- [183] J. Skalska, M. Frontczak-Baniewicz, and L. Strużyńska, "Synaptic degeneration in rat brain after prolonged oral exposure to silver nanoparticles," *Neurotoxicology*, vol. 46, pp. 145-154, 2015.
- [184] J. J. Kim, K. Konkel, L. McCulley, and I.-L. Diak, "Cases of Argyria Associated With Colloidal Silver Use," *Annals of Pharmacotherapy*, pp. 867-870, 2019.
- [185] M. S. Heydrnejad, R. J. Samani, and S. Aghaeivanda, "Toxic effects of silver nanoparticles on liver and some hematological parameters in male and female mice (*Mus musculus*)," *Biological Trace Element Research*, vol. 165, no. 2, pp. 153-158, 2015.
- [186] R. Tiwari *et al.*, "Oral subchronic exposure to silver nanoparticles causes renal damage through apoptotic impairment and necrotic cell death," *Nanotoxicology*, vol. 11, no. 5, pp. 671-686, 2017.
- [187] R. E. Elle *et al.*, "Dietary exposure to silver nanoparticles in Sprague–Dawley rats: effects on oxidative stress and inflammation," *Food and Chemical Toxicology*, vol. 60, pp. 297-301, 2013.
- [188] T. R. Fennell *et al.*, "Disposition of intravenously or orally administered silver nanoparticles in pregnant rats and the effect on the biochemical profile in urine," *Journal of Applied Toxicology*, vol. 37, no. 5, pp. 530-544, 2017.
- [189] I. L. Bergin *et al.*, "Effects of particle size and coating on toxicologic parameters, fecal elimination kinetics and tissue distribution of acutely ingested silver nanoparticles in a mouse model," *Nanotoxicology*, vol. 10, no. 3, pp. 352-360, 2016.
- [190] A. d. C. Martins Jr *et al.*, "Evaluation of distribution, redox parameters, and genotoxicity in Wistar rats co-exposed to silver and titanium dioxide nanoparticles," *Journal of Toxicology and Environmental Health, Part A*, vol. 80, no. 19-21, pp. 1156-1165, 2017.
- [191] T. Garcia *et al.*, "Oral subchronic exposure to silver nanoparticles in rats," *Food and Chemical Toxicology*, vol. 92, pp. 177-187, 2016.

- [192] D. Lafuente *et al.*, "Effects of oral exposure to silver nanoparticles on the sperm of rats," *Reproductive Toxicology*, vol. 60, pp. 133-139, 2016.
- [193] J. Skalska, B. Dąbrowska-Bouta, and L. Strużyńska, "Oxidative stress in rat brain but not in liver following oral administration of a low dose of nanoparticulate silver," *Food and Chemical Toxicology*, vol. 97, pp. 307-315, 2016.
- [194] P. Orłowski *et al.*, "Tannic acid-modified silver nanoparticles for wound healing: The importance of size," *International Journal of Nanomedicine*, vol. 13, pp. 991-1007, 2018.
- [195] S. Zhang, X. Liu, H. Wang, J. Peng, and K. K. Y. Wong, "Silver nanoparticle-coated suture effectively reduces inflammation and improves mechanical strength at intestinal anastomosis in mice," *Journal of Pediatric Surgery*, vol. 49, no. 4, pp. 606-613, 2014.
- [196] A. A. García, A. M. Rodríguez Martín, E. Serra Baldrich, E. Manubens Mercade, and L. Puig Sanz, "Allergic contact dermatitis to silver in a patient treated with silver sulphadiazine after a burn," *Journal of the European Academy of Dermatology and Venereology*, vol. 30, no. 2, pp. 365-366, 2016.
- [197] E. Özkaya, "A rare case of allergic contact dermatitis from silver nitrate in a widely used special patch test marker," *Contact Dermatitis*, vol. 61, no. 2, pp. 120-122, 2009.
- [198] M. Wang, X. Lai, L. Shao, and L. Li, "Evaluation of immunoresponses and cytotoxicity from skin exposure to metallic nanoparticles," *International Journal of Nanomedicine*, vol. 13, pp. 4445-4459, 2018.
- [199] Y. Zhu *et al.*, "Penetration of silver nanoparticles into porcine skin ex vivo using fluorescence lifetime imaging microscopy, Raman microscopy, and surface-enhanced Raman scattering microscopy," *Journal of Biomedical Optics*, vol. 20, no. 5, pp. 051006-051015, 2014.
- [200] M. Korani, S. M. Rezayat, and S. A. Bidgoli, "Sub-chronic dermal toxicity of silver nanoparticles in guinea pig: special emphasis to heart, bone and kidney toxicities," *Iranian Journal of Pharmaceutical Research: IJPR*, vol. 12, no. 3, pp. 511-519, 2013.
- [201] C. A. Austin *et al.*, "Distribution and accumulation of 10 nm silver nanoparticles in maternal tissues and visceral yolk sac of pregnant mice, and a potential effect on embryo growth," *Nanotoxicology*, vol. 10, no. 6, pp. 654-661, 2016.
- [202] Z. Wang *et al.*, "Evaluation of the biological fate and the transport through biological barriers of nanosilver in mice," *Current Pharmaceutical Design*, vol. 19, no. 37, pp. 6691-6697, 2013.

- [203] D. K. Tiwari, T. Jin, and J. Behari, "Dose-dependent in-vivo toxicity assessment of silver nanoparticle in Wistar rats," *Toxicology Mechanisms and Methods*, vol. 21, no. 1, pp. 13-24, 2011.
- [204] Y. Xue *et al.*, "Acute toxic effects and gender-related biokinetics of silver nanoparticles following an intravenous injection in mice," *Journal of Applied Toxicology*, vol. 32, no. 11, pp. 890-899, 2012.
- [205] Y. Zhang *et al.*, "Silver nanoparticles decrease body weight and locomotor activity in adult male rats," *Small*, vol. 9, no. 9-10, pp. 1715-1720, 2013.
- [206] T. X. Garcia, G. M. J. Costa, L. R. Franca, and M.-C. Hofmann, "Sub-acute intravenous administration of silver nanoparticles in male mice alters Leydig cell function and testosterone levels," *Reproductive Toxicology*, vol. 45, pp. 59-70, 2014.
- [207] H. Guo *et al.*, "Intravenous administration of silver nanoparticles causes organ toxicity through intracellular ROS-related loss of inter-endothelial junction," (in eng), *Particle Fibre and Toxicol*, vol. 13, pp. 21-34, 2016.
- [208] H. Wen *et al.*, "Acute toxicity and genotoxicity of silver nanoparticle in rats," *PloS one*, vol. 12, no. 9, pp. e0185554-e018570, 2017.
- [209] A. K. Vidanapathirana *et al.*, "Acute intravenous exposure to silver nanoparticles during pregnancy induces particle size and vehicle dependent changes in vascular tissue contractility in Sprague Dawley rats," *Reproductive Toxicology*, vol. 75, pp. 10-22, 2018.
- [210] K. E. Driscoll *et al.*, "Intratracheal instillation as an exposure technique for the evaluation of respiratory tract toxicity: uses and limitations," *Toxicological Sciences*, vol. 55, no. 1, pp. 24-35, 2000.
- [211] Y. Arai, T. Miyayama, and S. Hirano, "Difference in the toxicity mechanism between ion and nanoparticle forms of silver in the mouse lung and in macrophages," *Toxicology*, vol. 328, pp. 84-92, 2015.
- [212] J. H. Lee, K. Ahn, S. M. Kim, K. S. Jeon, J. S. Lee, and I. J. Yu, "Continuous 3-day exposure assessment of workplace manufacturing silver nanoparticles," *Journal of Nanoparticle Research*, vol. 14, no. 9, pp. 1134-1144, 2012.
- [213] J. R. Roberts *et al.*, "Pulmonary and cardiovascular responses of rats to inhalation of silver nanoparticles," (in eng), *Journal of Toxicology and Environmental Health*, vol. 76, no. 11, pp. 651-68, 2013..
- [214] X. He *et al.*, "Lung deposition and extrapulmonary translocation of nanoceria after intratracheal instillation," *Nanotechnology*, vol. 21, no. 28, pp. 285103-285112, 2010.
- [215] D. L. Gray, L. A. Wallace, M. C. Brinkman, S. S. Buehler, and C. La Londe, "Respiratory and cardiovascular effects of metals in ambient particulate

- matter: a critical review," in *Reviews of Environmental Contamination and Toxicology*: Springer, pp. 135-203, 2015.
- [216] V. C. Minarchick *et al.*, "Pulmonary cerium dioxide nanoparticle exposure differentially impairs coronary and mesenteric arteriolar reactivity," *Cardiovascular Toxicology*, vol. 13, no. 4, pp. 323-337, 2013.
- [217] P. A. Stapleton, A. B. Abukabda, S. L. Hardy, and T. R. Nurkiewicz, "Cardiovascular Responses to Environmental Stress: Xenobiotic pulmonary exposure and systemic cardiovascular response via neurological links," *American Journal of Physiology-Heart and Circulatory Physiology*, vol. 309, no. 10, pp. H1609-H1620, 2015.
- [218] R. F. Hamilton, S. Buckingham, and A. Holian, "The effect of size on Ag nanosphere toxicity in macrophage cell models and lung epithelial cell lines is dependent on particle dissolution," *International Journal of Molecular Sciences*, vol. 15, no. 4, pp. 6815-6830, 2014.
- [219] K. A. Huynh and K. L. Chen, "Aggregation kinetics of citrate and polyvinylpyrrolidone coated silver nanoparticles in monovalent and divalent electrolyte solutions," *Environmental Science & Technology*, vol. 45, no. 13, pp. 5564-5571, 2011.
- [220] M. Tejamaya, I. Römer, R. C. Merrifield, and J. R. Lead, "Stability of citrate, PVP, and PEG coated silver nanoparticles in ecotoxicology media," *Environmental Science & Technology*, vol. 46, no. 13, pp. 7011-7017, 2012.
- [221] A. Raj, P. Shah, and N. Agrawal, "Dose-dependent effect of silver nanoparticles (AgNPs) on fertility and survival of *Drosophila*: An in-vivo study," *PloS One*, vol. 12, no. 5, pp. e0178051-e0178065, 2017.
- [222] P. Hartemann *et al.*, "Nanosilver: Safety, health and environmental effects and role in antimicrobial resistance," *Materials Today*, vol. 18, no. 3, pp. 122-123, 2015.
- [223] S. Zhang, C. Du, Z. Wang, X. Han, K. Zhang, and L. Liu, "Reduced cytotoxicity of silver ions to mammalian cells at high concentration due to the formation of silver chloride," *Toxicology in Vitro*, vol. 27, no. 2, pp. 739-744, 2013.
- [224] M. E. Quadros and L. C. Marr, "Silver nanoparticles and total aerosols emitted by nanotechnology-related consumer spray products," *Environmental Science & Technology*, vol. 45, no. 24, pp. 10713-10719, 2011.
- [225] K. C. Stone, R. R. Mercer, P. Gehr, B. Stockstill, and J. D. Crapo, "Allometric relationships of cell numbers and size in the mammalian lung," *American Journal of Respiratory Cell and Molecular Biology*, vol. 6, no. 2, pp. 235-243, 1992.
- [226] A. R. R. Péry, C. Brochot, P. H. M. Hoet, A. Nemmar, and F. Y. Bois, "Development of a physiologically based kinetic model for 99 m-technetium-

- labelled carbon nanoparticles inhaled by humans," *Inhalation Toxicology*, vol. 21, no. 13, pp. 1099-1107, 2009.
- [227] J. Chen *et al.*, "Quantification of extrapulmonary translocation of intratracheal-instilled particles in vivo in rats: effect of lipopolysaccharide," *Toxicology*, vol. 222, no. 3, pp. 195-201, 2006.
- [228] A. Nemmar, S. Al-Salam, S. Beegam, P. Yuvaraju, and B. H. Ali, "The acute pulmonary and thrombotic effects of cerium oxide nanoparticles after intratracheal instillation in mice," *International Journal of Nanomedicine*, vol. 12, pp. 2913-2922, 2017.
- [229] A. Nemmar, S. Al-Salam, P. Yuvaraju, S. Beegam, and B. H. Ali, "Emodin mitigates diesel exhaust particles-induced increase in airway resistance, inflammation and oxidative stress in mice," *Respiratory Physiology & neurobiology*, vol. 215, pp. 51-57, 2015.
- [230] A. Nemmar, S. Al-Salam, P. Yuvaraju, S. Beegam, and B. H. Ali, "Exercise Training Mitigates Water Pipe Smoke Exposure-Induced Pulmonary Impairment via Inhibiting NF- κ B and Activating Nrf2 Signalling Pathways," *Oxidative Medicine and Cellular Longevity*, vol. 2018, pp. 1-10, 2018.
- [231] M. Al Za'abi, S. Al Salam, Y. Al Suleimani, P. Manoj, A. Nemmar, and B. H. Ali, "Gum Acacia Improves Renal Function and Ameliorates Systemic Inflammation, Oxidative and Nitrosative Stress in Streptozotocin-Induced Diabetes in Rats with Adenine-Induced Chronic Kidney Disease," *Cellular Physiology and Biochemistry*, vol. 45, no. 6, pp. 2293-2304, 2018.
- [232] C. A. Drummond *et al.*, "Reduction of Na/K-ATPase affects cardiac remodeling and increases c-kit cell abundance in partial nephrectomized mice," *American Journal of Physiology-Heart and Circulatory Physiology*, vol. 306, no. 12, pp. H1631-H1643, 2014.
- [233] N. Haberl *et al.*, "Cytotoxic and proinflammatory effects of PVP-coated silver nanoparticles after intratracheal instillation in rats," *Beilstein Journal of Nanotechnology*, vol. 4, pp. 933-940, 2013.
- [234] C. Volker, M. Oetken, and J. Oehlmann, "The biological effects and possible modes of action of nanosilver," (in eng), *Reviews of Environmental Contamination and Toxicology*, vol. 223, pp. 81-106, 2013.
- [235] G. R. S. Budinger *et al.*, "Particulate matter-induced lung inflammation increases systemic levels of PAI-1 and activates coagulation through distinct mechanisms," *PloS One*, vol. 6, no. 4, pp. e18525-e18534, 2011.
- [236] N. L. Mills *et al.*, "Adverse cardiovascular effects of air pollution," *Nature Reviews Cardiology*, vol. 6, no. 1, pp. 36-44, 2009.
- [237] L. M. Faddah, N. A. A. Baky, N. M. Al-Rasheed, and N. M. Al-Rasheed, "Biochemical responses of nanosize titanium dioxide in the heart of rats

- following administration of idepenone and quercetin," *African Journal of Pharmacy and Pharmacology*, vol. 7, no. 38, pp. 2639-2651, 2013.
- [238] N. A. A. Baky, L. M. Faddah, N. M. Al-Rasheed, and A. J. Fatani, "Induction of inflammation, DNA damage and apoptosis in rat heart after oral exposure to zinc oxide nanoparticles and the cardioprotective role of α -lipoic acid and vitamin E," *Drug Research*, vol. 63, no. 05, pp. 228-236, 2013.
- [239] Z. Du *et al.*, "Cardiovascular toxicity of different sizes amorphous silica nanoparticles in rats after intratracheal instillation," *Cardiovascular Toxicology*, vol. 13, no. 3, pp. 194-207, 2013.
- [240] H. B. Bostan *et al.*, "Cardiotoxicity of nano-particles," *Life Sciences*, vol. 165, pp. 91-99, 2016.
- [241] A. C. Maritim, a. Sanders, and J. B. Watkins Iii, "Diabetes, oxidative stress, and antioxidants: a review," *Journal of Biochemical and Molecular Toxicology*, vol. 17, no. 1, pp. 24-38, 2003.
- [242] A. Nemmar *et al.*, "Ultras-small superparamagnetic iron oxide nanoparticles acutely promote thrombosis and cardiac oxidative stress and DNA damage in mice," *Particle and Fibre Toxicology*, vol. 13, no. 1, pp. 22-33, 2015.
- [243] N. A. Holland, "Intratracheal instillation of silver nanoparticles exacerbates cardiac ischemia/reperfusion injury in male sprague-dawley rats," pp. 1-125, 2014.
- [244] A. Valavanidis, T. Vlachogianni, and C. Fiotakis, "8-hydroxy-2'-deoxyguanosine (8-OHdG): A critical biomarker of oxidative stress and carcinogenesis," (in eng), *Journal of Environmental Science and Health*, vol. 27, no. 2, pp. 120-39, Apr 2009.
- [245] B. Trouiller, R. Reliene, A. Westbrook, P. Solaimani, and R. H. Schiestl, "Titanium dioxide nanoparticles induce DNA damage and genetic instability in vivo in mice," *Cancer Research*, pp. 0008-5472, 2009.
- [246] N. J. Siddiqi, M. A. K. Abdelhalim, A. K. El-Ansary, A. S. Alhomida, and W. Y. Ong, "Identification of potential biomarkers of gold nanoparticle toxicity in rat brains," *Journal of Neuroinflammation*, vol. 9, no. 1, pp. 123-130, 2012.
- [247] P. Ma *et al.*, "Intraperitoneal injection of magnetic Fe₃O₄-nanoparticle induces hepatic and renal tissue injury via oxidative stress in mice," *International Journal of Nanomedicine*, vol. 7, pp. 4809-4818, 2012.
- [248] Y. Gavrieli, Y. Sherman, and S. A. Ben-Sasson, "Identification of programmed cell death in situ via specific labeling of nuclear DNA fragmentation," *The Journal of Cell Biology*, vol. 119, no. 3, pp. 493-501, 1992.

- [249] T. Pálmai-Pallag and C. Z. Bachrati, "Inflammation-induced DNA damage and damage-induced inflammation: a vicious cycle," *Microbes and Infection*, vol. 16, no. 10, pp. 822-832, 2014.
- [250] A. Nemmar *et al.*, "Diesel exhaust particles induce impairment of vascular and cardiac homeostasis in mice: ameliorative effect of emodin," *Cellular Physiology and Biochemistry*, vol. 36, no. 4, pp. 1517-1526, 2015.
- [251] V. M. Silva, N. Corson, A. Elder, and G. Oberdörster, "The rat ear vein model for investigating in vivo thrombogenicity of ultrafine particles (UFP)," *Toxicological Sciences*, vol. 85, no. 2, pp. 983-989, 2005.
- [252] B. Furie and B. C. Furie, "The molecular basis of blood coagulation," *Cell*, vol. 53, no. 4, pp. 505-518, 1988.
- [253] K. Landin, L. Tengborn, and U. Smith, "Elevated fibrinogen and plasminogen activator inhibitor (PAI-1) in hypertension are related to metabolic risk factors for cardiovascular disease," *Journal of Internal Medicine*, vol. 227, no. 4, pp. 273-278, 1990.
- [254] Y. Aso, "Plasminogen activator inhibitor (PAI)-1 in vascular inflammation and thrombosis," *Frontiers in Bioscience*, vol. 12, no. 8, pp. 2957-2966, 2007.
- [255] A. Nemmar *et al.*, "Amorphous silica nanoparticles impair vascular homeostasis and induce systemic inflammation," *International Journal of Nanomedicine*, vol. 9, pp. 2779-2789, 2014.
- [256] A. Erdely *et al.*, "Cross-talk between lung and systemic circulation during carbon nanotube respiratory exposure. Potential biomarkers," *Nano Letters*, vol. 9, no. 1, pp. 36-43, 2008.
- [257] K. Maeda, T. Tsutamoto, A. Wada, T. Hisanaga, and M. Kinoshita, "Plasma brain natriuretic peptide as a biochemical marker of high left ventricular end-diastolic pressure in patients with symptomatic left ventricular dysfunction," *American Heart Journal*, vol. 135, no. 5, pp. 825-832, 1998.
- [258] C. Hall, "Essential biochemistry and physiology of (NT-pro) BNP," *European Journal of Heart Failure*, vol. 6, no. 3, pp. 257-260, 2004.
- [259] A. Radomski *et al.*, "Nanoparticle-induced platelet aggregation and vascular thrombosis," *British Journal of Pharmacology*, vol. 146, no. 6, pp. 882-893, 2005.
- [260] P. A. Stapleton, C. R. McBride, J. Yi, A. B. Abukabda, and T. R. Nurkiewicz, "Estrous cycle-dependent modulation of in vivo microvascular dysfunction after nanomaterial inhalation," *Reproductive Toxicology*, vol. 78, pp. 20-28, 2018.

- [261] D. Tsikas, "Review Methods of quantitative analysis of the nitric oxide metabolites nitrite and nitrate in human biological fluids," *Free Radical Research*, vol. 39, no. 8, pp. 797-815, 2005.
- [262] S. Elmore, "Apoptosis: a review of programmed cell death," *Toxicologic Pathology*, vol. 35, no. 4, pp. 495-516, 2007.
- [263] X. Chen and H. J. Schluesener, "Nanosilver: a nanoparticle in medical application," *Toxicology Letters*, vol. 176, no. 1, pp. 1-12, 2008.
- [264] A. Shimada, N. Kawamura, M. Okajima, T. Kaewamatawong, H. Inoue, and T. Morita, "Translocation pathway of the intratracheally instilled ultrafine particles from the lung into the blood circulation in the mouse," *Toxicologic Pathology*, vol. 34, no. 7, pp. 949-957, 2006.
- [265] T. Kato *et al.*, "Evidence that exogenous substances can be phagocytized by alveolar epithelial cells and transported into blood capillaries," *Cell and Tissue Research*, vol. 311, no. 1, pp. 47-51, 2003.
- [266] J. Lademann *et al.*, "Penetration of titanium dioxide microparticles in a sunscreen formulation into the horny layer and the follicular orifice," *Skin Pharmacology and Physiology*, vol. 12, no. 5, pp. 247-256, 1999.
- [267] Y. Y. Zhang and J. Sun, "A study on the bio-safety for nano-silver as anti-bacterial materials," *Zhongguo yi liao qi xie za zhi= Chinese Journal of Medical Instrumentation*, vol. 31, no. 1, pp. 36-8, 2007.
- [268] C. S. Yah, G. S. Simate, and S. E. Iyuke, "Nanoparticles toxicity and their routes of exposures," *Pakistan Journal of Pharmaceutical Sciences*, vol. 25, no. 2, pp. 299-314, 2012.
- [269] A. Nemmar, S. Beegam, P. Yuvaraju, J. Yasin, A. Shahin, and B. H. Ali, "Interaction of amorphous silica nanoparticles with erythrocytes in vitro: role of oxidative stress," *Cellular Physiology and Biochemistry*, vol. 34, no. 2, pp. 255-265, 2014.
- [270] C. B. Kim, S. Shin, and S.-H. Song, "Hemorheological changes caused by lead exposure," *Clinical Hemorheology and Microcirculation*, vol. 55, no. 3, pp. 341-348, 2013.
- [271] A. Nemmar, S. Zia, D. Subramanian, I. Al-Amri, M. A. Al Kindi, and B. H. Ali, "Interaction of diesel exhaust particles with human, rat and mouse erythrocytes in vitro," *Cellular Physiology and Biochemistry*, vol. 29, no. 1-2, pp. 163-170, 2012.
- [272] S. Lu *et al.*, "Efficacy of simple short-term in vitro assays for predicting the potential of metal oxide nanoparticles to cause pulmonary inflammation," *Environmental Health Perspectives*, vol. 117, no. 2, pp. 241-248, 2009.

- [273] B. W. Neun and M. A. Dobrovolskaia, "Method for analysis of nanoparticle hemolytic properties in vitro," *Characterization of Nanoparticles Intended for Drug Delivery*, pp. 215-224, 2011.
- [274] A. Nemmar, S. Al-Maskari, B. H. Ali, and I. S. Al-Amri, "Cardiovascular and lung inflammatory effects induced by systemically administered diesel exhaust particles in rats," *American Journal of Physiology-Lung Cellular and Molecular Physiology*, vol. 292, no. 3, pp. L664-L670, 2007.
- [275] G. Lefevre *et al.*, "Evaluation of lipid peroxidation by measuring thiobarbituric acid reactive substances," vol. 56, 3 ed., pp. 305-319, 1998.
- [276] M. Foller *et al.*, "Participation of leukotriene C4 in the regulation of suicidal erythrocyte death," *Acta Physiologica Polonica*, vol. 12, no. 3, pp. 135-145, 2009.
- [277] P. Pignatelli *et al.*, "Carnitine inhibits arachidonic acid turnover, platelet function, and oxidative stress," *American Journal of Physiology-Heart and Circulatory Physiology*, vol. 284, no. 1, pp. H41-H48, 2003.
- [278] M. Walsh, R. J. Lutz, T. G. Cotter, and R. O'Connor, "Erythrocyte survival is promoted by plasma and suppressed by a Bak-derived BH3 peptide that interacts with membrane-associated Bcl-XL," *Blood*, vol. 99, no. 9, pp. 3439-3448, 2002.
- [279] J. Choi, V. Reipa, V. M. Hitchins, P. L. Goering, and R. A. Malinauskas, "Physicochemical Characterization and In Vitro Hemolysis Evaluation of Silver Nanoparticles," *Toxicological Sciences*, vol. 123, no. 1, pp. 133-143, 2011.
- [280] S. Krajewski *et al.*, "Hemocompatibility evaluation of different silver nanoparticle concentrations employing a modified Chandler-loop in vitro assay on human blood," *Acta biomaterialia*, vol. 9, no. 7, pp. 7460-7468, 2013.
- [281] R. Shrivastava, P. Kushwaha, Y. C. Bhutia, and S. J. S. Flora, "Oxidative stress following exposure to silver and gold nanoparticles in mice," *Toxicology and industrial health*, vol. 32, no. 8, pp. 1391-1404, 2016.
- [282] T. Kwon *et al.*, "Optimizing hemocompatibility of surfactant-coated silver nanoparticles in human erythrocytes," *Journal of nanoscience and nanotechnology*, vol. 12, no. 8, pp. 6168-6175, 2012.
- [283] M. A. Munger *et al.*, "In vivo human time-exposure study of orally dosed commercial silver nanoparticles," *Nanomedicine: Nanotechnology, Biology and Medicine*, vol. 10, no. 1, pp. 1-9, 2014.
- [284] K. J. Smock, R. L. Schmidt, G. Hadlock, G. Stoddard, D. W. Grainger, and M. A. Munger, "Assessment of orally dosed commercial silver nanoparticles on human ex vivo platelet aggregation," *Nanotoxicology*, vol. 8, no. 3, pp. 328-333, 2014.

- [285] S.-Q. Li *et al.*, "Nanotoxicity of TiO₂ nanoparticles to erythrocyte in vitro," *Food and Chemical Toxicology*, vol. 46, no. 12, pp. 3626-3631, 2008.
- [286] Y. Zhao, X. Sun, G. Zhang, B. G. Trewyn, I. I. Slowing, and V. S. Y. Lin, "Interaction of mesoporous silica nanoparticles with human red blood cell membranes: size and surface effects," *ACS Nano*, vol. 5, no. 2, pp. 1366-1375, 2011.
- [287] H. J. Johnston, G. Hutchison, F. M. Christensen, S. Peters, S. Hankin, and V. Stone, "A review of the in vivo and in vitro toxicity of silver and gold particulates: particle attributes and biological mechanisms responsible for the observed toxicity," *Critical Reviews in Toxicology*, vol. 40, no. 4, pp. 328-346, 2010.
- [288] M. Geiser *et al.*, "Ultrafine particles cross cellular membranes by nonphagocytic mechanisms in lungs and in cultured cells," *Environmental Health Perspectives*, vol. 113, no. 11, pp. 1555-1560, 2005.
- [289] D. M. Underhill and A. Ozinsky, "Phagocytosis of microbes: complexity in action," *Annual Review of Immunology*, vol. 20, no. 1, pp. 825-852, 2002.
- [290] J. J. Bogdanska, P. Korneti, and B. Todorova, "Erythrocyte superoxide dismutase, glutathione peroxidase and catalase activities in healthy male subjects in Republic of Macedonia," *Bratislavske Lekarske Listy*, vol. 104, no. 3, pp. 108-114, 2003.
- [291] C. S. S. Reddy, M. V. V. Subramanyam, R. Vani, and S. A. Devi, "In vitro models of oxidative stress in rat erythrocytes: effect of antioxidant supplements," *Toxicology in Vitro*, vol. 21, no. 8, pp. 1355-1364, 2007.
- [292] S. Misra, C. Hamilton, and S. Niyogi, "Induction of oxidative stress by selenomethionine in isolated hepatocytes of rainbow trout (*Oncorhynchus mykiss*)," *Toxicology in Vitro*, vol. 26, no. 4, pp. 621-629, 2012.
- [293] M. Holcik, "Do mature red blood cells die by apoptosis?," *TRENDS in Genetics*, vol. 18, no. 3, p. 121, 2002.
- [294] F. Lang, K. S. Lang, P. A. Lang, S. M. Huber, and T. Wieder, "Mechanisms and significance of eryptosis," *Antioxidants & Redox Signaling*, vol. 8, no. 7-8, pp. 1183-1192, 2006.
- [295] E. Daugas, C. Cande, and G. Kroemer, "Erythrocytes: death of a mummy," *Cell Death and Differentiation*, vol. 8, no. 12, pp. 1131-1133, 2001.
- [296] M. Jemaà, M. Fezai, R. Bissinger, and F. Lang, "Methods Employed in Cytofluorometric Assessment of Eryptosis, the Suicidal Erythrocyte Death," *Cellular Physiology and Biochemistry*, vol. 43, no. 2, pp. 431-444, 2017.
- [297] F. Rosário, P. Hoet, C. Santos, and H. Oliveira, "Death and cell cycle progression are differently conditioned by the AgNP size in osteoblast-like cells," *Toxicology*, vol. 368, pp. 103-115, 2016.

- [298] M. Föllner, S. M. Huber, and F. Lang, "Erythrocyte programmed cell death," *IUBMB life*, vol. 60, no. 10, pp. 661-668, 2008.
- [299] F. Lang *et al.*, "Erythrocyte ion channels in regulation of apoptosis," in *Cell Volume and Signaling*: Springer, pp. 211-217, 2004.
- [300] E. Pretorius, J. N. du Plooy, and J. Bester, "A comprehensive review on eryptosis," *Cellular Physiology and Biochemistry*, vol. 39, no. 5, pp. 1977-2000, 2016.
- [301] D. Bratosin *et al.*, "Programmed cell death in mature erythrocytes: a model for investigating death effector pathways operating in the absence of mitochondria," *Cell Death and Differentiation*, vol. 8, no. 12, pp. 1143-1156, 2001.
- [302] C. P. Berg *et al.*, "Human mature red blood cells express caspase-3 and caspase-8, but are devoid of mitochondrial regulators of apoptosis," *Cell Death & Differentiation*, vol. 8, no. 12, pp. 1197-1206, 2001.
- [303] F. Lang, E. Lang, and M. Föllner, "Physiology and pathophysiology of eryptosis," *Transfusion Medicine and Hemotherapy*, vol. 39, no. 5, pp. 308-314, 2012.
- [304] W. Utembe, K. Potgieter, A. B. Stefaniak, and M. Gulumian, "Dissolution and biodurability: Important parameters needed for risk assessment of nanomaterials," *Particle and Fibre Toxicology*, vol. 12, no. 1, pp. 11-23, 2015.
- [305] L. G. Hooper and J. D. Kaufman, "Ambient air pollution and clinical implications for susceptible populations," *Annals of the American Thoracic Society*, vol. 15, no. Supplement 2, pp. S64-S68, 2018.

List of Publications

Ferdous Z, Al-Salam S, Greish YE, Ali BH, Nemmar A. Pulmonary exposure to silver nanoparticles impairs cardiovascular homeostasis: Effects of coating, dose and time. *Toxicology and Applied Pharmacology*, 367:36-50, 2019.

Ferdous Z, Beegam S, Tariq S, Ali BH, Nemmar A. The in vitro effect of polyvinylpyrrolidone and citrate coated silver nanoparticles on erythrocytic oxidative damage and eryptosis. *Cellular Physiology and Biochemistry*. 49(4):1577-88, 2018.